5. HYDROGEOLOGICAL CHARACTERISATION OF THE STUDY AREA

5.1. Characterisation of groundwater recharge

No systematic recharge studies have been conducted in the area of investigation. National datasets such as the Groundwater Assessment Projected II (GRA II) (DWAF, 2006) or Vegter's (1995) recharge map can be used to obtain a first estimate of regional recharge. The distribution of recharge based on the GRA II dataset is presented in Figure 5.1. The GRA II dataset is based on the chloride method and adjusted to account for factors such as depth to groundwater, landcover, variation of MAP and slope. Groundwater recharge in the Limpopo WMA is approximately 702 million m^3/a (assuming recharge being 2% of mean annual precipitation (MAP) and 376 million m^3/a in the Luvuvhu/Letaba WMA (2% to 3% of MAP).

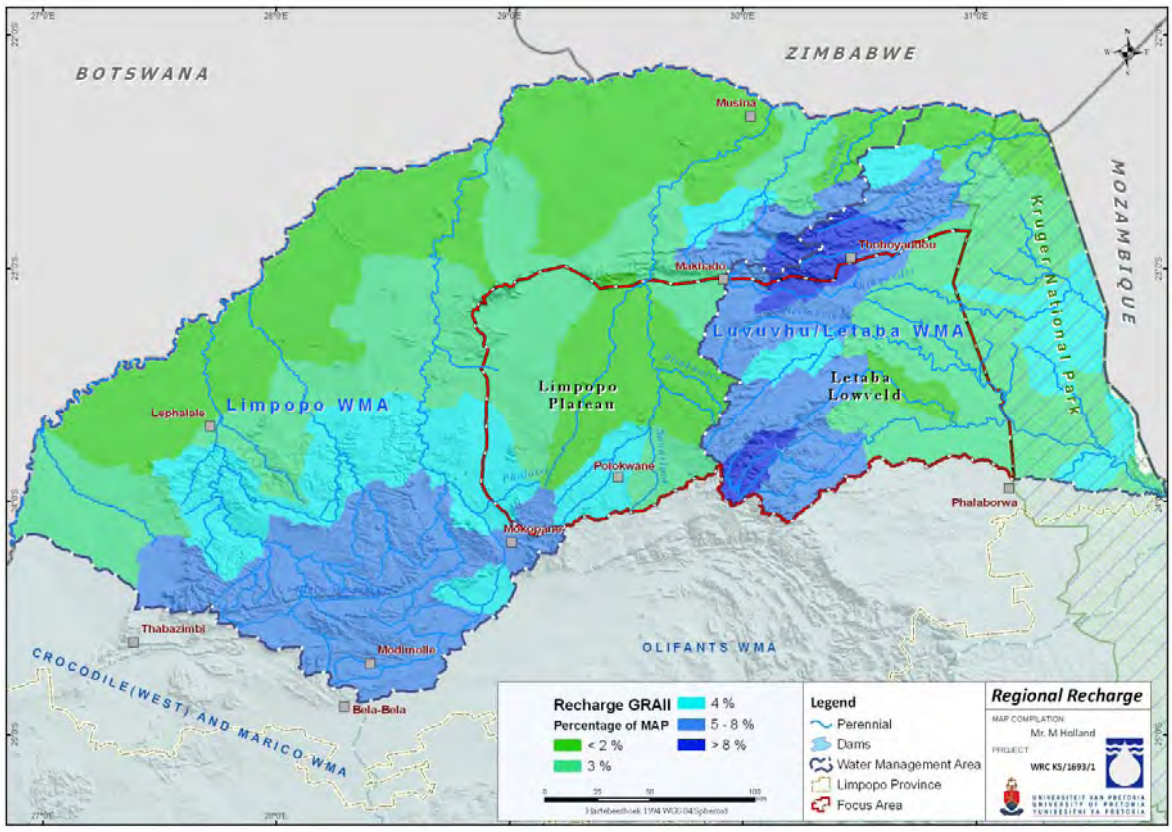

Figure 5.1. Regional recharge map for the Limpopo Province.

5.1.1. Recharge estimates (Chloride Mass Balance)

Regional and local estimates of recharge were obtained using chloride concentrations in rainwater and groundwater, together with annual rainfall. Three bulk rainfall stations were installed in the area for the application of the CMB and isotope characterization. Unusually high chloride values for rainfall obtained at the start of the study suggest that these samples were influenced by aerosol deposits and dry depositions indicating that the bulk rainfall collectors overestimated the total

chloride deposition. Therefore, a couple of manual rainfall samples were collected during the study. Further chloride concentrations were obtained from the Department of Water Affairs[1] as part of the National Rainwater Monitoring Programme which operates five rainfall sampling collectors in the Blouberg and Taaiboshgroet area. Table 5.1 lists the chloride values obtained from the sampled rainwater of the individual rainfall event as well as the bulk rainfall samples from the DWA. Based on the results chloride concentrations range from 0.39 to 7.3 mg/ℓ. However, according to Bean (2003) chloride values above 5 mg/ℓ represent site-specific enrichment within the given sampling period and would result in an over-estimation of recharge.

Table 5.1. Summary of borehole characteristics in the study area.

Site	*Sample ID*	*Date*	*Cl (mg/l)*	*Comment*
Mufeba (UP1)	MERS 1	08-Mar-08	6.3	Bulk sample (Could be polluted)
Bochum (UP2)	BORS 1	09-Mar-08	7.3	
Rawesi (UP3)	CORS 1	09-Mar-08	6.3	
Mufeba (UP1)	RA 1	03-Mar-09	0.61	Event based
Rawesi (UP3)	RAW 2	15-Mar-09	0.39	Event based
Rawesi 2 (UP3)	RAS 3	15-Mar-09	0.77	Event based
Bochum (UP2)	BC1	15-Mar-09	0.69	Event based
Polokwane (UP4)	Rain2	01-Feb-10	0.34	Event based
DWA (1 to 5) Taaiboschgroet Area*	Blouberg Eldorado Greenfields Langjan Rosyth	2002/2003 late summer	0.68	Bulk Rainfall Collectors
		2003/2004 early summer	1.34	
		2003/2004 Mid summer	0.91	
		2003/2004 late summer	0.44	
		2003/2004 winter	1.96	
		2004/2005 Early Summer	0.80	
		2004/2005 Late Summer	1.43	
		2005/2006 Mid summer	0.63	
		2005/2006 Late summer	0.57	

*- Based on the harmonic mean chloride values of five stations within the Taaiboshgroet area.

Excluding erroneous values an average concentration of 0.69 mg/ℓ is obtained. The spatial location of the sampling rainfall collector sites are shown in Figure 5.2, together with the distribution of chloride content in groundwater from over 4 000 boreholes.

[1] E-mail correspondence (2009) – Eddie van Wyk (Hydrological Services - Department of Water Affairs)

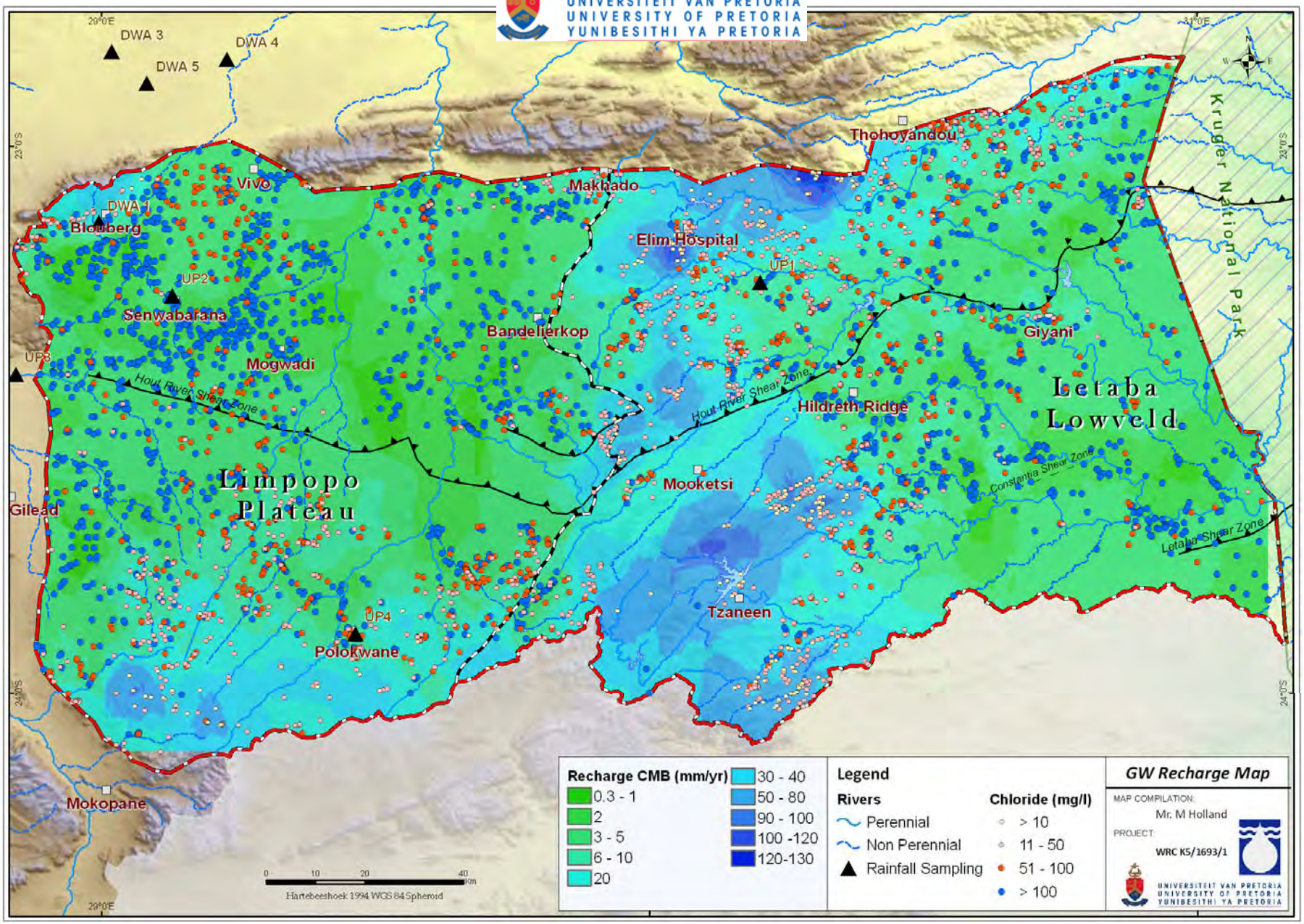

Figure 5.2. Annual recharge map based on the CMB-method.

Interpolations from the CMB results were based on the Kriging techniques, while site specific results are shown in Table 5.2. The average concentrations of groundwater in boreholes surrounding the localities (10 km radius) were used to determine the average rate of recharge per year. Recharge rates vary from 0.4 to 4.6 % of MAP. Active recharge zones are related to the higher lying areas associated with the main surface water drainage divides (i.e. along the Great Escarpment and to the south of Polokwane).

Table 5.2. Recharge estimates based on the CMB for selected localities in the study area.

Locality	Annual Rainfall (mm)*	Chloride (mg/l)		Average Recharge	
		Cl_{rf}	Cl_{gw}	Mm/year	% of MAP
Chloe	365	0.6	147.3	1.5	**0.4**
Mogwadi	392	0.7	153.7	1.8	0.5
Tzaneen	950	0.75	10.2	70.0	7.4
Mara	454	0.6	77.2	3.5	0.8
Palmaryville	916	0.75	26.1	26.4	2.9
Polokwane	455	0.6	40.1	6.8	1.5
Rossbach	912	0.75	10.8	63.4	**7.0**
Shangoni	446	0.7	76.1	4.1	0.9
Soekmekaar	648	0.7	15.2	29.8	4.6

*- South African Weathers Services.

5.1.2. Aquifer response to recharge

Over 50 boreholes are currently installed with continuous groundwater level loggers within the study area as part of the Limpopo (DWA) regional office monitoring network. The available groundwater levels from these stations extend back to between 2005 and 2006. A summary of the short term water level data obtained from selected monitoring boreholes is presented in Table 5.3 and illustrated spatially in Figure 5.3.

Table 5.3. Summary of short term monitoring groundwater level data for selected stations.

Station	Start		Downloaded		WL Fluctuation#		
	Date	WL*	Date	WL*	Min*	Max*	Dh (m)
A6N0586	Mar-06	4.2	Aug-09	4.4	5.2	3.5	1.7
A7N0019	Jan-06	12.6	Aug-09	13.3	14.9	8.2	**6.7**
A7N0041	Jul-06	6.8	Aug-09	7.1	8.6	8.2	0.4
A7N0524	Oct-05	31.2	May-09	31.7	32.1	31.0	1.2
A7N0637	Jul-05	9.6	Aug-09	9.4	12.3	6.5	**5.8**
A9N0008	Sep-05	6.1	Aug-09	6.6	14.9	8.2	**6.7**
B8N0504	Sep-06	25.6	Aug-09	26.9	28.0	25.4	2.5
B8N0510	Sep-06	19.7	Aug-09	18.8	19.8	16.8	3.0
B8N0514	Mar-06	22.1	Aug-09	19.0	22.1	18.9	3.2
B8N0517	Mar-06	19.3	Aug-09	18.7	20.4	17.3	3.1
B8N0518	Mar-05	11.9	Aug-09	12.9	12.9	10.4	2.5
B8N0521	Oct-05	8.3	Aug-09	8.2	8.4	6.9	1.5

*- meters below ground level.
#- The largest amplitude of the groundwater level over the measurement period and the difference between them.

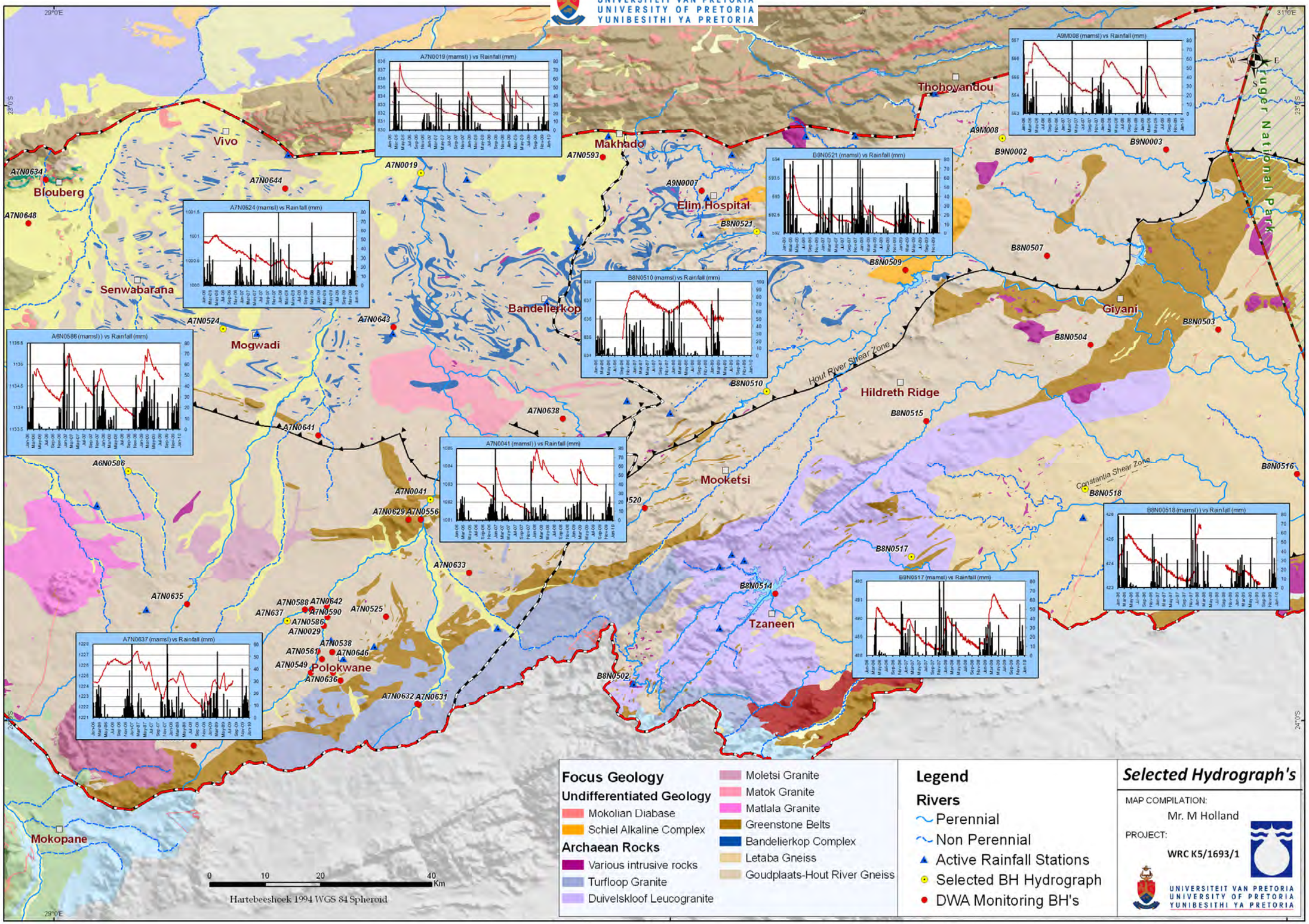

Figure 5.3. Spatial distribution of monitoring boreholes and selected water level hydrographs for the period Jan-06 to Dec-09 (A3 map) (red lines represent daily water levels while black columns represent monthly rainfall).

Generally, groundwater levels fluctuate according to the characteristics of precipitation events (i.e. amount, duration, and intensity) and various hydrogeological variables (i.e. topography, thickness of the unsaturated zone, and matrix composition of saturated and unsaturated materials) (Moon et al., 2004). Groundwater level fluctuations from the observed hydrographs vary between 0.4 and 6.7 m with a mean hydrostatic fluctuation of 3.2 m. Extreme fluctuations of more than 5 m may relate to anthropogenic influences on groundwater levels (i.e. A7N0524 is located near the Mogwadi (Dendron) irrigation groundwater control area).

An indication of the hydrostatic response trends were based on daily water level measurements together with daily rainfall data (Figure 5.3). For comparative purposes all hydrographs were based on a four year period (January 2006 to December 2009). The response of the aquifer to recharge displays well-identified seasonal water-level fluctuations. Therefore, it is expected that during the four year monitoring period, data permitting four distinct recharge periods should be observed. A typical natural hydrograph response for the study area is illustrated in Figure 5.4.

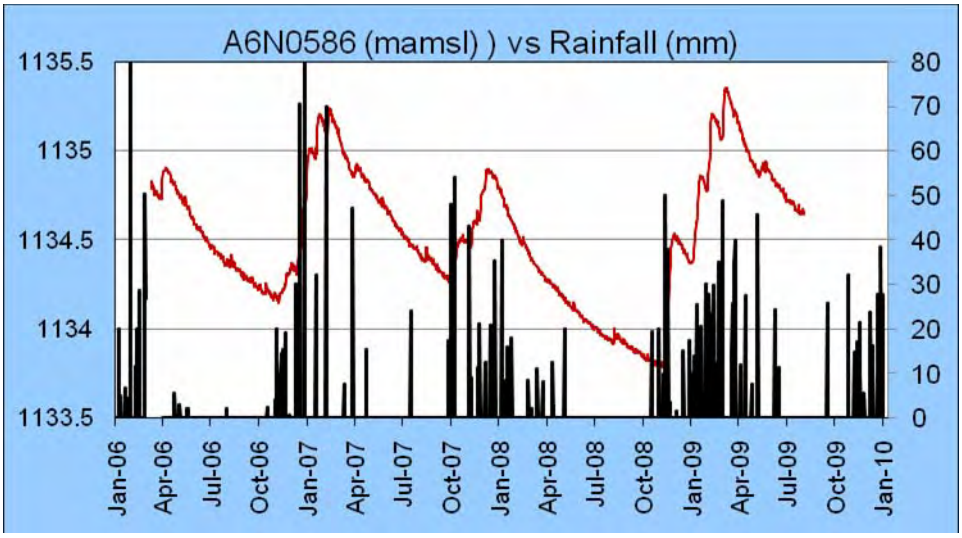

Figure 5.4. Hydrograph of monitoring station A6N0586 for the period (Jan-06 to Dec-09).

The Hydrological Year in South Africa is the period from 1 October to 30 September, as the lowest river and spring discharge (base flow) is typically observed at this time. The recession of the groundwater levels generally occurred during the second half of the Hydrological Year, i.e. from Apr/May to October. The following general observations are made:

- Maximum groundwater levels are mostly encountered during February or March.
- The period of groundwater recharge depends on the duration of the rainfall season.
- A three to four month lag is seen between the onset of the rainy season and peak water levels.
- Rapid increases in water levels are associated with extreme single rainfall events, while progressive increases are related to long periods of low intensity rainfall events.
    - During these significant rainfall periods (i.e. 2006/2007 season) groundwater levels increase to above the preceding year's level and the recession period is often reduced considerably.

- A typical exponential water level decline is observed after the rainy season.

- In contrast during below average rainfall periods the succeeding recession period may continue throughout the season with little or no recharge at all (i.e. Figure 5.5).
  - This is also evident in monitoring boreholes A7N0019, B80509 and B80518 (Figure 5.3) for the periods between Jan and March 2007.
- Where a strong relationship between rainfall and water level (aquifer) response exist active recharge occurs.

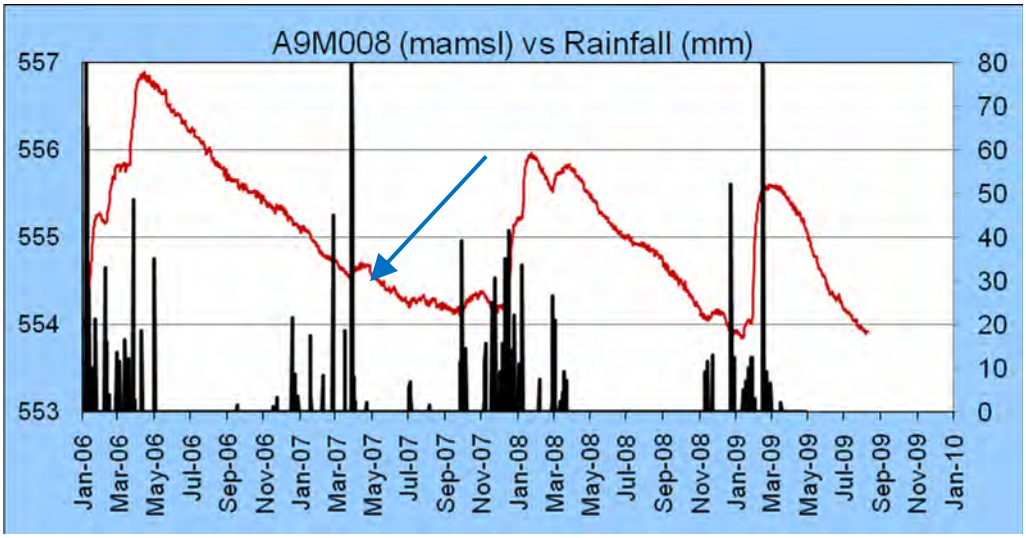

Figure 5.5. Hydrograph of monitoring station A9M008 for the period (Jan-06 to Dec-09).

Impact of rainfall variability on groundwater levels

The monthly groundwater level fluctuations for selected stations are presented together with the monthly rainfall data from the closest rainfall station in Appendix A. Only 12 monitoring stations cover periods of at least 20 years. Figure 5.6 illustrates monthly groundwater level data versus the annual rainfall departure from the MAP.

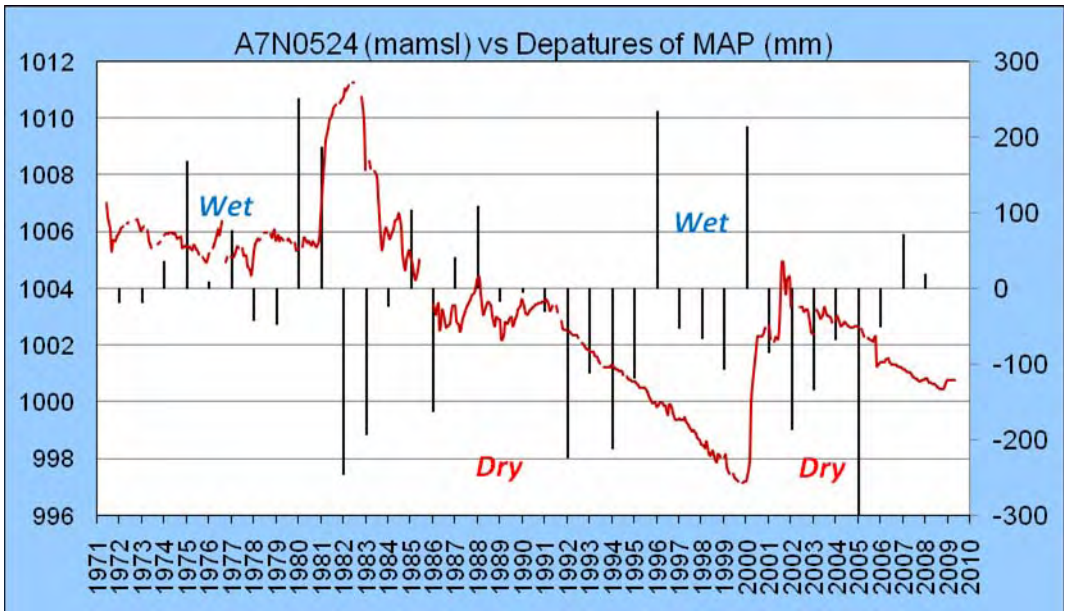

Figure 5.6. Hydrograph of long term monitoring station A7N0524 near Mogwadi (1971 to 2009).

According to Meyer (2005) major wet periods was experienced during 1971/72 to 1980/81 and again from 1993/94 to 2002/03, while a major dry period was experienced during 1982/1983 to 1992/1993. The wet and dry cycles have a major impact on groundwater recharge which can be easily distinguished from Figure 5.6.

The monitoring borehole is located approximately 3 km from the Mogwadi (Dendron) irrigation scheme. Jolly (1986) indicated an increase in groundwater abstraction for irrigation from 9 million m^3/a in 1968 to 21 million m^3/a in 1986 (no recent estimates are available). Although evidence of over-abstraction is aggravated by below average rainfall, the groundwater level declined by 6 m since the early 1970s. Groundwater levels declined steadily for a decade from 1990 to 2000, despite this being regarded as a wet period. According to Masiyandima (2009) certain management interventions were implemented in the 1990s which together with an above average rainfall for 2000 lead to a recovery of groundwater levels in 2001/2002. Continued decline of the groundwater level suggest that management interventions were not effective in controlling over abstraction. The groundwater level declines are also enhanced by a number of consecutive below average rainfall years and are also evident in monitoring station A7N0549 near Polokwane (Figure 5.7).

Figure 5.8 shows the large variability in rainfall over the last 100 years from the Polokwane rainfall station. There is a good relationship with major wet and dry cycles (11 and 18 years) identified by Meyer (2005) for southern Africa. The last decade can be regarded as the most years with below average rainfall for the entire 104 year record, which will definitely have an influence on groundwater recharge.

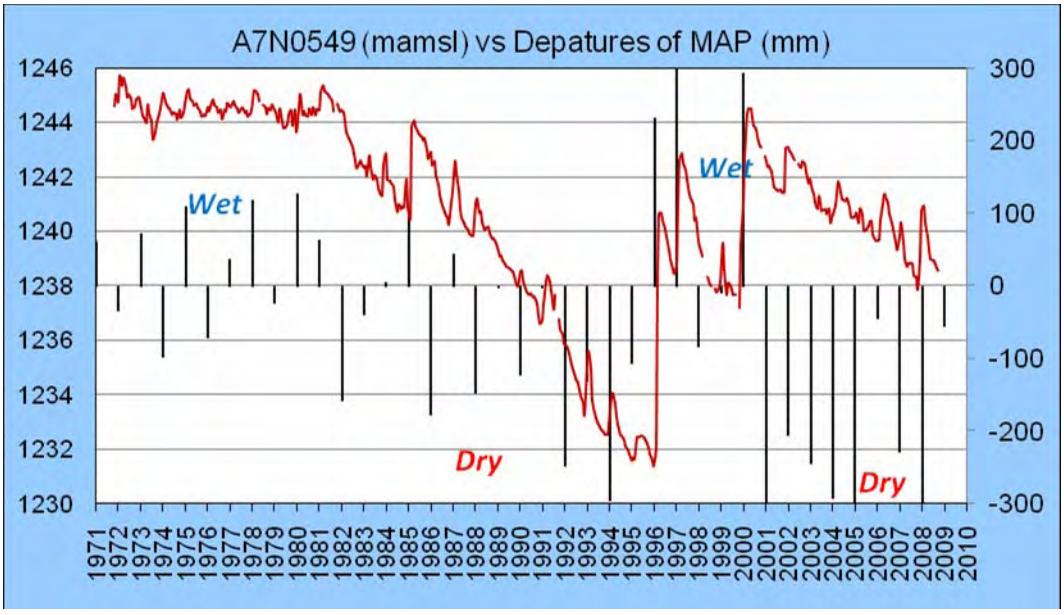

Figure 5.7. Hydrograph of long term monitoring station A7N0549 near Polokwane (1971 to 2009).

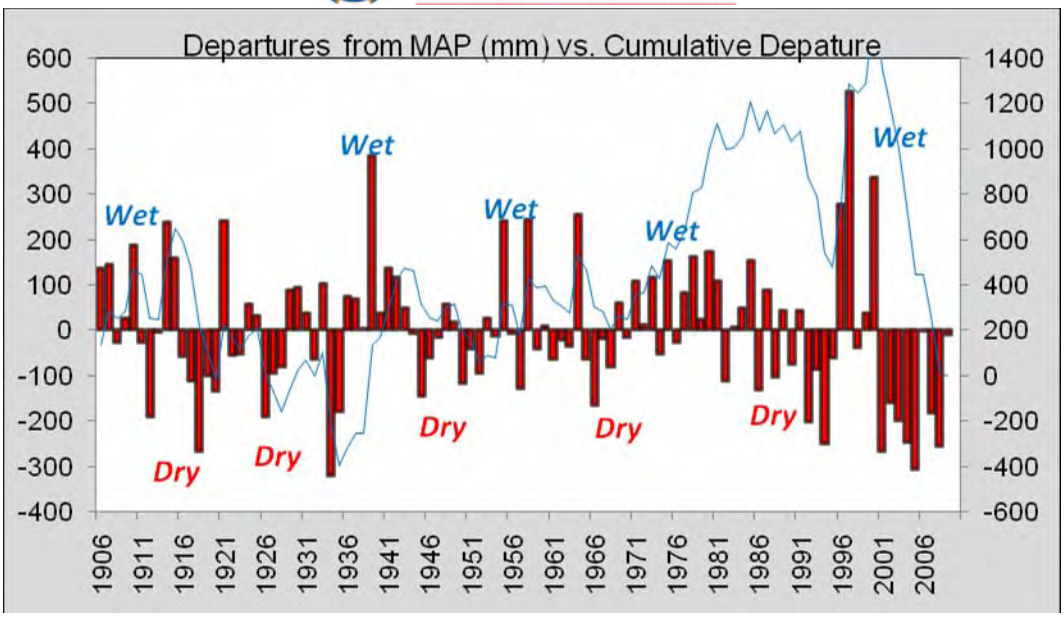

Figure 5.8. Annual deviation from the average rainfall, together with the cumulative departure for the 104-year rainfall record of Polokwane.

Cumulative rainfall departure (CRD)

The recharge excel spreadsheet (developed by Xu and Van Tonder, 2000) is used to simulate recharge for the selected monitoring stations within the study area. The results of the CRD simulations are shown in Appendix B and the recharge estimates obtained based on the results are shown in Table 5.4. Due to the limited period of monitoring the CRD recharge values differ in some cases considerably from the CMB estimates. The CMB method estimates recharge over an extensive period as opposed to the shorter term CRD simulation.

Table 5.4. Recharge estimations based on the CRD method.

Site	Station	Date		CRD Recharge	Area Km^2	CMB Recharge
		Start	*End*			
Polokwane	A7N0549	Dec-92	Oct-08	1.8 %	20	1.5 %
Thohoyandou	A9M009	Jan-06	Aug-09	2.3 %	12	1.9 %
Nwamitwa	B8N0517	Mar-06	Oct-09	1.7 %	25	2.5 %
Chloe	A6N0586	Mar-06	Aug-09	1.4 %	15	0.4 %
Mara	A7N0019	Mar-06	Aug-09	1.5 %	35	0.9 %
Rossbach	B8N0521	Jan-06	Aug-09	2.5 %	20	7 %

Groundwater Flow

Groundwater levels from approximately 360 boreholes were used to construct a groundwater contour map for two areas within the Limpopo Plateau and Letaba Lowveld (Figure 5.9). The potential correlation between the measured head (static water level) and topography (surface elevation) was investigated by cross-plotting the data for each dataset (Appendix C). A very good correlation between the measured head and topography is obvious (R^2 = 0.99.) The observed correlation is used to improve the interpolation of water levels in data-scarce environments (Bayesian interpolation). In general, the water table is a subdued reflection of the topography.

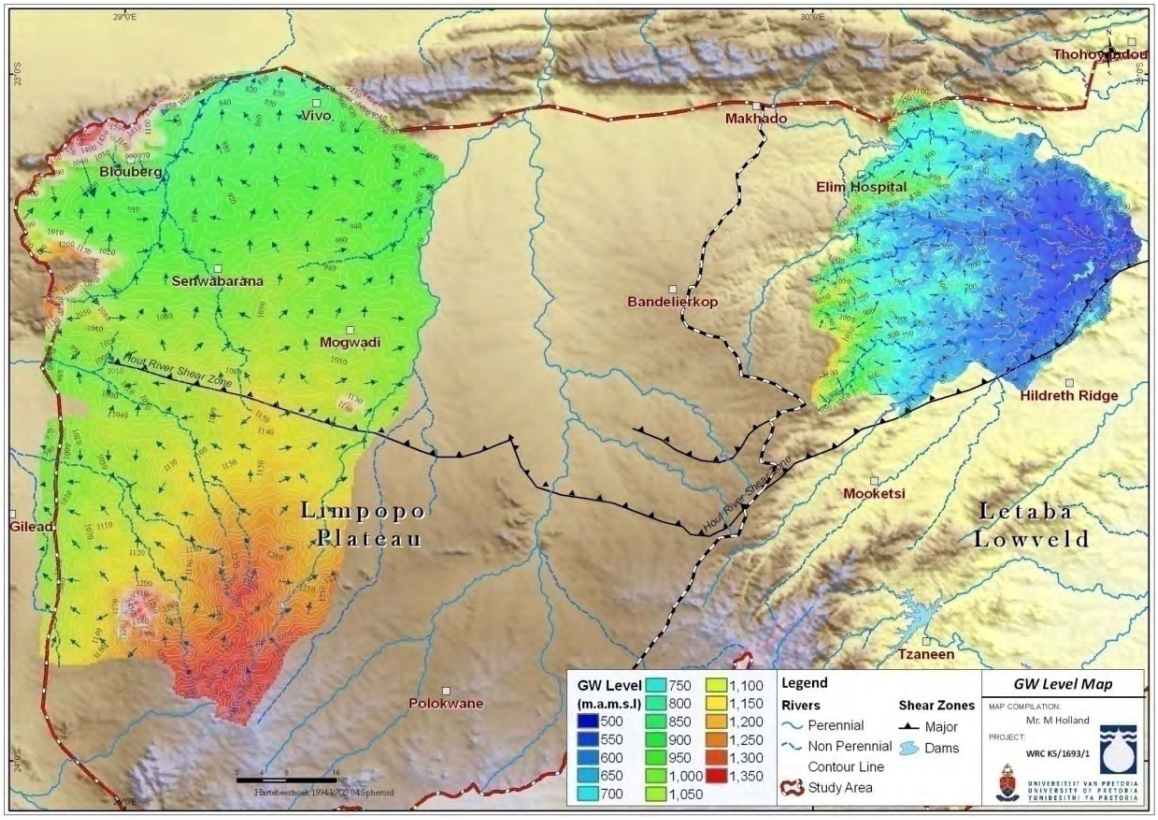

Figure 5.9. Groundwater contour map of two selected areas and derived flow vectors.

5.2. Geochemical description

To determine the spatial variation in the groundwater chemistry, a hierarchical cluster analysis (HCA) was applied to classify the large number of analysis into groups that are similar to each other but distinct from other groups (see section 3.3). The relationship of the statistically defined clusters of samples was then related to its geographic location.

5.2.1. Interpretation of results

Based on the visual assessment of the rescaled distance in the dendrogram, three distinct hydrochemical clusters were identified for each of the sub-areas (Limpopo Plateau and Letaba Lowveld) (Appendix D). A summary of the chemical data is presented in Table 5.5. The three groups of each sub-area represent trends between the main water types observed in the study area. In gross chemical terms, Group I and V samples are characterised by low mineralisation as indicated by the low electrical conductivity (EC) and a relative enrichment in bicarbonate, attributed to a fresh, recently recharged groundwater. Group II and IV samples show a general increase in mineralisation which is rich in bicarbonate with increasing sodium, potassium and EC concentrations, suggesting groundwater that is actively being mixed. Group III and VI are distinguished by significantly higher chloride, sodium and nitrate content and can be considered as relatively old groundwater at the end of chemical development.

Table 5.5. Mean values for the clusters distinguished by the hierarchical cluster analysis (EC in mS/m, all other in mg/l).

Parameter	Limpopo Plateau				Letaba Lowveld			
	Group I	*Group II*	*Group III*	*TOTAL*	*Group IV*	*Group V*	*Group VI*	*TOTAL*
Nr. of BH's	*235*	*364*	*208*	*807*	*333*	*196*	*364*	*893*
pH	8.1	8.2	8.2	8.2	8.1	8.0	8.1	8.1
EC	67.7	119.0	283.4*	146.4	73.8	41.4	196.8*	116.8
Na	75.3	119.6	301.0*	153.5	53.3	26.7	209.5*	111.1
Ca	33.2	54.2	119.5	64.9	42.6	28.9	83.7	56.4
Mg	25.5	50.5	108.8	58.2	41.1	17.6	80.8	52.1
K	5.0	12.5	14.6	10.8	3.9	1.6	5.5	4.0
HCO_3	309.0	399.4	469.5	391.2	346.3	195.7	519.0	383.7
SO_4	15.2	29.8	99.8	43.6	14.6	6.3	47.8	26.3
Cl	46.4	155.0	614.3*	241.7*	52.2	22.3	326.7*	157.5
NO_3	19.7	37.1	64.4*	39.1	20.0	6.9	58.4*	32.8
F	0.7	0.4	0.7	0.6	0.4	0.4	0.7	0.5
TDS	535.6	866.1	1802.3*	1011.2*	580.6	309.2	1342.5*	831.5
Dominant Facies	Na-HCO_3	Na-Mg-HCO_3	Na-Cl	-	Mg-HCO_3,	Ca-Mg-HCO_3	Na-Cl, Na-Mg-HCO_3	-

*- Within maximum allowable limits for drinking water in South Africa (SANS 2006).

As a result the dominant water types in Limpopo Plateau vary from a Na-HCO_3 to a Na-Mg-HCO_3 and Na-Cl groundwater facies and are explained as follows:

- The direct infiltration of Ca-HCO_3 dominated rainwater (Table 5.6) which evolved to a Na-HCO_3 facies due to the replacement of calcium by sodium through cation exchange in the aquifer matrix or alternatively due to the weathering of albite to kaolinite in the crystalline rocks, releasing sodium and bicarbonate.
- The Na-Cl facies is a result of prolonged residence and fluid-rock interaction times in the subsurface in areas of discharge (i.e. alluvium along rivers) or low recharge and also towards the foothills of the Blouberg Mountains (Figure 5.10).

Table 5.6. Chemical composition of rainfall within the study area (EC in mS/m, all other in mg/l).

Site	Mufeba (UP1)	Rawesi 2 (UP3)	Rawesi (UP3)	Rawesi 2 (UP3)	Bochum (UP2)
Date	03-Mar-09	09-Mar-09	15-Mar-09	15-Mar-09	15-Mar-09
pH	5.9	6.4	5.8	7.26	7.08
EC	0.84	4.18	0.45	5	3
Na	0.8	0.5	0.4	0.3	0.05
Ca	0.5	2.3	0.5	1.55	0.7
Mg	0.1	0.3	0.2	0.25	0.08
K	0.4	0.6	<0.1	0.81	0.2
HCO_3	6	24	6	19.2	12.12
SO_4	1.1	3.7	1.4	2.74	1.13
Cl	1	2.1	1	1.77	0.69
NO_3	0.3	0.9	1.2		
Facies	Na-Ca-HCO3	Ca-HCO3-SO4*	Ca-HCO3-SO4-Cl*	Ca-HCO3-SO4*	Ca-HCO3
EN %	-22	-52	-41	-52	-66

*- Bulk rainfall sample may be polluted.

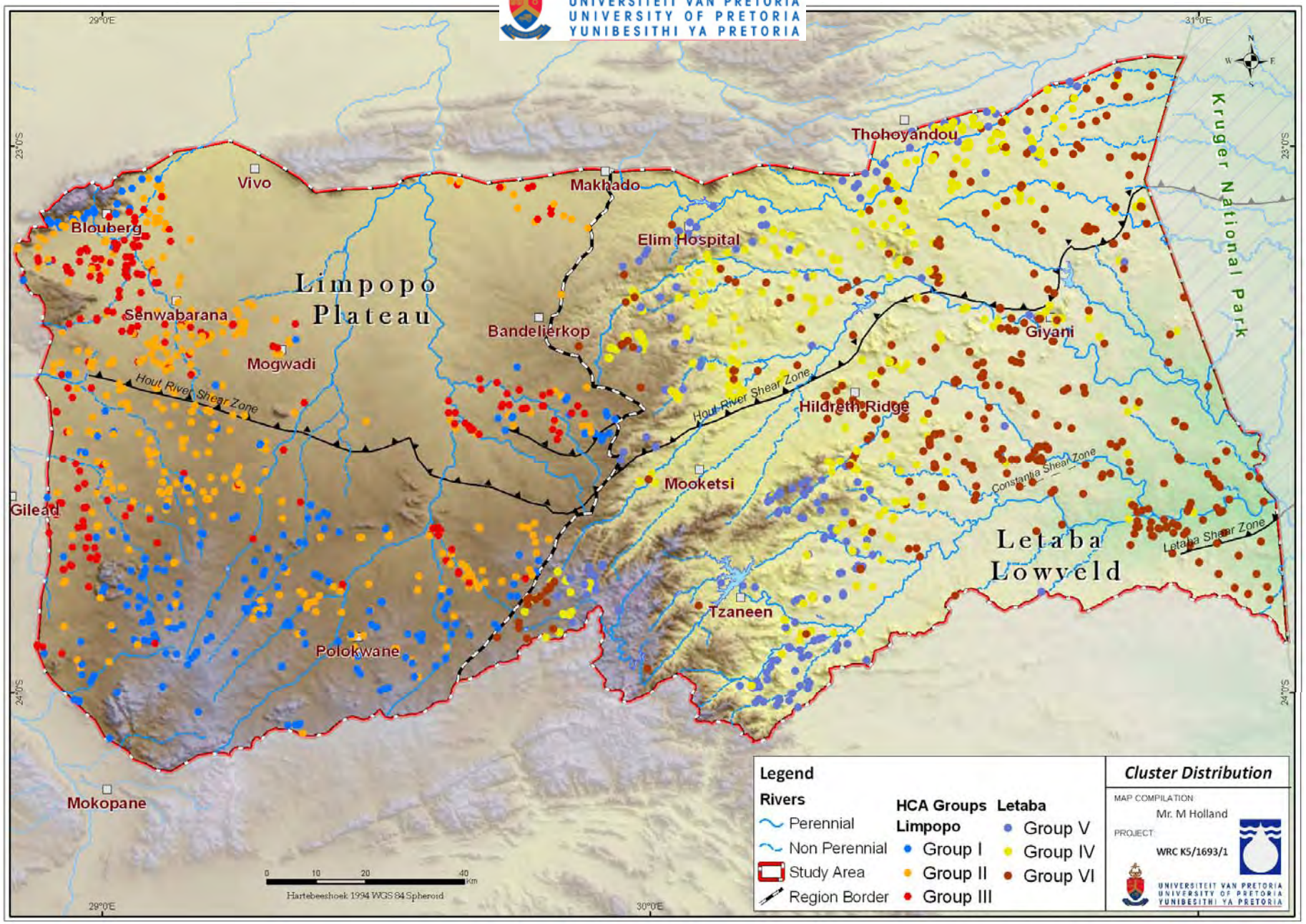

Figure 5.10. Spatial distribution of the hydrochemical groups identified by the HCA.

Groundwater in the Letaba Lowveld is generally a fresher Mg-HCO_3 facies (in comparison with the Limpopo Plateau), with a recognizable pattern of elevated mineralization with reduced precipitation/recharge. The dominant Mg-HCO_3 may be explained by the abundance of ferromagnesian minerals present within the rocks of the area, by ion exchange processes or the precipitation of calcite ($SI_{(calcite)}$ = 0.8). The water chemistry appears to evolve from a Ca-Mg-HCO_3 towards a Na-Cl predominance. The direction of this trend is consistent with increasing specific conductance and groundwater flow, (see Figure 5.9) which is generally related to the relative age and the length of the groundwater flow paths. The high degree of spatial and statistical coherence (Figure 5.10) supports the regional hydrochemical model, where changes in water chemistry are a result of increasing rock-water interactions along hydrological flow paths.

5.2.2. Discussion of stable isotope data

The isotopic ratios (δD and $\delta^{18}O$) of groundwater samples for each region within the study area are plotted in Figure 5.11, relative to the global meteoric water line (GMWL). A number of boreholes plot between the GMWL and a hypothetical local meteoric water line (LMWL) (including the single rainfall sample collected), suggesting that recharge seems to take place rapidly, possibly via preferred pathways in higher lying areas preventing any significant evaporation. Although not very distinct some samples are enriched in their heavy isotopic content due to significant kinetic (non-equilibrium) evaporation, suggesting evaporative losses of rainwater before infiltration. Thus, the recharge of partially evaporated water takes place in this area. There is also a distinct difference between groundwater samples observed between regions, clearly indicating the influence of more local rainfall regimes. Unfortunately not enough isotope rainfall data is available to reflect the particular rainfall selectivity between the four regions. The spatial setting of boreholes sampled for isotopes is presented in Figure 5.12.

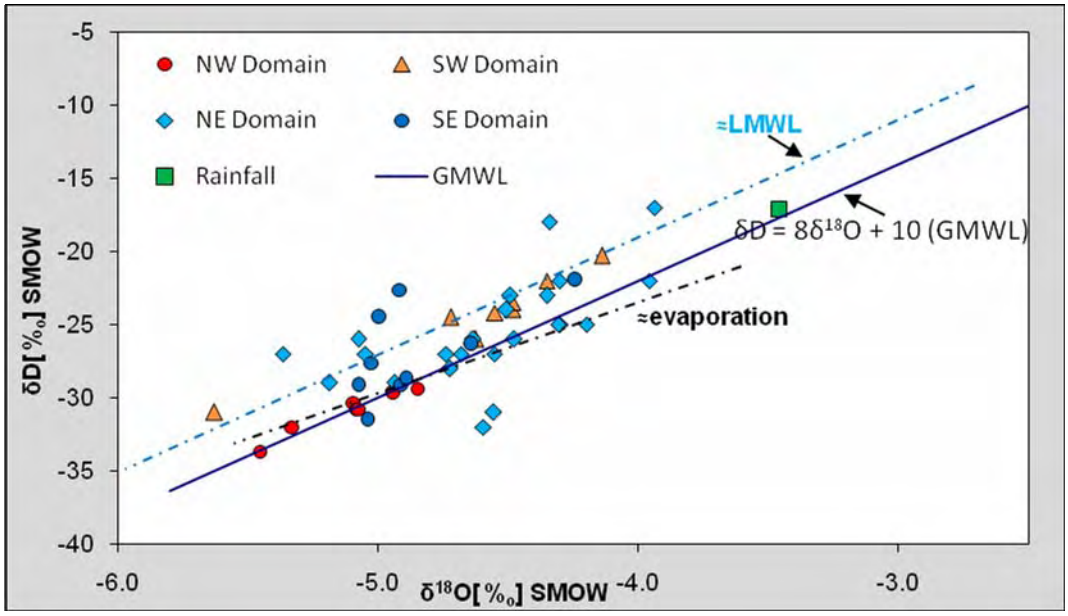

Figure 5.11. Groundwater and precipitation isotopic compositions, depicted with the GMWL.

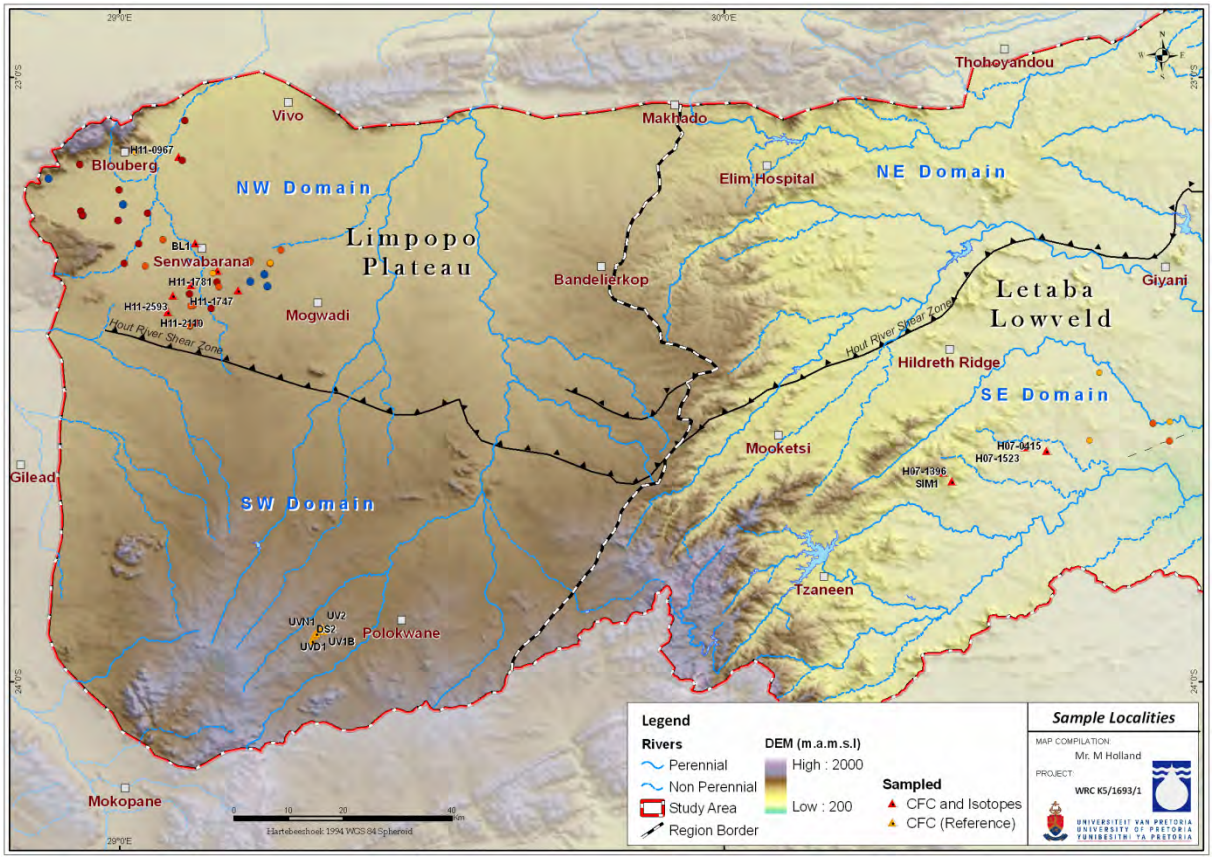

Figure 5.12. Location isotope groundwater samples.

5.2.3. Groundwater dating

Radiocarbon and tritium

The majority of ^{14}C samples plot between 85 and 95 pMC and the $\delta^{13}C$ between -5 and -7‰ (Figure 5.13). The ^{14}C content does not vary significantly and is consistent with that of very recent water that has only been slightly diluted with dissolved carbonate. Initial ^{14}C concentrations of 80 and 90% was suggested by Verhagen et al., 2009 for the Bochum (Senwabarwana) area and Talma and Weaver (2003) used an initial ^{14}C of 85-100% for the Leeukuil area 10 km west of Polokwane. One sample from Region D shows an increase in $\delta^{13}C$, evidence of ongoing isotope exchange or dilution processes with aquifer material, but the bulk of the samples Region B and D are within -9 and -12‰, which may be a reflection of the grassland vegetation in the area. Generally, these samples have ^{14}C values that have similar trends to the bulk of the samples, suggesting that there has been no major dilution of ^{14}C which affects relative ages or residence times.

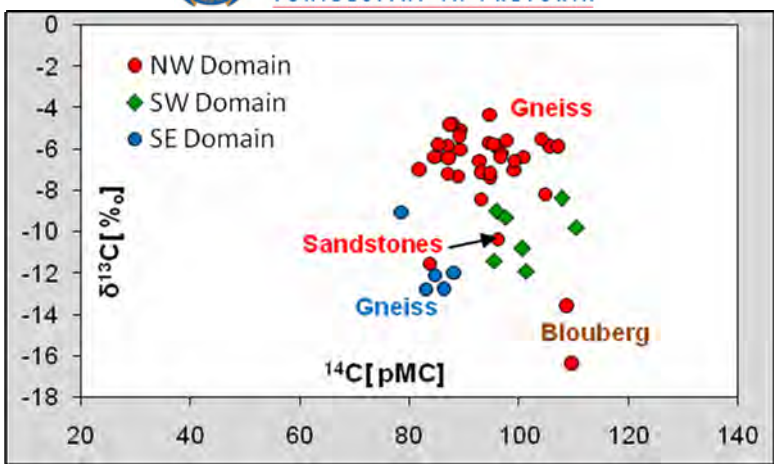

Figure 5.13. Scatter-plot of $\delta^{13}C$ and against ^{14}C for all samples.

A plot of ^{14}C against ^{3}H together with the inferred MRT values calculated by the exponential mixing model by Verhagen (2000) is shown on Figure 5.14. The ^{14}C values can be interpreted as ground water mean residence times ranging from a few decades up to about 1 000 years, implying fairly rapidly turned-over ground water.

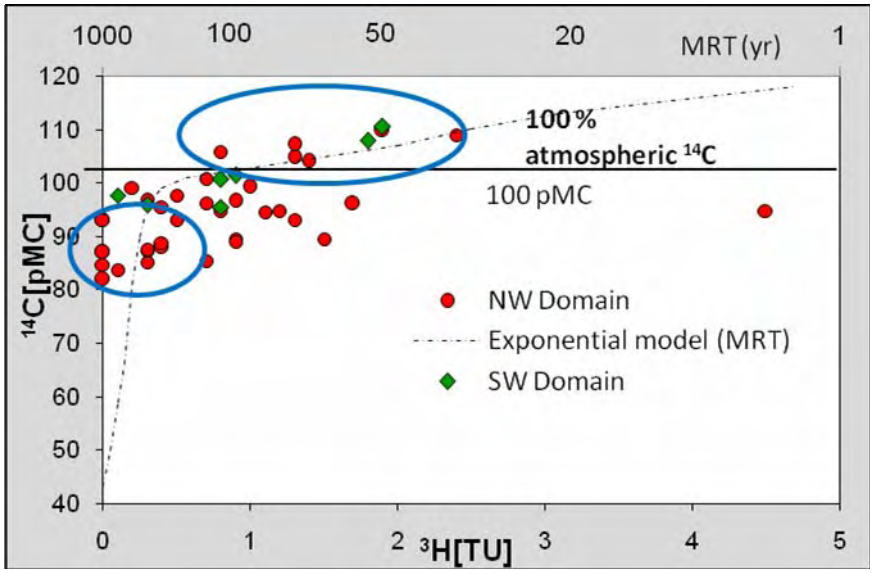

Figure 5.14. Scatter-plot of $\delta^{13}C$ and against ^{3}H. Also shown are plots of expected exponential model values for $\delta^{13}C$ and ^{3}H showing mean residence time (MRT) (Adapted from, Verhagen, 2000).

Groundwater radiocarbon values of > 100 pMC can be interpreted as falling in the thermonuclear era, i.e. recharged over the past three and a half decades. In this time-span, interpretations can be constrained further by tritium. Many radiocarbon values of > 100 pMC accompanied by tritium > 1TU may be ascribed to post-1963 (thermonuclear) recharge. Another group of samples with values of ^{14}C < 90 pMC and ^{3}H < 1 TU represent older water with an approximate mean residence time of between 500 and 1000 years. Tritium samples with no radiocarbon analysis proved futile

in determining ages of groundwater, since tritium values did not exceed 3 TU representing a mixture of old and recent water (pre- and post bomb testing) (Figure 5.15).

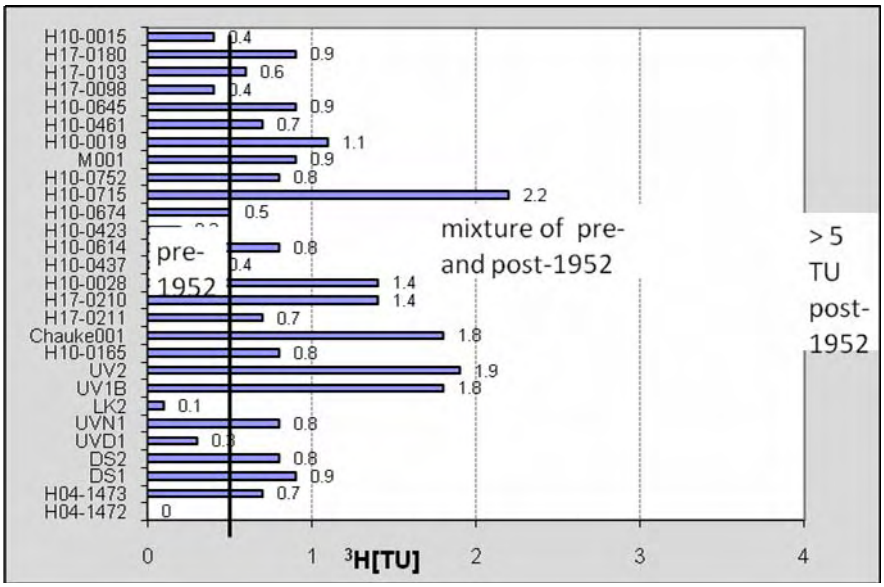

Figure 5.15. Results of tritium.

Chlorofluorocarbons

It is important to note that only a limited number of CFC samples could be taken and results should be seen as the basis for future CFC applications in the Limpopo basement aquifers. Table 5.7 shows the concentrations of CFCs, SF_6 and selected chemical parameters found in each of the boreholes. Samples for this investigation were collected from boreholes in the NW and SE domain within quaternary catchment A72A and B81F respectively (Figure 5.16).

Table 5.7. Chemical composition of rainfall within the study area.

Region	Site	CFC-12 (pmol/l)	CFC-11 (pmol/l)	SF_6 (fmol/l)	Cl (mg/l)	NO_3 (mg/l)	Elevation (mamsl)	Air Temp*
NW Domain	H11-0967	0.93	1.33	0.69	140	51.6	893	19.5
	BL1	0.51	1.23	0.98	239	43	975	19.5
	H11-1781	0	0.06	***3.57***	243	12.9	1018	19.5
	H11-1535	1.43	0.26	0.82	188	47.3	1023	19.5
	H11-2593	0.39	0.56	1.02	242	26.2	1045	19.5
	H11-1747	0.13	0.09	0.1	185	18.1	1060	19.5
	H11-2110	0.2	0.14	0.29	224	21.9	1060	19.5
SW Domain	UV2#	0.3	0.15	-	67	28.4	1320	18.5
	UVN1#	0.07	0.03	-	28	16.8	1321	18.5
	UVD1#	0.07	0.01	-	28	3.9	1325	18.5
	UV1B#	0.62	0.3	-	50	18.1	1331	18.5
	DS2#	0.3	0.1	-	26	10.8	1338	18.5
	LK2#	0.26	0.13	-	62	21.9	1340	18.5
	DS1#	0.27	0.14	-	23	52.5	1386	18.5
SE Domain	H07-0415	0.14	0.3	0.1	228	43	492	20.5
	H07-1523	0.01	0.45	0.25	169	275.2	521	20.5
	H07-1396	0.64	0.21	0.1	33	0.9	700	20.5

	SIM1	1.18	1.59	1.28	12	6.9	840	20.5

[#] - Samples captured from Talma and Weaver (2003).

*- Mean annual temperature of recharge location.

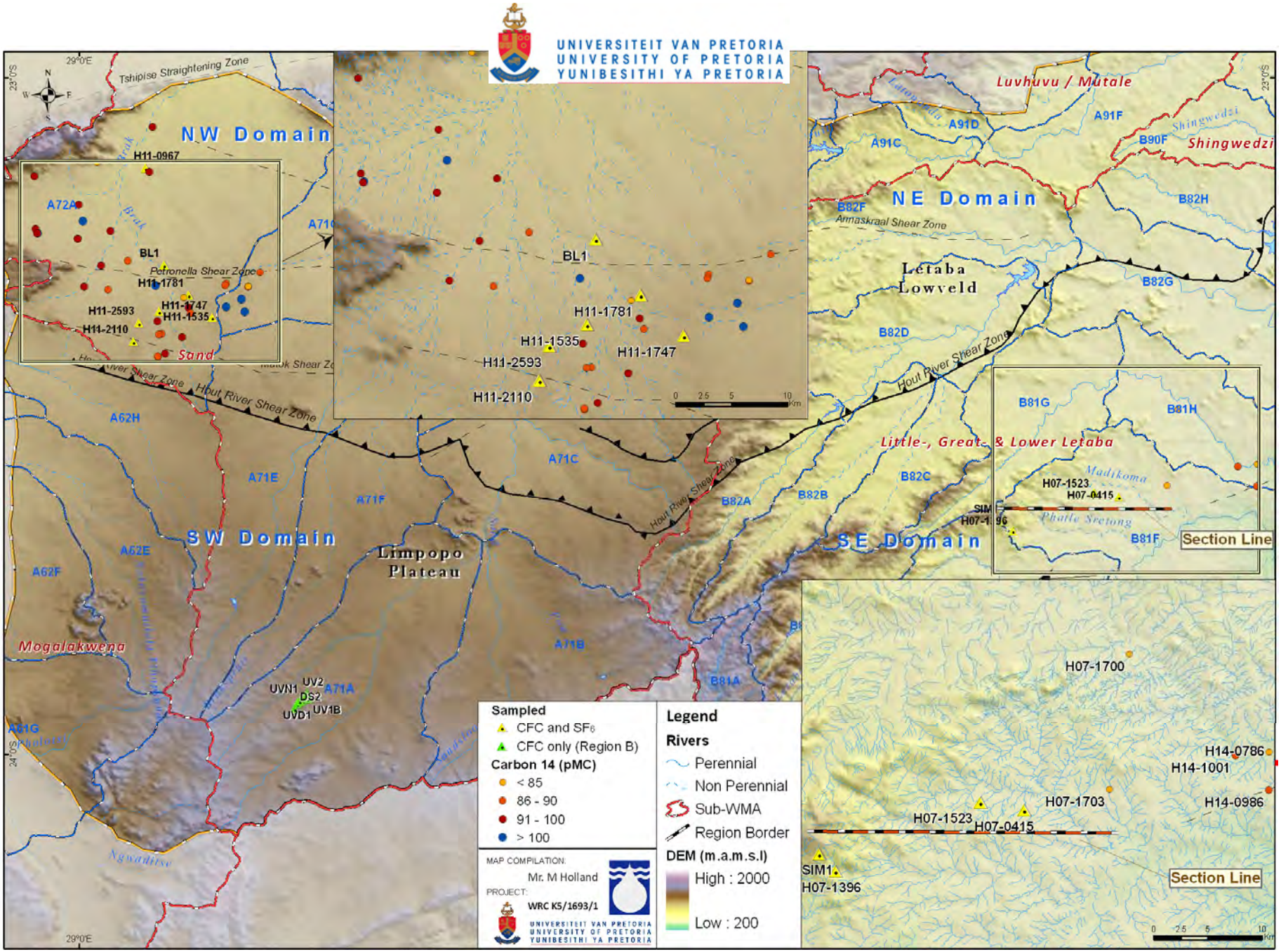

Figure 5.16. Spatial distribution of CFC samples together with carbon 14 samples.

Modern air saturated water at 10ºC is calculated to have a concentration of 2.97 pmol/L for CFC-12, 5.40 pmol/L for CFC-11 and 2.3 fmol/L for SF_6 (IAEA, 2006). All groundwater samples fit within these guidelines except sample H11-1781 with a SF_6 concentration above modern atmospheric concentrations, suggesting a sampling or analysis error, or some natural or anthropogenic addition of SF_6. Theoretical variations in the concentrations of CFC-11 and CFC-12 were constructed using cases of piston flow and binary mixing (Figure 5.17).

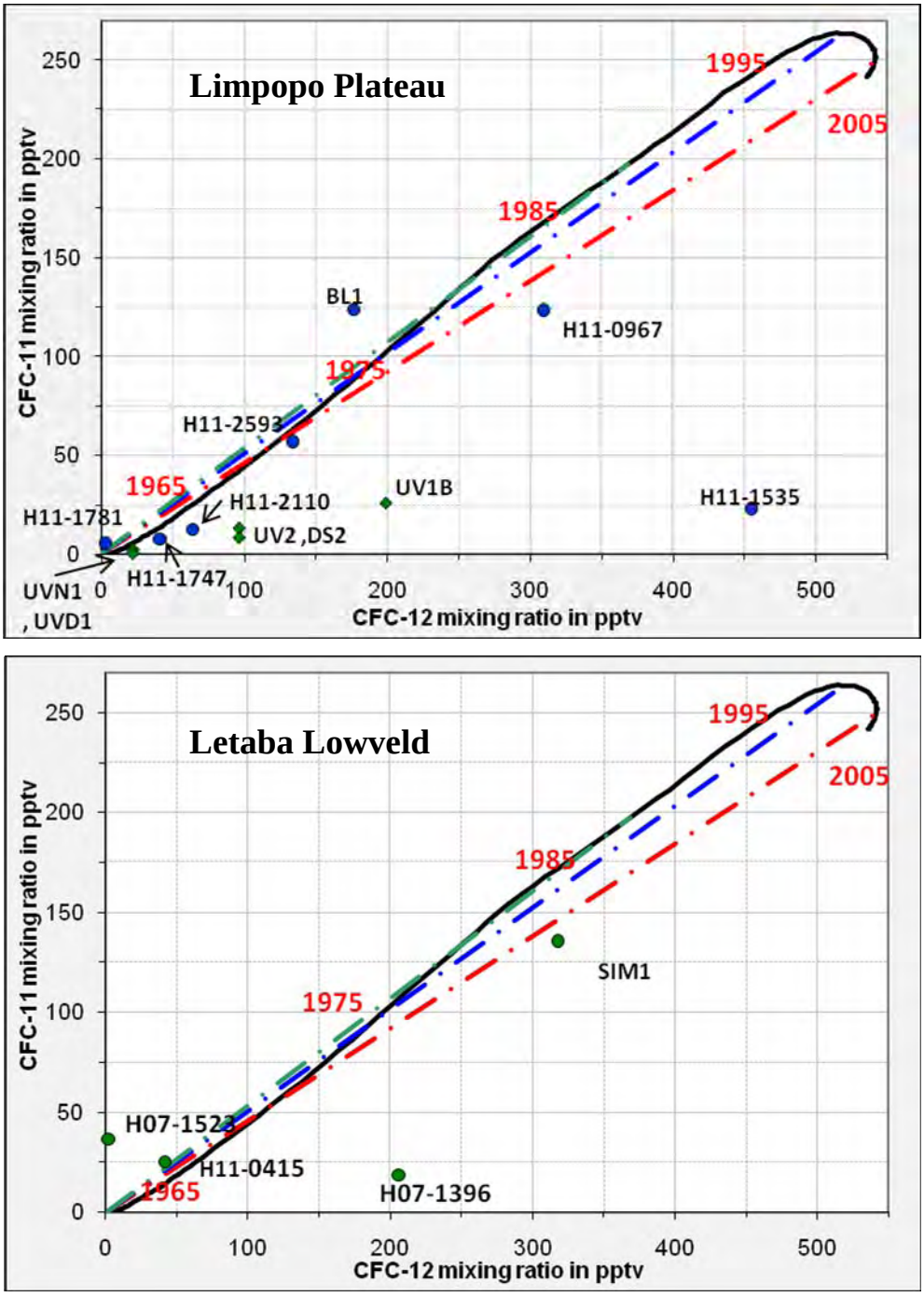

Figure 5.17. Tracer plots comparing CFC-11 and CFC-12 concentrations for southern hemisphere air. The solid lines represent unmixed (piston) flow with selected apparent ages ('1985'). The dashed line shows one example of binary mixing for the case of water recharged in 1985, 1995 and 2005 diluted with old, CFC-free water.

The region bounded by the CFC input function (solid line) and the mixing line represents the range of CFC-11 and CFC-12 concentrations that can be expected in waters if air–water equilibrium and mixing with old, CFC-free water account for the observed variations in CFC concentrations. Samples plotting outside the region bounded by piston flow and binary mixing (see, for example, H07-1396, H11-1535 and UVB1) have been affected by other processes such as contamination, degradation or an introduction of excess air that have altered the CFC concentrations from air–water equilibrium values. These lower CFC-11/CFC-12 ratios are most likely due to degradation of CFC-11 and have been observed in some studies (i.e. Bockgård et al., 2004). CFC-11 and CFC-12 have similar input data curves which doesn't allow for differentiation between exponential binary and piston flow. In contrast, Figure 5.18 shows SF_6 versus CFC-12 plot for the Limpopo Plateau samples.

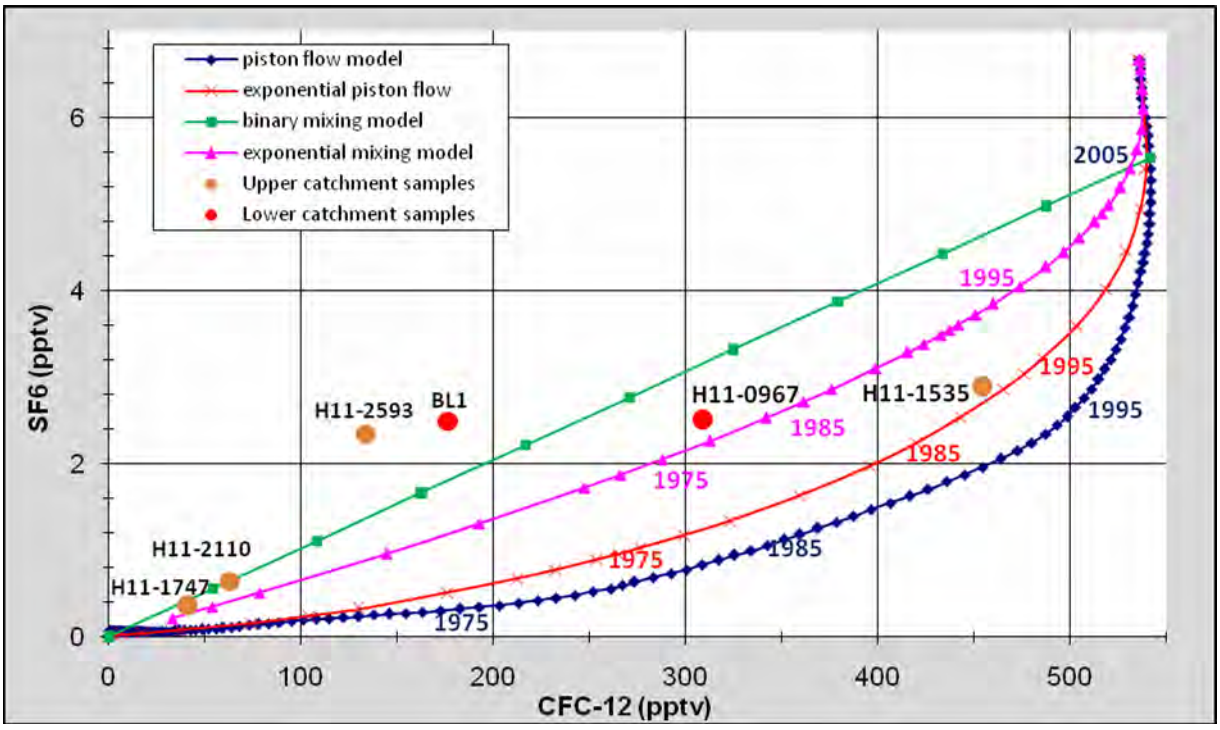

Figure 5.18. CFC-12 and SF6 groundwater data overlaid on the ideal mixing model curves. Samples categorised as upper or lower catchment (quaternary drainage A72A) (Figure 5.16).

A number of samples plot outside the region bounded by piston flow and binary mixing (2002 to pre-CFC) (see, for example, H11-2593, BL1) and may have been affected by SF_6 contamination. All other samples plot within the region bounded by the binary mixing model and piston flow model. The boreholes that were sampled are essentially in the upper Brak River catchment (A72A) with two samples in the middle and lower parts of the catchment (BL1 and H11-0967). The youngest sample H11-1535 (apparent age of 20 years, 1990) is located up gradient of these samples. It is expected that the upper catchment represent younger water related to more recent recharge events. From previous discussions it seems that this sample may have been contaminated by CFC-12 (see, Figure 5.17). However, a number of samples (H11-2110 and H11-1747) in the upper catchment consist of apparent ages of 45 to 50 years and plot between the BMM and EMM curve. Despite the high SF_6/CFC-12 ratio in samples H11-2593 and BL1, these boreholes are

down gradient from each other and have an apparent age of 35 and 40 years. The sample (H11-0967) in the lower catchment plot close to the EMM curve and have an apparent age of 30 years (1980).

Based on the results the direction of inferred flow lines based on the groundwater gradient (see section, 5.1.2) does not coincide with the direction of increasing water age. Samples from quaternary drainage A72A present a complex chemical model with highly mineralised water, with no clear flow regime suggesting a highly heterogeneous system with a number of likely flow paths (i.e. recent recharge from fractures exposed to the surface or high lying areas; old groundwater from river losses or diffuse flow). This is clearly illustrated in a correlation plot of apparent age vs. elevation in Figure 5.19 where high lying areas does not necessarily relate to younger age. In contrast CFC samples from the south-eastern domain (quaternary drainage B81F) indicate that younger waters are related to higher lying areas while older sample are related to lower lying areas (Figure 5.19). It must be highlighted that these samples do not relate to an identified flow path but rather indicate the variations observed between the higher and lower lying samples.

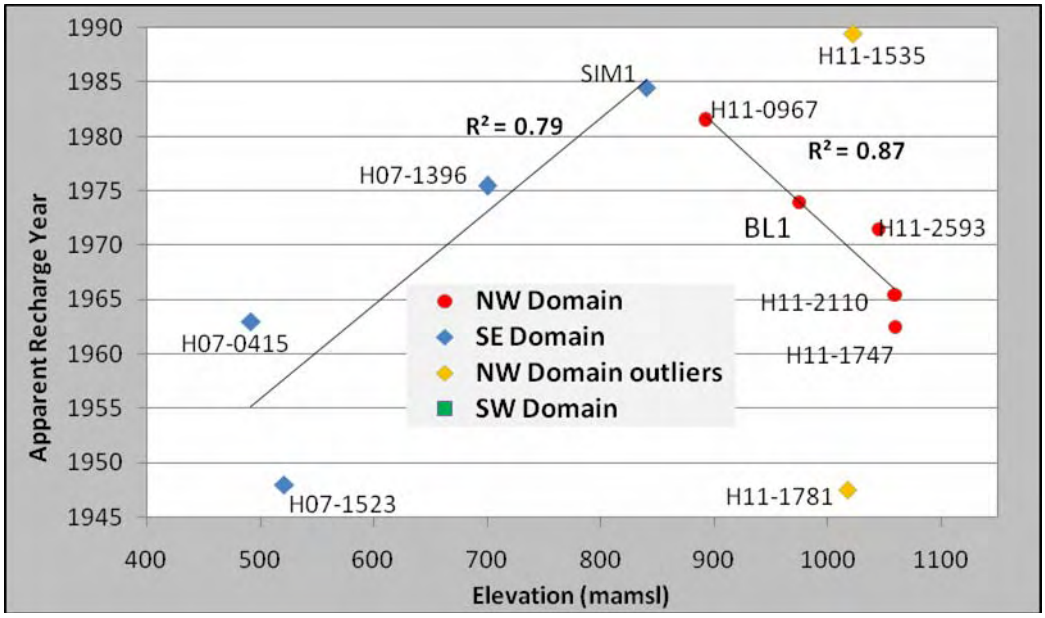

Figure 5.19. CFC-12 and SF6 groundwater data overlaid on the ideal mixing model curves. Selected sites have been labelled

Generally samples representing the upper catchment (SIM1 and H07-1396) lie close to the exponential piston- and piston flow models (Figure 5.20). These samples are located on the Tzaneen escarpment with an apparent age of 25 years (1985) and 35 years (1975) respectively. In the low reaches of the catchment sample H07-0415 is much older with an apparent age of 45 years (1965), while sample H11-1523 has a CFC-12 concentration below detection limit and is therefore pre-CFC age. These samples may indicate exponential mixing suggesting mixing between the old groundwater and modern water from recent recharge.

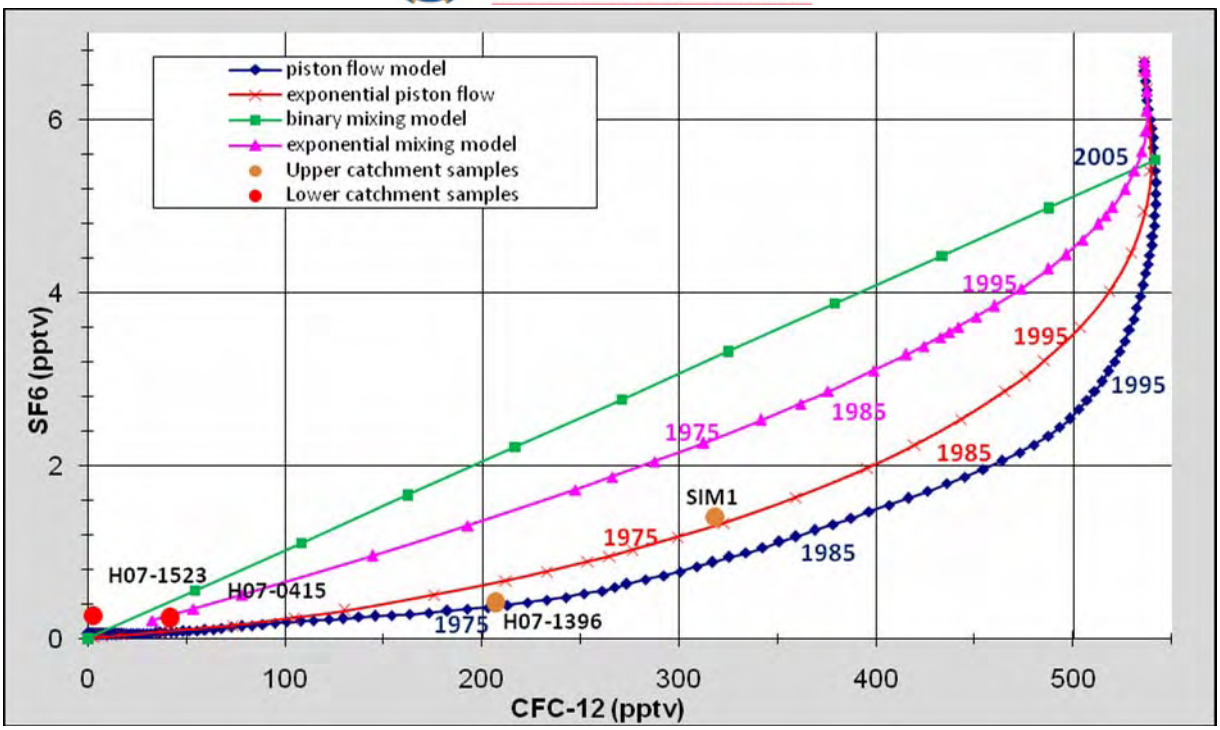

Figure 5.20. CFC-12 and SF6 groundwater data overlaid on the ideal mixing model curves. Selected sites have been labelled.

Ideally flow paths should have been identified and sampled; however, in this case the sparse distribution of samples allows us only to infer a regional concept of groundwater flow regimes from the higher to lower lying areas (Figure 5.21). The model suggest that deeper groundwater, recharged from higher lying unconfined conditions (i.e. Tzaneen escarpment) moves down gradient from under (semi-)confined conditions towards low lying discharge areas. Loosing ephemeral rivers may lose evaporative younger water to the older groundwater system in the area, especially along drainages incised into the basement rock with a thin or absent alluvium and/or regolith layer.

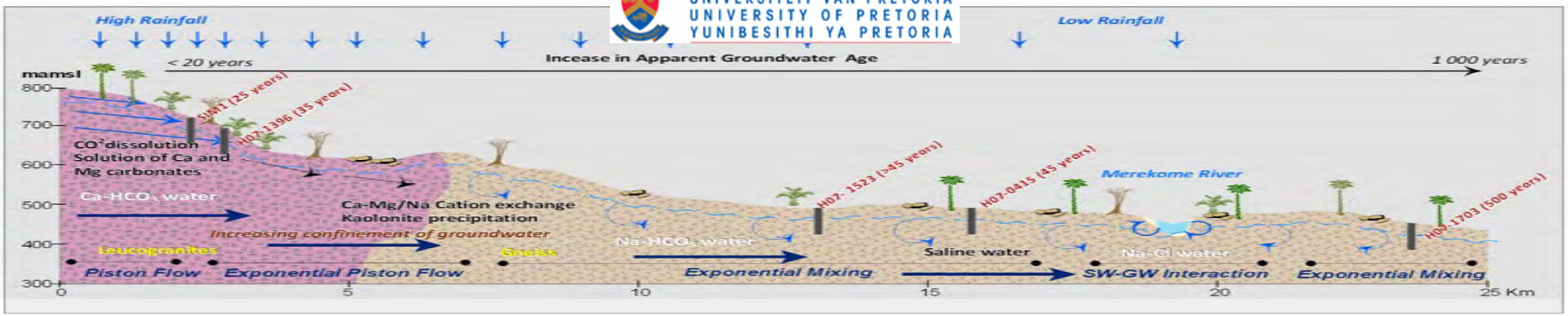

Figure 5.21. Cross-section of the hypothetical hydrochemical model for the Merokome River catchment (B81F) (Section line illustrated in Figure 5.16). Based on the CFC and carbon 14 results.

5.2.4. Groundwater quality hazards

Table 5.8 presents the overall drinking guideline classification of the major ion chemistry of the Limpopo Plateau and Letaba Lowveld basement aquifer region under investigation. Results show that many rural groundwater supplies exceed the acceptable limits for drinking water.

Table 5.8. Potability classification of the area of investigation (EC in mS/m, all other in mg/l).

SANS 241:2006	EC	Ca	Mg	Na	K	SO_4	Cl	NO_3 as N	F	TDS
Class I Rec. operational Limit	< 150	< 150	< 70	< 200	< 50	< 400	< 200	< 10	< 1	
Class II Max. allowable limited	150-370	150-300	70-100	200-400	50-100	400-600	200-600	10-20	1-1.5	
Exceeding Class II (Consumption period)	7 years								1 year	
Limpopo Plateau										
	EC	**Ca**	**Mg**	**Na**	**K**	**SO_4**	**Cl**	**NO_3 as N**	**F**	**TDS**
Class I	70%	94%	75%	85%	99%	99%	73%	54%	87%	96%
Class II	26%	4%	15%	11%	1%	0%	20%	27%	5%	0%
> Class II	4%	2%	9%	4%	0%	1%	6%	19%	8%	4%
Letaba Lowveld										
	EC	**Ca**	**Mg**	**Na**	**K**	**SO_4**	**Cl**	**NO_3 as N**	**F**	**TDS**
Class I	75%	95%	72%	87%	100%	99%	78%	53%	88%	95%
Class II	19%	3%	12%	8%	0%	0%	14%	14%	4%	0%
> Class II	6%	2%	16%	6%	0%	1%	8%	33%	8%	5%

The most noticeable elements of concern for water consumption are nitrate (measured as nitrogen (N)) and fluoride. In addition, several samples show major ion concentrations (i.e. Mg, Na, Cl) and subsequently electric conductivities beyond acceptable limits. This can mostly be related to evaporative concentration of elements in discharge areas or due to low recharge values as well as long residence times for selected samples. According to Marais (1999), the single most important reason for groundwater sources in South Africa being declared unfit for drinking is nitrate levels exceeding 10 mg/l (as N). The main inputs of nitrate to groundwater in rural environments are derived from anthropogenic activities such as inappropriate on-site sanitation and wastewater treatment, improper sewage sludge, drying and disposal, and livestock concentration at watering points near boreholes. The extensive occurrence of nitrate in groundwater in uninhabited regions (see Appendix E) suggest non-anthropogenic sources possibly related to evaporative enrichment of dry and wet deposition, biogenic point sources through N-fixing organisms, or to a geogenic origin (Tredoux and Talma, 2006). In contrast to nitrate, the occurrence of fluoride is primarily

controlled by geology and climate. Therefore, there are no preventative measures under the given spatial limits of water supply to avoid contamination.

Heterotrophic bacterial counts are used to indicate the general microbiological quality of water, i.e. the amount of bacteria present in the water. The total coliform bacteria count, which includes bacteria from the faecal group, is an indicator of the general sanitary quality of the groundwater, with many of these bacterial colonies originating potentially from an aquatic environment. The total faecal coliform bacteria count, which is related to human or animal faecal pollution, refers to probable faecal pollution of water. The presence of coliform bacteria implies the potential presence of waterborne pathogens (DWAF, 1996). According to the Department of Water Affairs' water quality guidelines (DWAF, 1996) for domestic use, the total heterotrophic bacterial plate count of all groundwater samples from both areas indicates a slight or increased risk of bacterial infection and infectious disease transmission. Fourteen groundwater samples show a significantly increased risk for infectious disease transmission according to the total coliform bacterial range and two samples indicates a significant risk for faecal coliform and e.coli (Table 5.9).

Table 5.9. Microbiological analyses for all samples collected.

Allowable compliance contribution (DWAF, 1996)*				
95% min.	*100*	*Not detected*	*Not detected*	*Not detected*
4% min.	*1 000*	*10*	*1*	*Not detected*
1% min.	*10 000*	*100*	*10*	*1*
Sample	**Heterotrophic *count/ml***	**Total Coliform *count/100ml***	**Faecal Coliforms *count/100ml***	**E.Coli *count/100ml***
Nr of Samples	51	19	10	10
Compliance 4% min.	45	4	5	5
Compliance 1% min.	11	14	2	2

* The allowable compliance contribution shall be at least 95% to the limits indicated with a maximum of 4% and 1% respectively.

5.3. Pumping test analysis

5.3.1. Aquifer response classification

Due to the intrinsic difficulty in identifying an appropriate theoretical model that fits the observed pumping test data, a classification scheme based on the typical drawdown behaviours encountered in the study area was identified. The observed datasets (2 359 boreholes) were visually compared to a set of typical diagnostic plots as discussed in section 3.4.2 in order to identify which model can be used to best interpret the data. The schematic diagnostic plots of the typical drawdown behaviours identified for the study area basement lithologies are conceptualised in Table 5.10.

Table 5.10. Most typical diagnostic plots encountered in the Basement aquifers under investigation.

TYPE 1: Theis model (infinite two-dimensional confined aquifer) – Approximate straight line type **387** boreholes (16 % of all BH's)	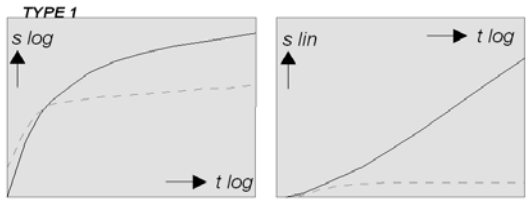
TYPE 2: Double porosity or unconfined porous aquifer – approximate S-type **568** boreholes (24 % of all BH's) (80 % have distinct double porosity dip)	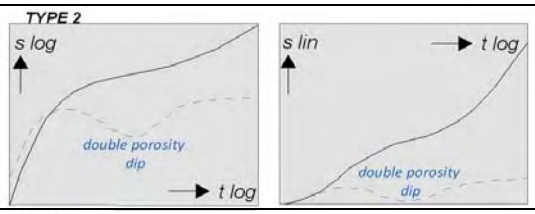
Variation 2: Fracture dewatering - Stepwise drawdown **514** boreholes (22 % of all BH's) (87 % have distinct double porosity dip) (54 % suggest dewatering of fractures)	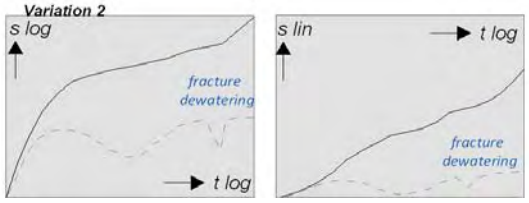
TYPE 3: Constant-head or leaky aquifer – Drawdown stabilizes May also represent too low pumping rates or too short duration to stress the aquifer **569** boreholes (24 % of all BH's)	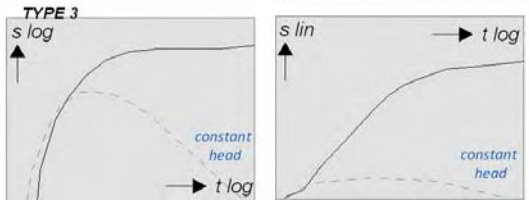
TYPE 4: Single fracture or general radial flow (GRF) model – Steepening of drawdown response **106** boreholes (4% of all BH's)	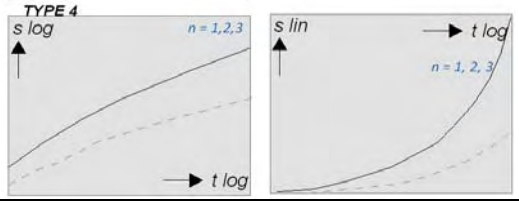
TYPE 5: Porous aquifer with limited extent (closed reservoir) Boundary conditions is distinct in this group but may be observed in all of the above **215** boreholes (9% of all BH's)	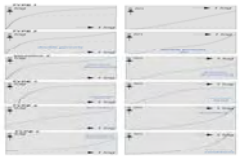

Type 1, Variation 2 and Type 3 drawdown curve categories have typically above average transmissivity and recommended yields, type curves provide the most Type 5 have below average recommended yields in line with increased drawdowns observed during testing (Table 5.11). These low yielding boreholes have low transmissivities and the lowest potential in terms of bulk water supply. The relatively high average drawdown achieved for Type 3 curves in comparison with the population average indicates that near steady state conditions were reached in most cases. Accordingly, the low drawdown averages of Type 1 curves may indicate that in most cases unsteady state conditions prevailed (typical Theis type-curve) at the end of the test. Variation 2 which represent distinct fracture dewatering curves has the highest constant rate averages and be regarded as the most productive aquifer types.

Table 5.11. Summary of selected hydrogeological parameters for the different drawdown behaviours.

Class	Nr. of BH's	Rec. Yield ℓ/s per day	Transmissivity m^2/d	Constant Rate ℓ/s per day	Drawdown during test
TYPE 1	387	1.2	34.7	4.8	17.6
TYPE 2	568	0.9	24.1	3.4	21.7
Variation 2	514	1.4	35.1	5.5	18.8
TYPE 3	569	1.2	31.2	4.4	23.8
TYPE 4	106	1.0	36.8	4.8	18.9
TYPE 5	215	0.4	12.5	2.1	30.2
All	**2359**	**1.1**	**29.4**	**4.3**	**20.4**

TYPE 1 (Theis)

These refer to an ideal confined, unconsolidated, homogeneous and isotropic aquifer. These assumptions are hardly applicable to basement (fractured) rock aquifers unless a dense network of interconnected fractures intersects the rock and builds a continuum comparable to a porous aquifer. A series of borehole drawdown behaviours can be matched with a typical Theis-curve (unsteady-state) equation (Figure 5.22). Early time behaviour is characterised by linear flow with a slope of 0.5 and may be indicative of fracture flow. Late times the derivative stabilises indicating infinite acting radial flow. The start of radial flow indicates the time at which the fractured reservoir behaves as homogenous.

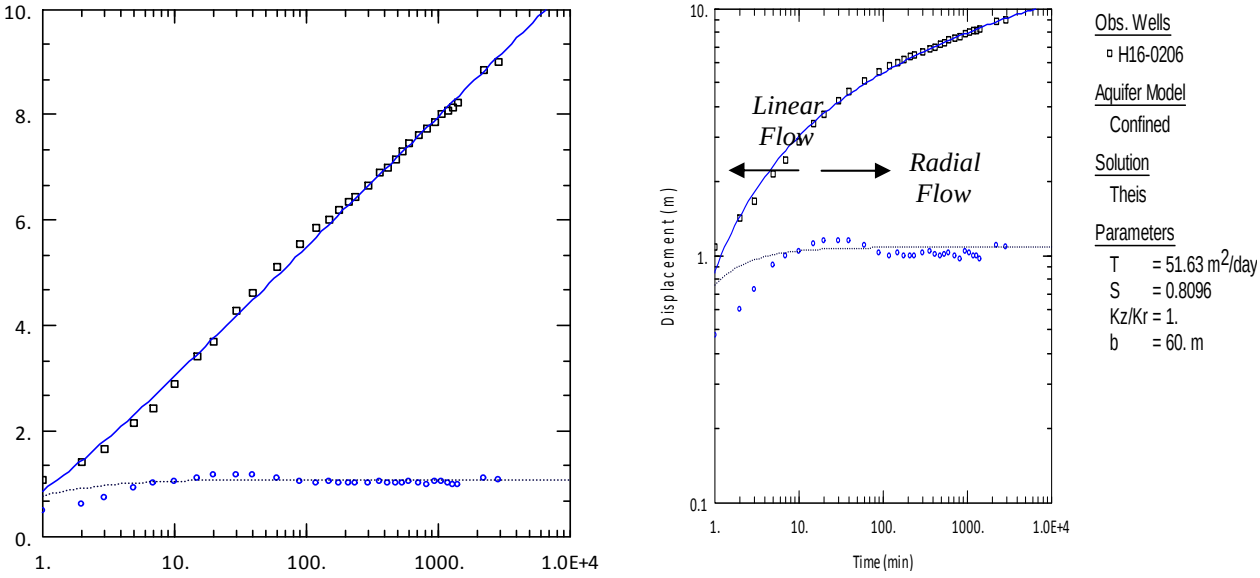

Figure 5.22. Diagnostic plots (semi- log, log-log and derivative) of a 48 hour constant rate pumping test fitted with a Theis solution (borehole H16-0206).

The shape of the recovery-curve may provide valuable additional information in cases where the drawdown-curve was disturbed due to variations in the pumping rate. In this example the recovery data fitted with a Theis recovery method (in addition to the Agarwal plot) confirms the homogenous behaviour identified in the drawdown-curve (Figure 5.23). In the absence of no flow boundary conditions both (drawdown and recovery) curves must show the same behaviour due to superposition (Van Tonder et al., 2002).

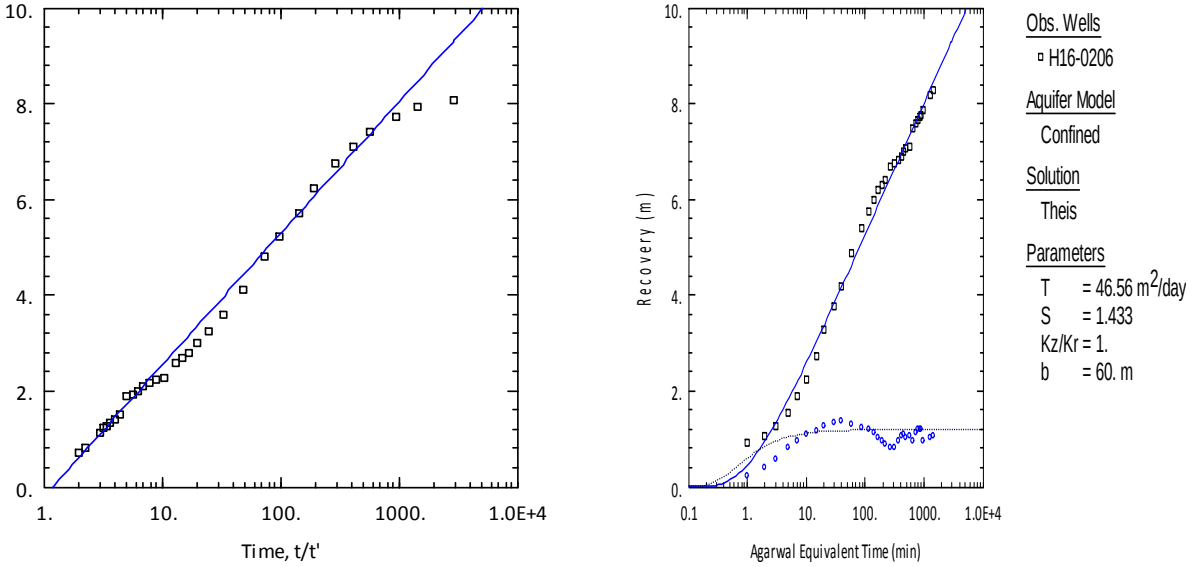

Figure 5.23. Diagnostic plots (semi-log) of the recovery data of borehole H16-0206 fitted with a conventional Theis-recovery solution (left) and a Theis solution for the Agarwal plot (right).

TYPE 2 (Unconfined or double porosity)

The most common behaviour of all boreholes tested in the study area is an inflection of the drawdown at intermediate times, reflected by a pronounced double porosity dip in the derivative. Early pumping times indicate the depletion of a first reservoir that is well connected to the pumping well (i.e. fractures or the saturated zone of an unconfined aquifer). At intermediate pumping times the drawdown is stabilised by a delayed flux provided by a second compartment of the aquifer, which can be either 1) the vertical delayed recharge from the overlying, less permeable part in an unconfined aquifer (Neuman 1974; Moench, 1997) or 2) the drainage of matrix blocks in fractured aquifers (Moench, 1984; Barker, 1988). At late time, the system either tends toward a typical infinite acting radial flow asymptote or boundary conditions may be encountered. In the first instance the semi-log plot shows the characteristic parallel straight line segment at early and late pumping times, while a no-flow boundary is characterised by a doubling of the value of the derivative (Ehlig-Economides et al. 1994; Van Tonder et al., 2002). Borehole H17-0774 were fitted with both an unconfined Neuman (1974) and double porosity Moench (1984) solution (Figure 5.24 and Figure 6.6). In both cases a good curve fit was achieved highlighting the difficulty in choosing an appropriate model. A detailed description of the geology and conceptual model will greatly assist in choosing the correct analytical model.

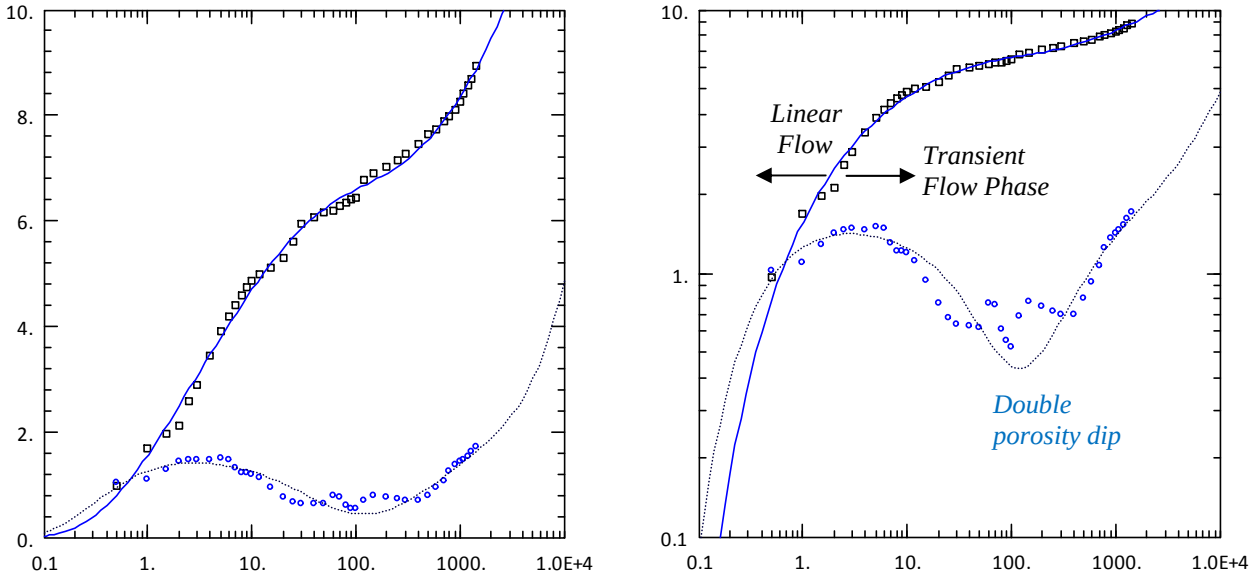

Figure 5.24. Diagnostic plots (semi- log, log-log and derivative) of a 24 hour constant rate pumping test with an unconfined solution (borehole H17-0774).

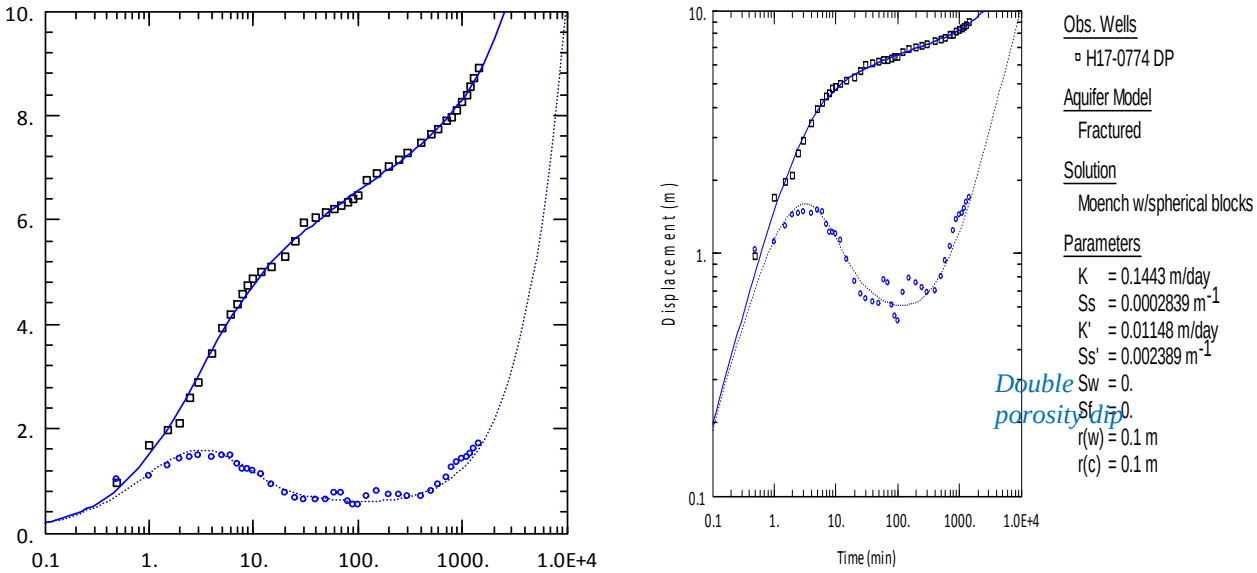

Figure 5.25. Diagnostic plots (semi- log, log-log and derivative) of borehole H17-0774 fitted with a fractured (double porosity) solution.

Variation 2

The drawdown behaviour is characterised by distinct dips (fracture dewatering) during late times of the associated derivative data (Figure 5.26). In this conceptual model the early flow towards the well is from fracture storage, supported at intermediate times by drainage of the rock matrix before water is derived from both systems at late times with frequent dewatering of discrete fracture systems. Once these fractures are dewatered, a marked increase in drawdown and decrease in transmissivity becomes apparent.

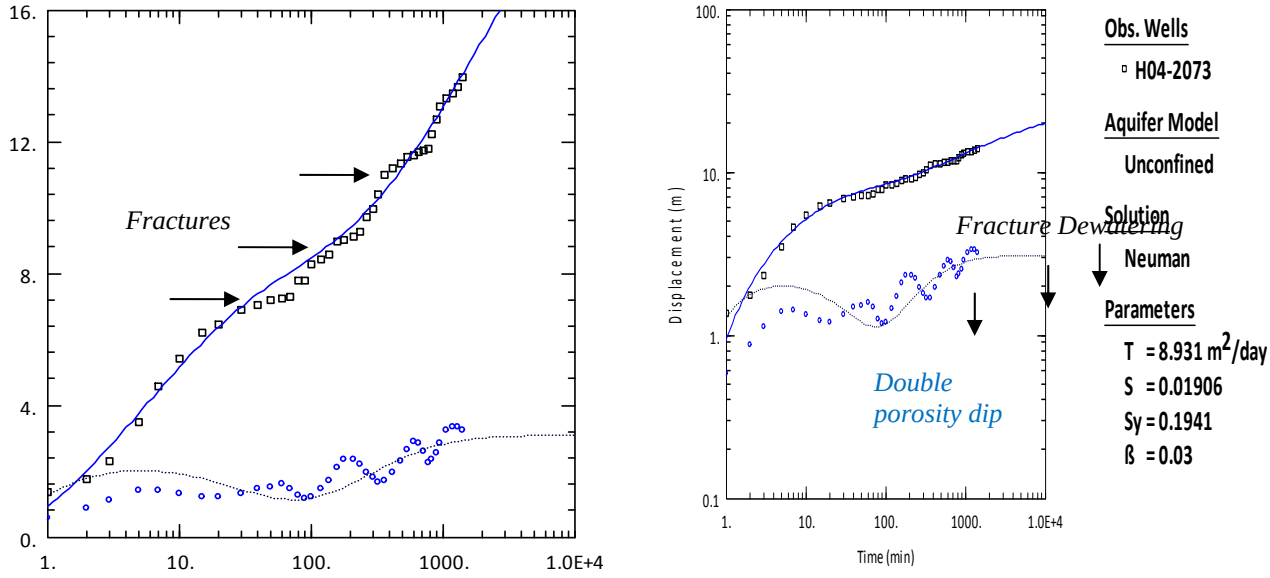

Figure 5.26. Diagnostic plots (semi- log, log-log and derivative) of a 24 hour constant rate pumping test fitted with a fractured (double porosity) solution (borehole H04-2073).

In the example illustrated in Figure 5.26 a number of discrete fractures (water strikes) were evidently dewatered. Although a conventional fracture solution was used, more disturbed drawdown curves (due to the dewatering of fractures) make the evaluation complicated and often only parts of the curve can be modelled. The recovery-curve methods provide an alternative approach for fitting of the pumping test where the drawown curve have been affected by fracture dewatering (Figure 5.27).

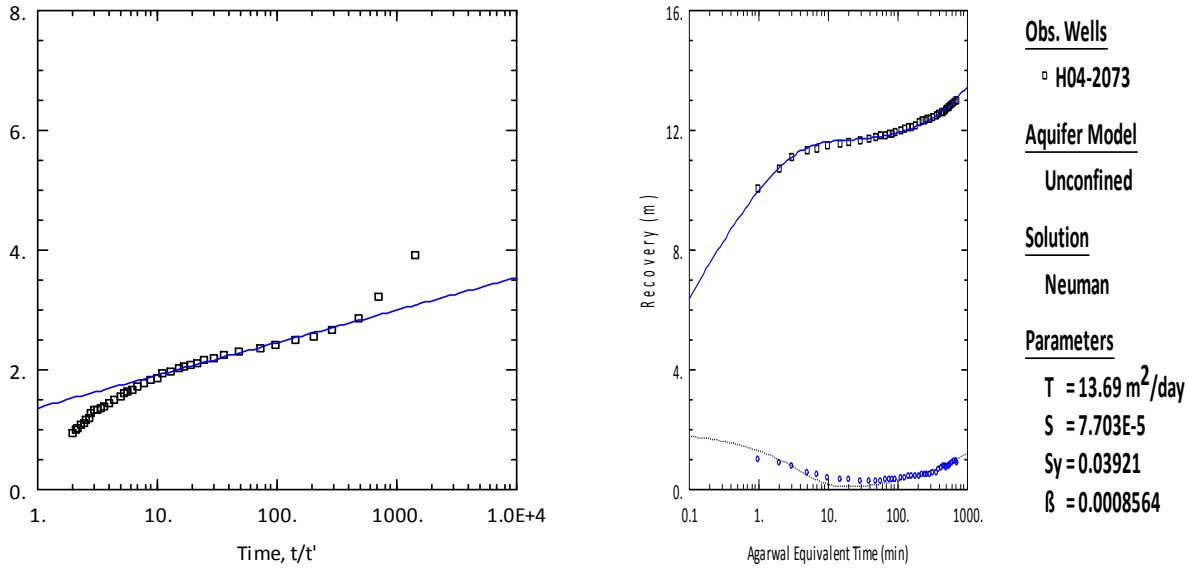

Figure 5.27. Diagnostic plots (semi-log) of the recovery data of borehole H04-2073 fitted with a conventional Theis-recovery solution (left) and a fractured (double porosity) solution for the Agarwal plot (right).

TYPE 3 (Leaky or Constant Head)

At early pumping times, a Theis-type curve is observed (0 to 100 minutes), at intermediate times, water from the aquitard leaking into the aquifer. Eventually, at late times all the leakage through the aquitard becomes constant and the flow towards the well reaches steady state (Figure 5.28).

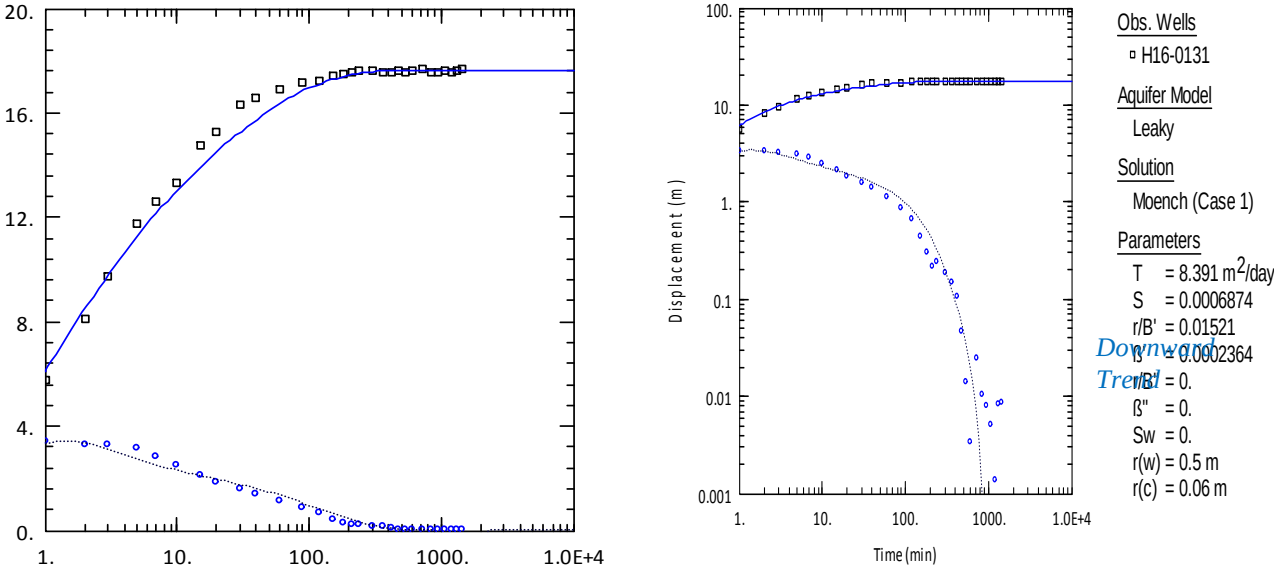

Figure 5.28. Diagnostic plots (semi- log, log-log and derivative) of a 24 hour constant rate pumping test fitted with a leaky aquifer solution (borehole H16-0131).

A similar behaviour (leakage) is observed when the cone of depression reaches a recharge boundary (constant-head). Renard et al. (2009) noted that in theory a leaky aquifer case can be distinguished from a constant head case by looking at the shape of the derivative). The derivative tends towards zero earlier in the case of a leaky aquifer much faster than in the constant head case (see Figure 2.4, section 2.4.2).

TYPE 4 (Single Fracture – General radial flow)

Type 4 can be regarded as a fractured aquifer system characterised by an early period in which the effect of the fracture dominates and very little water is contributed by the aquifer (matrix). The flow towards the well takes place in the fracture only and is parallel (i.e. linear in the fault). At intermediate times water is supplied by the fracture and matrix. The extensive occurrence of near vertical dykes, lineaments and shear zones (see section 4.3) in the crystalline rock, in addition to the fact that most boreholes are completed once a single moderate- or high-yielding fracture is encountered, it is to be expected that a number of drawdown behaviours can be fitted with a single fracture model. An example is borehole H03-3269 (Figure 5.29), which seemingly targeted the Matok shear zone. In this case it was assumed that the fracture zone (set of vertical fractures) acted as a conduit and based on the drawdown behaviour the curve was idealised with a single vertical fracture model (Gringarten et al., 1974). A fracture half-length of 100 m was assumed (although fracture half-lengths of several hundreds of meters, up to above 1000 m are encountered in study area).

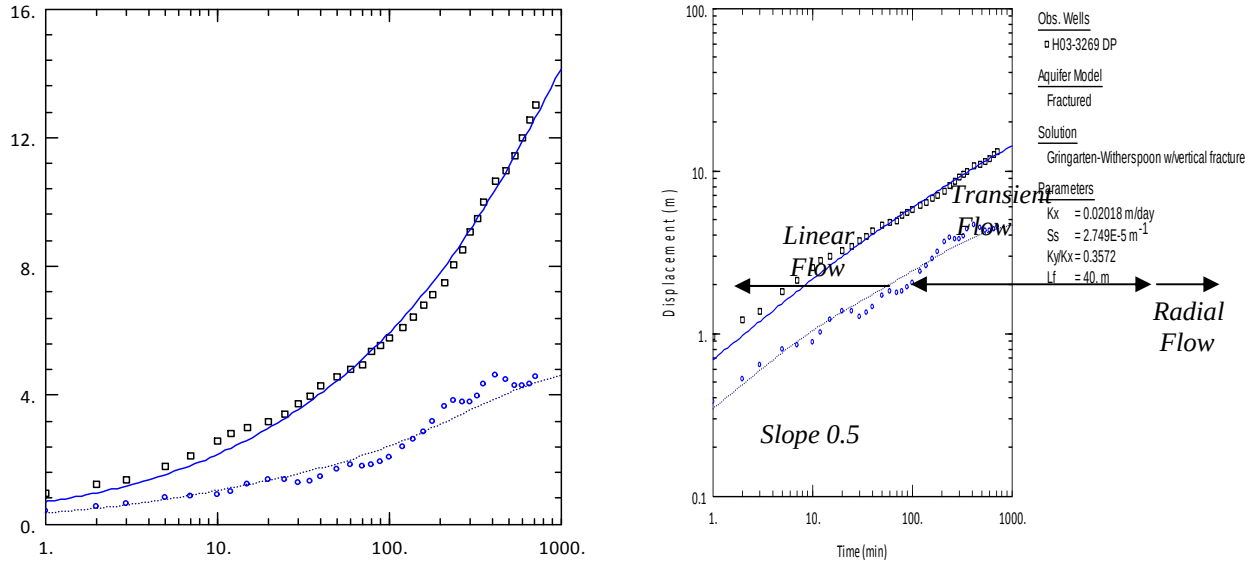

Figure 5.29. Diagnostic plots (semi- log, log-log and derivative) of a 12 hour constant rate pumping test fitted with a single fracture (Gringarten et al., 1974) model (H03-3269).

TYPE 5 (Closed reservoir)

A feature of these type-curves is the obvious influence of barrier boundaries which increases the rate of drawdown as the limits of the fissure systems are reached by the pumping effects (Figure 5.30). The shape of the drawdown has a characteristic steepening in the semi-log, log-log and derivative plots. Interestingly 50 % of Type 5 tests were pumped for 8 hours or less and achieved the highest drawdown (Table 5.11).

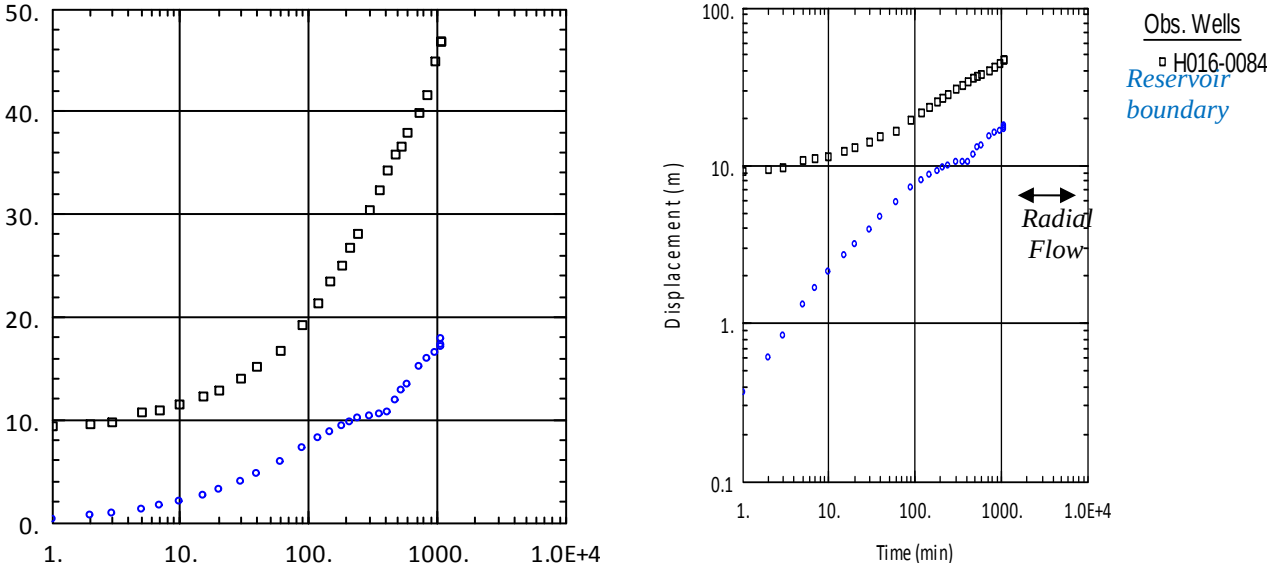

Figure 5.30. Diagnostic plots (semi- log, log-log and derivative) of borehole H16-0084, indicating reservoir boundaries.

This may be a clear indication of an excessive pumping rate, where the aquifer could simply not supply efficient water to the borehole to sustain the discharge rate chosen. In these cases, parameter estimation is extremely difficult and the test should be repeated with a lower pumping rate.

Summary of aquifer characterisation

The exact shape of the diagnostic plot (drawdown behaviour) depends on the values of the hydraulic (and physical) parameters that control them. These typical behaviours can occur over shorter or longer periods, which is in some cases extremely clear and in others more difficult to identify. Therefore the curves shown in the preceding section are indicative of a certain category of response and not strictly identical with a single response that one should expect in field situations. Analyses of pumping tests in crystalline basement aquifers do not satisfy the underlying assumptions for porous media. In particular:

- basement rock aquifers are neither homogenous nor isotropic,
- the aquifer often represents semi-confined to unconfined conditions,
- flow from fractures will neither be two-dimensional radial, nor will it be constrained to a single one-dimensional channel. The characteristic of the fracture network determine the flow geometry, and
- well bore storage and skin is not negligible, and can overlie other effects, which are important for the parameter estimation (Van Tonder et al., 2002; Misstear et al., 2006).

5.3.2. Hydraulic parameters

The locations of all pumping tests conducted within the project framework are illustrated in Figure 5.31.

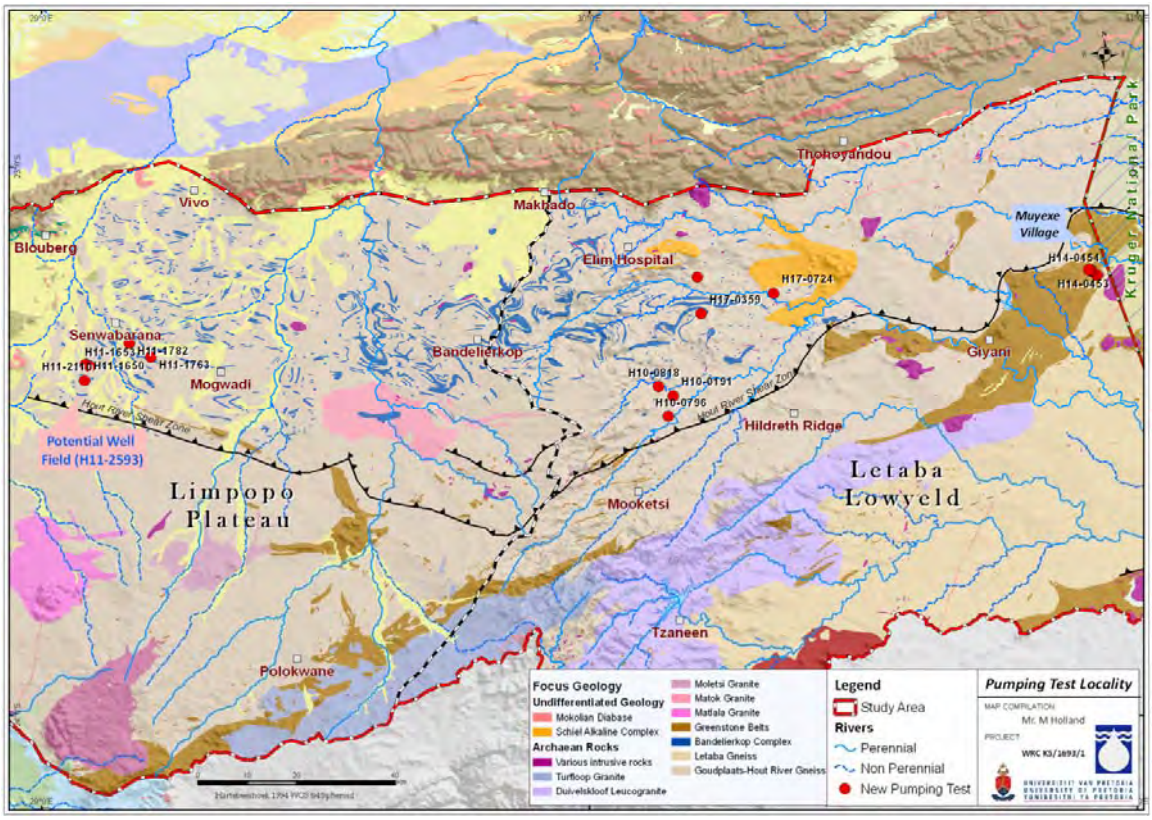

Figure 5.31. Location of pumping tests conducted in the study area.

The hydraulic parameters obtained from the pumping test analysis and the analytical solutions applied for the curve matching procedure are summarised in Table 5.12. The representative values for T and S were obtained from the aquifer test analysis using the pumped and observation boreholes (if available). Although well loss and well efficiency was not a priority for this assessment it was analysed for some boreholes. In most cases well losses exceeded 3 800 ec^2/m^5, which can be regarded as severe losses according to Walton (1962) (Appendix F). The confidence level of the determined hydraulic parameters (T and S) generally increases if observation boreholes are present. The arithmetic average storativity value determined is 5.E-02 and 7.E-03 for the Limpopo Plateau and Letaba Lowveld respectively, coinciding closely with the chosen constant storativity value of 1.E-03 used in the analysis (FC-method) of the GRIP dataset.

Table 5.12. Hydraulic test analysis results (test details is given in Appendix F).

Area	BH Nr.	Applied solution	Aquifer Type	T m^2/d	S	Observation BH's	Theis Recovery-method
Limpopo Plateau	H11-1650#	Barker	Fractured	330	2.E-01	H11-1651 (301m), H11-1652 (255m)	470
	H11-1653#	Moench	Fractured	220	2.E-03	H11-1651 (398m), H11-1652 (441m), H11-1654 (451m)	344
	H11-2110*	Neuman-Witherspoon	Leaky	180	6.E-05	H11-2109 (211m)	310
	H11-1782*	Hantush-Jacob	Leaky	50	2.E-04	H11-1781 (48m)	30
	11-1763	Neuman-Witherspoon	Leaky	4	-	H11-1764 (120m)	9
Letaba Lowveld	H10-0818*	Hantush-Jacob	Leaky	47	9.E-04	H10-0823 (40m)	30
	H10-0796#	Neuman	Unconfined	7	1.E-03	H10-0100 (40m)	17
	H10-0191#	Hantush	Leaky	1	3.E-03	H10-0816 (180m)	20
	H14-0277*	Neuman	Unconfined	95	2.E-03	H14-0279 (220m)	137
	H14-0279*	Barker	Fractured	51	3.E-04	H14-1288 (50m), H14-1301 (250m)	130
	H14-0453*	Neuman	Unconfined	77	4.E-04	H14-0277 (130m), H14-0454 (290m)	170
	H17-0359	Neuman	Unconfined	4	-	_	10
	H17-0724	Neuman	Unconfined	1	-	_	15
	H17-0774	Neuman	Unconfined / Fractured	4	-	_	11
	H14-0454	Neuman	Unconfined	16	-	_	20
	H14-0275	Gringarten-Ramey	Fractured	43	-	-	45

* - Observation hole monitored with drawdown.

- Observation borehole monitored with no-influence.

5.4. Groundwater sustainability (source vs. resource)

The following discussion will show that the recommended 'sustainable' yield is non-unique and can be influenced by factors such as the constant rate during testing. It will also be highlighted that long term borehole yields are recommended without consideration of the combined (aquifer) yield.

5.4.1. Source yield

The most common factor influencing a proper analysis of a pumping test is insufficient drawdown achieved due to, a too low pumping rate or too short duration. If the aquifer is not stressed sufficiently it's impossible to identify the main fracture zone or possible boundary conditions. Two constant rate tests were performed on borehole H14-0279; in 2005 the test was conducted at a rate of 3.7 ℓ/s for 24 hrs and in 2009 the test was conducted at a rate of 6.2 ℓ/s for 48 hrs (Figure 5.32).

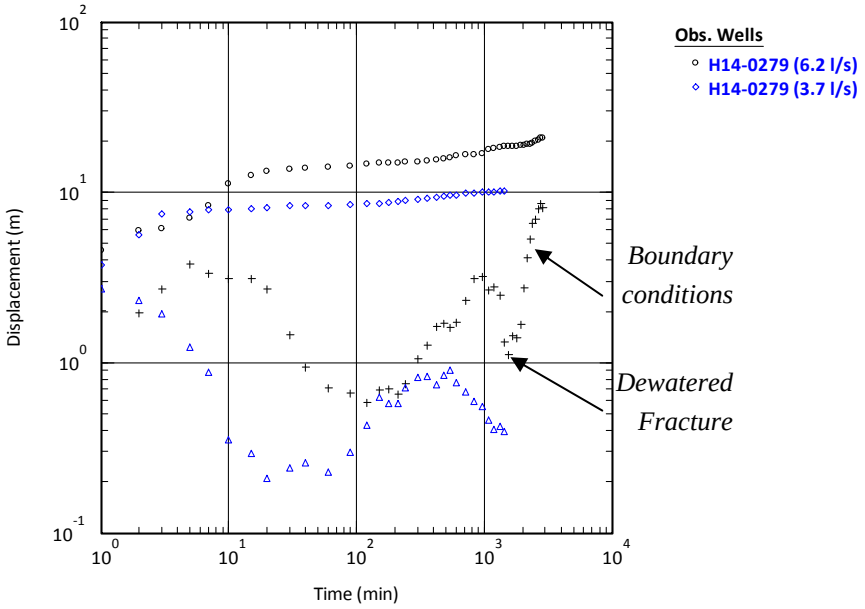

Figure 5.32. Semi logarithmic plot of borehole H14-0279 with two different constant discharge rates.

The pumping test data produced different drawdown curves. Although the position of the fracture is seen in both derivative plots, the dewatering of the fracture (or no-flow boundary) is only seen after 1 440 minutes (i.e. in the second test). By comparing the recommended yield results obtained from the FC spreadsheet it is evident that the higher constant rate estimated the lower 'sustainable' yield (Table 5.13).

Table 5.13. Comparison of the results for the two constant rates.

Constant Rate	**3.7 (ℓ/s)**		**6.2 (ℓ/s)**	
Date	2005		2009	
Rest Water level (m.b.g.l)	7.7		7.6	
Drawdown (Available) (m)	53		55	
Final Drawdown (24 hr) (m)	10.2			
Final Drawdown (48 hr) (m)	-		20.9	
Available drawdown	**Drawdown**	**Yield***	**Drawdown**	**Yield***
Main water strike@	19	2.7	19	1.4
Final Drawdown	10.2	1.9	20.9	1.3
Transmissivity (Late T m^2/day)	**30**		**7**	

@ - Distance from rest WL to main water strike (m) – BH Log
# - Estimated from the geometric mean of the end drawdown and main water strike
* - Recommended abstraction (ℓ/s per day).

Using the position of the main water strike as the available drawdown, the estimated yields are 2.7 and 1.4 ℓ/s respectively for the low and high rate tests. The 2.7 ℓ/s obtained from the lower rate test may therefore, be an over estimate of the 'sustainable' yield of borehole H14-0279. This clearly illustrates the problem encountered when using the main water strike as available drawdown when the achieved drawdown is far above the position of the main water strike. This is a common pitfall of the pumping tests conducted in the Limpopo Province, where the constant rate is often decided before hand without site specific considerations. Only a third of all boreholes tested in the study area, achieved a final drawdown of 80-90 % of the available drawdown (water level to the pump intake) (Figure 5.33).

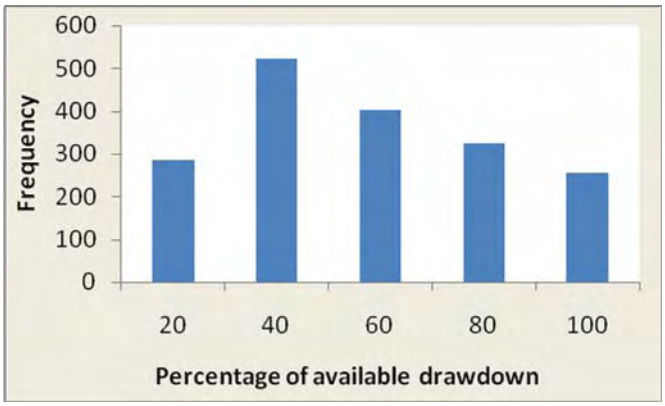

Figure 5.33. Distribution of drawdown percentage achieved from pumping tests in the study.

Another common shortfall of pumping tests conducted in the study area is pre-determined duration for the tests. Because boundary conditions were not encountered during the 24 hr pumping test it wasn't considered during the yield estimate and a recommended yield of 1.9 ℓ/s was determined (using the final drawdown as available drawdown). Considering the boundary conditions evident from the 48 hr test, 1.3 ℓ/s is recommended (Table 5.13). Almost 85% of boreholes tested in the study area were pumped for 24 hrs or less (Table 5.14). However, using the final drawdown during a test as available drawdown can be regarded as the minimum 'sustainable' yield of the borehole if the water strike has not been reached.

Table 5.14. Pumping test in the study area (GRIP dataset).

Hours	<12	12	24	48	72	96	Total
Nr. of Tests	335	547	1054	213	63	1	2213
Percentage	15%	25%	48%	10%	3%	0.1%	100%

These common shortfalls may be directly related to the poor emphasis on step-drawdown rates to accurately determine a constant rate that will ensure interpretable drawdown curves are obtained at the pumping well and observation points.

5.4.2. Resource yield

Pumping tests are probably the most important aquifer investigations techniques, however, as seen from the preceding discussion long term assured water supplies (30 years+) to a community

or village with substantial infrastructure investments are often based on a mere 12 or 24 hr pumping test. This can in theory lead to a sustainable source yield but an unsustainable resource yield. An example of such a case is the Upper Brak River catchment where numerous pumping tests were conducted for rural water supply purposes. The catchment lies to the west of the Dendron-Vivo groundwater control area where large scale irrigation has sustained (though not necessarily sustainably) agricultural activities in the region for the last 40 years. As illustrated in Figure 5.6 (section 5.1.2) and Figure 5.34 (insert) groundwater levels have declined by 6 m since the early 1970s. Considering that the impacts of groundwater consumption on the ecological environment are largely unknown the aquifer can be considered as being partially mined.

To evaluate the situation in the Upper Brak River catchment all recommended borehole yields were accumulated and compared to the rate of natural recharge (Table 5.15). Based on the results the area has a combined recommended yield of 10.4 Mm^3/a, which is almost twice the annual vertical recharge of 6 Mm^3/a (2% of MAP). Although not all of these boreholes are in operation and in most cases infrastructure (i.e. electricity) is required, the example does show that recommended source yields may exceed the resource yield (in this case recharge).

Table 5.15. Simplified water balance for the Upper Brak River catchment.

Area	Boreholes	Recharge	Rainfall	Recharge	Yield*
763 km^2	149 (mean yield of 2.2 *l/s*)	2%	392 mm/a	6 Mm^3/a	10.4 Mm^3/a

* - As determined by the FC-method for a 24 hr duty cycle.

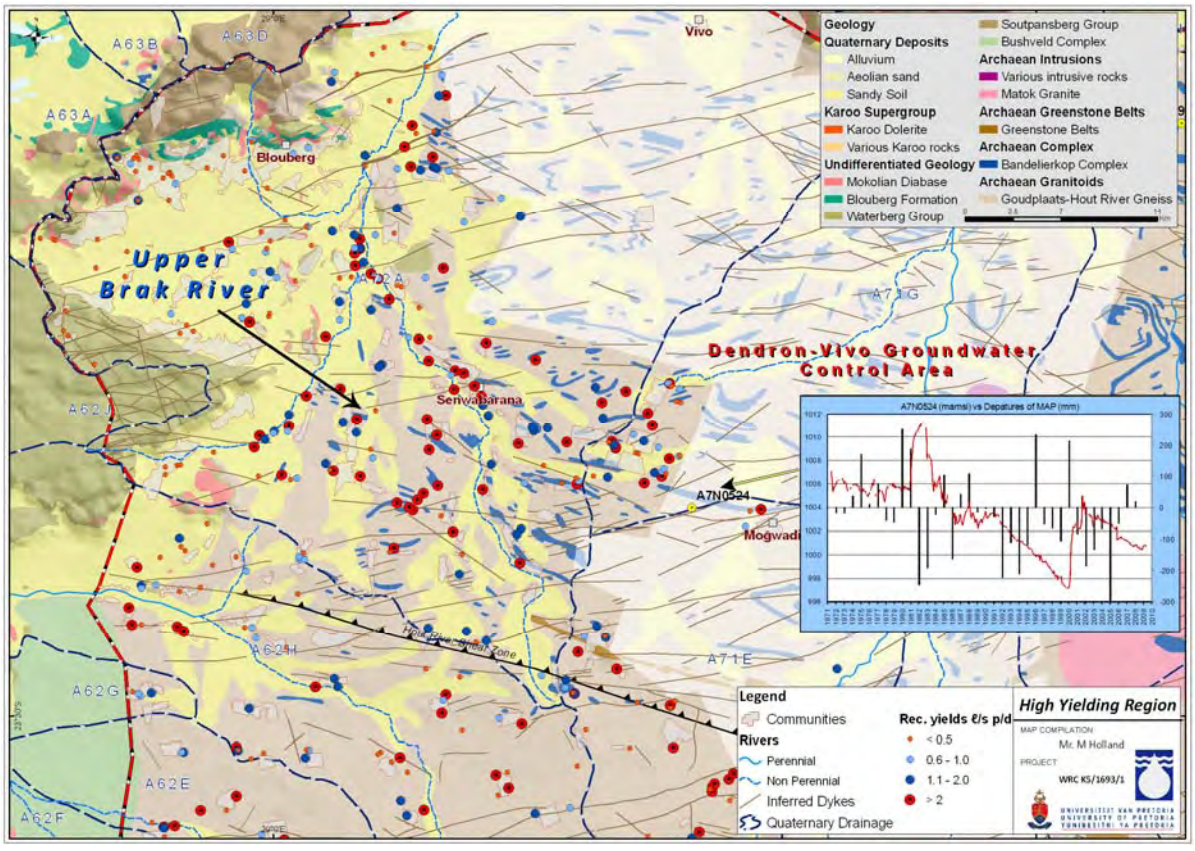

Figure 5.34. High groundwater potential area in the Upper Brak River catchment.

5.4.3. High yield test (potential well field)

Due to increasing water demand from the Blouberg local municipality this site (Brilliant Farm) has been earmarked as a potential well field. To further the understanding of aquifer behaviour in response to pumping especially in high yielding fractured bedrock, a constant discharge test was conducted on borehole (H11-2593) with at a rate of 55 ℓ/s for a period of just over 60 hours. The exceptional yield of 55 ℓ/s is arguably the highest constant rate test conducted to date on the Limpopo basement aquifers. Photo 2 shows the drilling and hydraulic testing of borehole H11-2593. Three observation boreholes were drilled at right angles to the large diameter pumping test hole (Figure 5.35) (Table 5.16).

Photo 2. Drilling and testing of borehole H11-2593.

Table 5.16. Summary of pumping and observation boreholes of high yield test.

BH ID	Area	Distance from abstraction hole (m)	BH Depth (m)	Start WL (m.b.g.l)	Drawdown (m)	End WL (m.b.g.l)
H11-2593	-	Pump Well	84	24.04	7.49	31.53
H11-2596	South	38	52	23.85	4.64	28.49
H11-1653		233	78	23.23	2.41	25.64
H11-2594	West	58	120	24.09	3.67	27.76
H11-1652		215	90	22.86	2.34	25.2
H11-2595	North	65	72	23.86	2.73	26.59

To identify inflow horizons and fractures, down-hole geophysics was conducted prior to the completion of the borehole (casing). Logging operations included a CCTV inspection, and the use of a natural gamma, electrical resistivity and neutron probe (Photo 3). An electrical conductivity and temperature log was completed after the completion of the borehole. Table 5.17 shows geophysical and fluid measurements and, the identification of the particular transmissive fractures in borehole H11-2593.

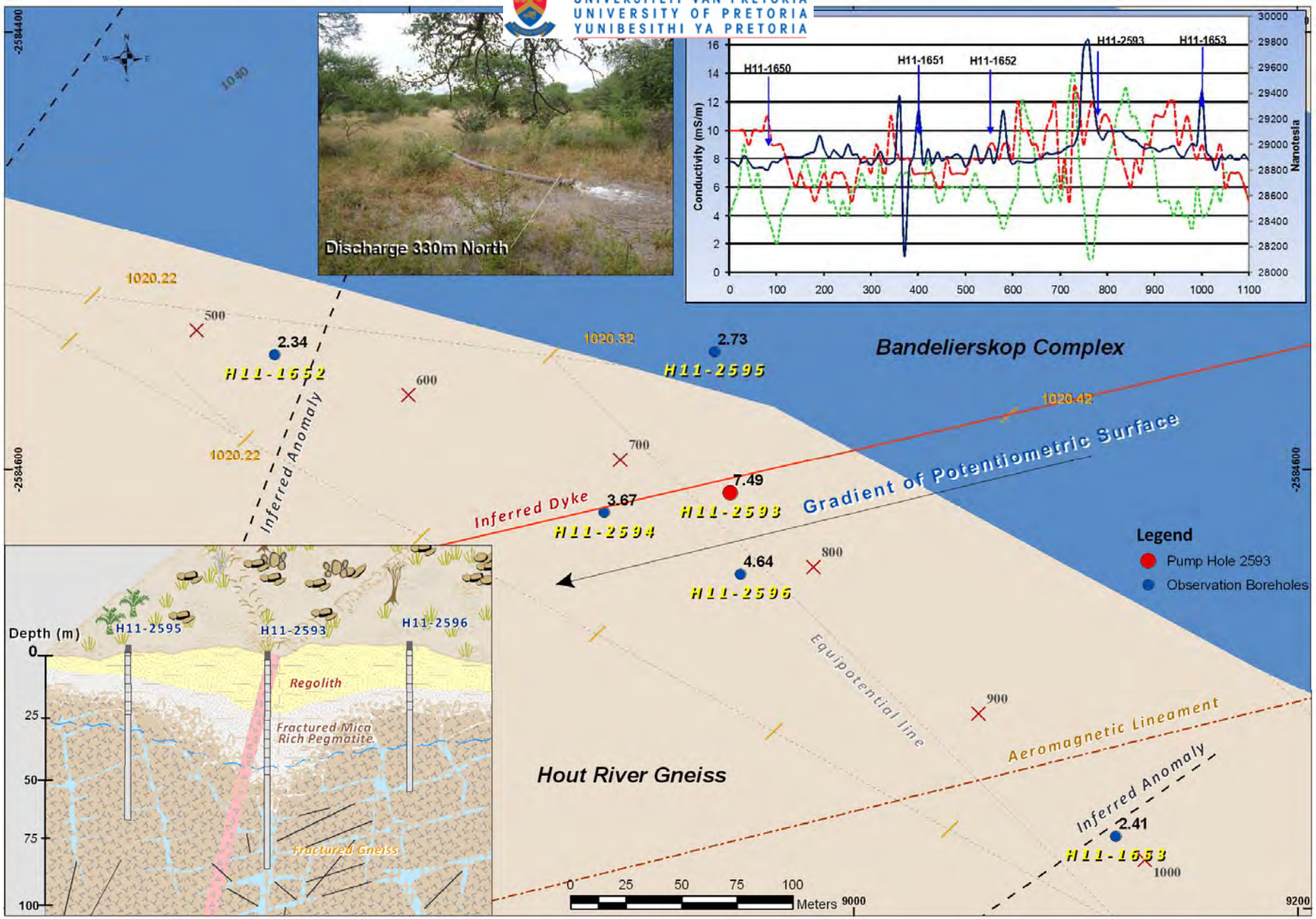

Figure 5.35. Borehole setting of pumping test conducted at the farm Brilliant (Drawdown achieved at the end of constant test is indicated on the map).

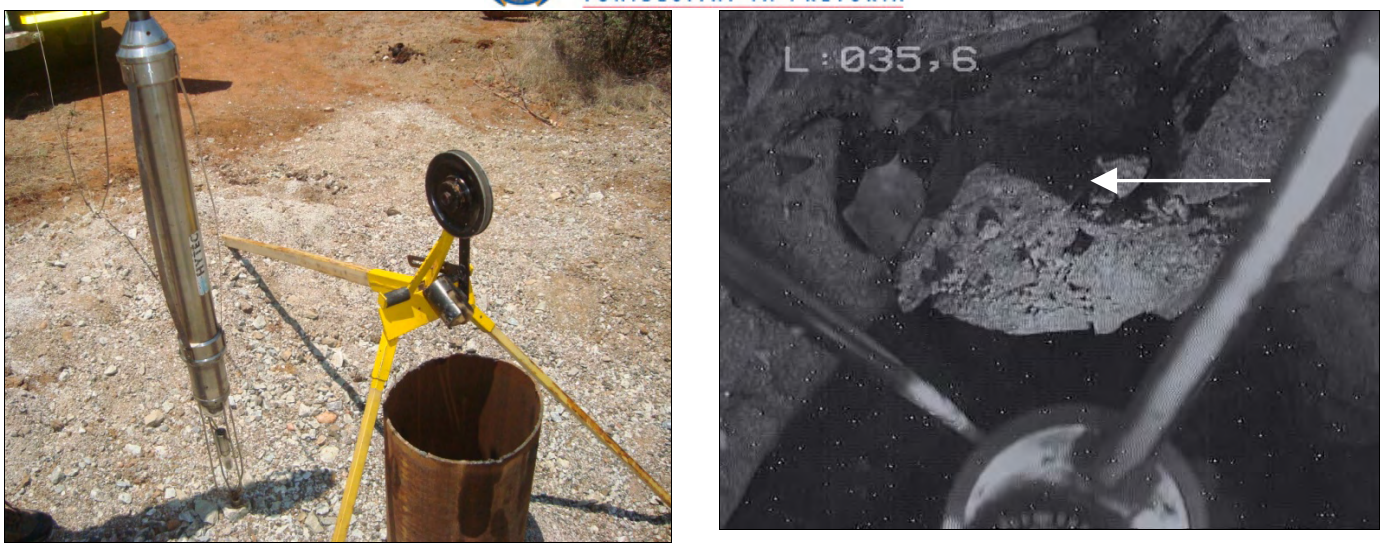

Photo 3. Geophysical and CCTV logging of borehole H11-2593, footage showing water strike at 36 m.b.g.l.

Based on the results the following interpretations are maid:

- The n*atural gamma* log clearly indicates an increase in radiation in the quartzitic zone (39 to 49 m.b.g.l). A high content of quartz, K-feldspar and plagioclase was clearly observed in the drill chips which are high in ^{40}K.
- Two distinct zones can be identified from the *resistivity* log. Low conductivity observed from 35 to 52 m.b.g.l. may indicate a porous fractured zone while an increase in conductivity from 52 m.b.g.l representing a zone of more solid (intact) rock. The base of weathering is inferred at 30 m.b.g.l.
- Decrease in the *neutron* signal between 35 and 38 m.b.g.l suggests the increased capture of neutrons due to higher hydrogen content. This indicates an increase in the amount of water due to higher water filled porosity, and although not clear, could be interpreted as locations of major flowing fractures.
- A sharp increase in electrical conductivity at 36 m.b.g.l and again at 42 m.b.g.l confirm this as the main water bearing zone with groundwater entering as discrete horizons or fissures with a slightly different conductivity. In addition, two distinct flow systems (highlighted on EC graph) are observed which represents limited vertical mixing between these two zones. A distinct drop in temperature at ≈35 m.b.g.l supports the notion of inflows from fractures.

Table 5.17. Results of geological, CCTV and geophysical logging of b

Geology (log)	Water Strike*	Natural Gamma (cps)	Electrical Resistivity (Ωm)	Neutron-N (cps)	Fluid Conductivity (mS/m) / Temp (C°)	CCTV (Images)
Coarse Calcareous weathered material, dominated by quartz Fine weathered material, particles coated with cement but are quartz dominated	RWL 24 m	0 6 12 18	70 170 270	0 1000	132 137 142 "EC" "Tempra ture"	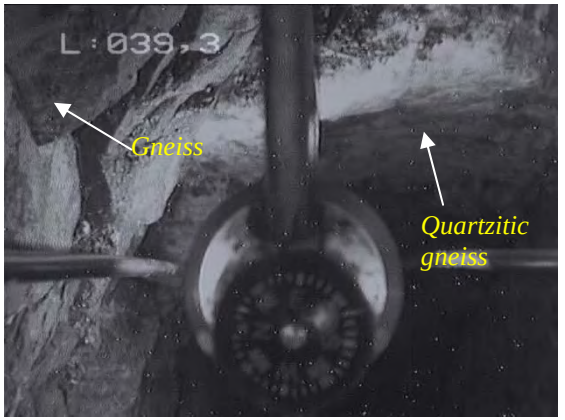
Weathered diabase, mainly fine grained black material with quartzofeldspathic gneiss	EWL#					
Fractured diabase, with some quartzofeldspathic gneiss	36 m 44 m					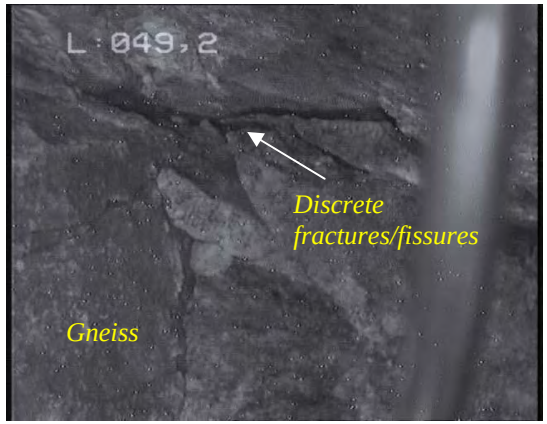
Coarse grained quartzofeldspathic gneiss (almost entirely quartzitic) Medium to coarse grained quartzofeldspathic gneiss	56 m 66 m					
Base of borehole 84 m	BH Diamater: 300 mm Casing: 250 mm solid to 17 m Perforated to 41 m		Rest Water Level: 24 m Pump installation: 39 m			

* - Drillers log.

- End water level (7.53 m drawdown).

During the constant discharge test, a drawdown of 7.53 m was achieved. From the drawdown curve a higher permeable zone were reached at 1 560 minutes, and lasted approximately 220 minutes, before it was dewatered. It's clearly visible as a distinct decrease followed by an increase of the derivative curve (Figure 5.36). This zone can be interpreted as the dewatering of a fracture or it can be related to the dewatering of a highly transmissive zone From the geophysical (geological) logging and the CCTV footage (Figure 5.36), this zone (30.5 m.b.g.l) can be regarded as a higher permeability basal breccia which represents the horizon of fracturing between the fresh rock and the regolith.

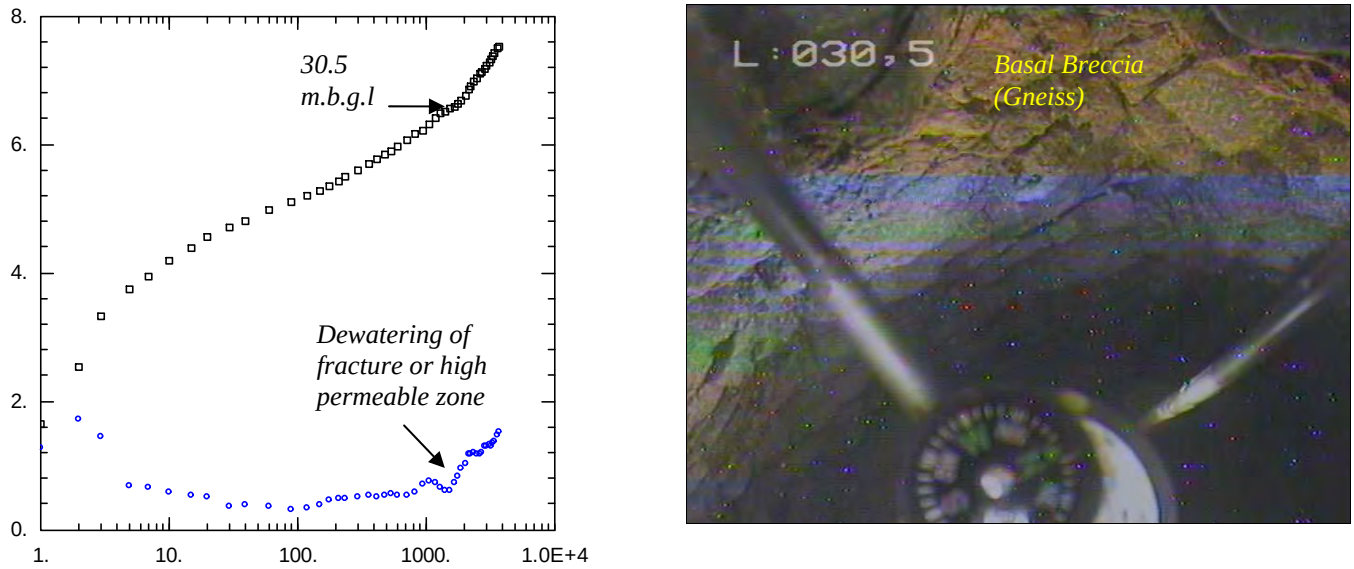

Figure 5.36. Diagnostic plot (semi- log and derivative) model and the CCTV footage of the inferred higher permeability zone.

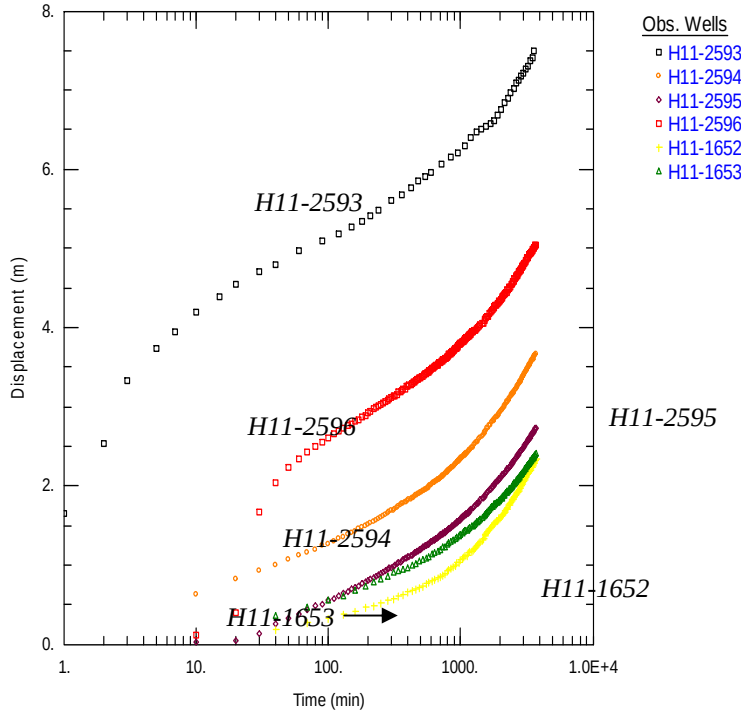

Figure 5.37. Diagnostic plot (semi- log and log-log) fitted with a fracture (Barker, 1988) model of pumping borehole (H11-2593) and observation boreholes (H11-2596 and H11-1653).

The distinct double porosity dip of the derivatives and the typical sigmoidal type drawdown behaviour of the pumping borehole suggest that a fractured aquifer model can be justified for the dataset. Figure 5.38 illustrates the curve fit of borehole H11-2593 with the general radial flow model by Barker (1988) and its extension to dual porosity.

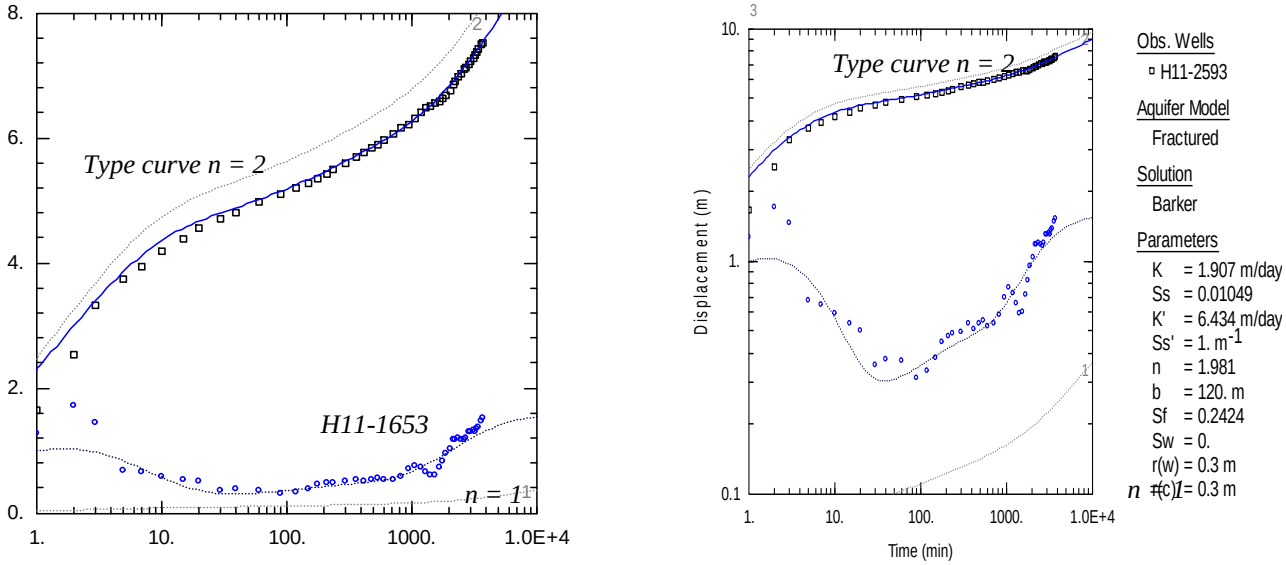

Figure 5.38. Diagnostic plot (semi- log and log-log) fitted with a fracture (Barker, 1988) model of pumping borehole (H11-2593) and observation boreholes (H11-2596 and H11-1653).

The diagnostic plot also indicate the family type curves of flow dimensions of n=1 and n= 2 respectively (see section 2.4.3). Early pumping times are characterised by well bore storage effects and flow through fractures, followed by a transient flow phase (contribution of the matrix flow) at intermediate times and finally a characteristic bilinear flow regime indicative of flow in fractures and the matrix (Figure 5.38). An increase in the value of the derivative and an upward trend in the time drawdown data at later pumping times are often interpreted as no-flow boundaries, which can be incorrect (Van Tonder, 2002). It may be related to the end of the hydraulic active fracture zone which was increasingly being stressed at later times. Van Tonder and Steyl (2010) have shown that the representative transmissivity in fractured aquifers decrease with time of a pumping test, except if the borehole was situated close to a river.

A slightly better hydraulic connection based on drawdown versus distance is observed between the observation boreholes to the south (H11-2596; H11-1653) and west (H11-2594; H11-1652) of the pumping borehole, compared to the observation borehole (H11-2595) to the north (see Table 5.16 and Figure 5.37). For this reason the observation boreholes were grouped and analysed accordingly to their observed behaviour with respect to the abstraction borehole. Observation borehole (H11-2596) to the south responded in a similar way to the pumping borehole indicating well bore storage at early times followed by bilinear flow at late pumping times (Figure 5.39). The furthest observation borehole to the south (east) (H11-1653) has a predominant linear flow regime at late pumping times, characterised by a linear derivative.

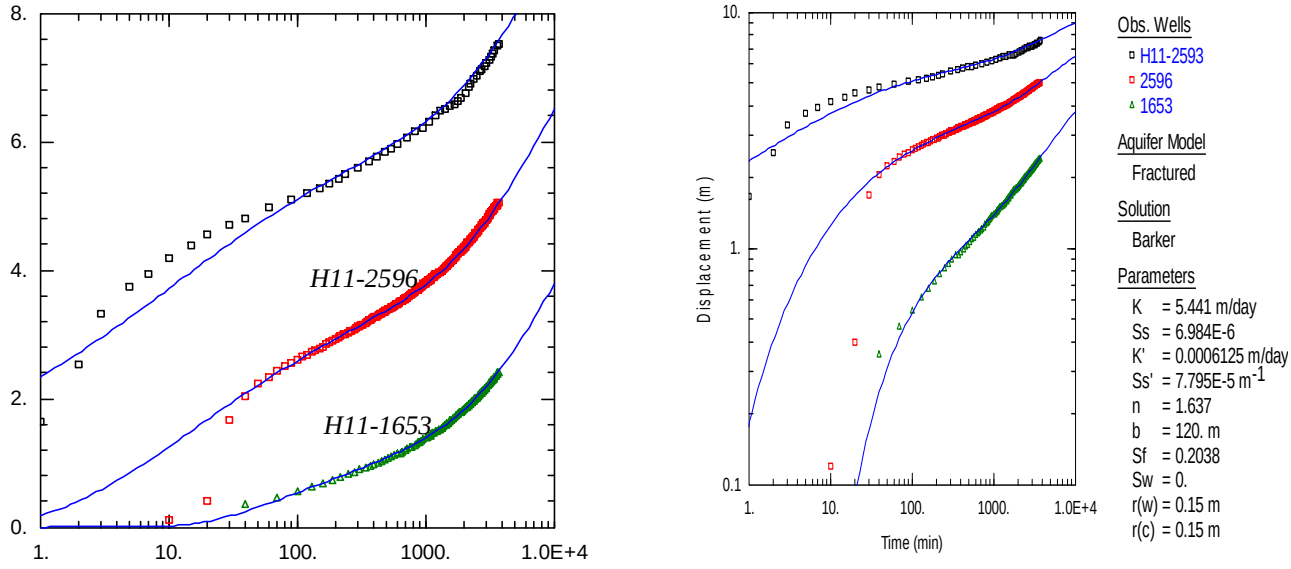

Figure 5.39. Diagnostic plot (semi- log and log-log) fitted with a fracture (Barker, 1988) model of pumping borehole (H11-2593) and observation boreholes (H11-2596 and H11-1653).

Similarly the furthest observation borehole to the west (H11-1652) shows linear flow followed by a transient flow phase (Figure 5.40). Observation borehole H11-2594 has predominantly a bilinear flow regime, which corresponds to the partial flow dimension of n = 1.5.

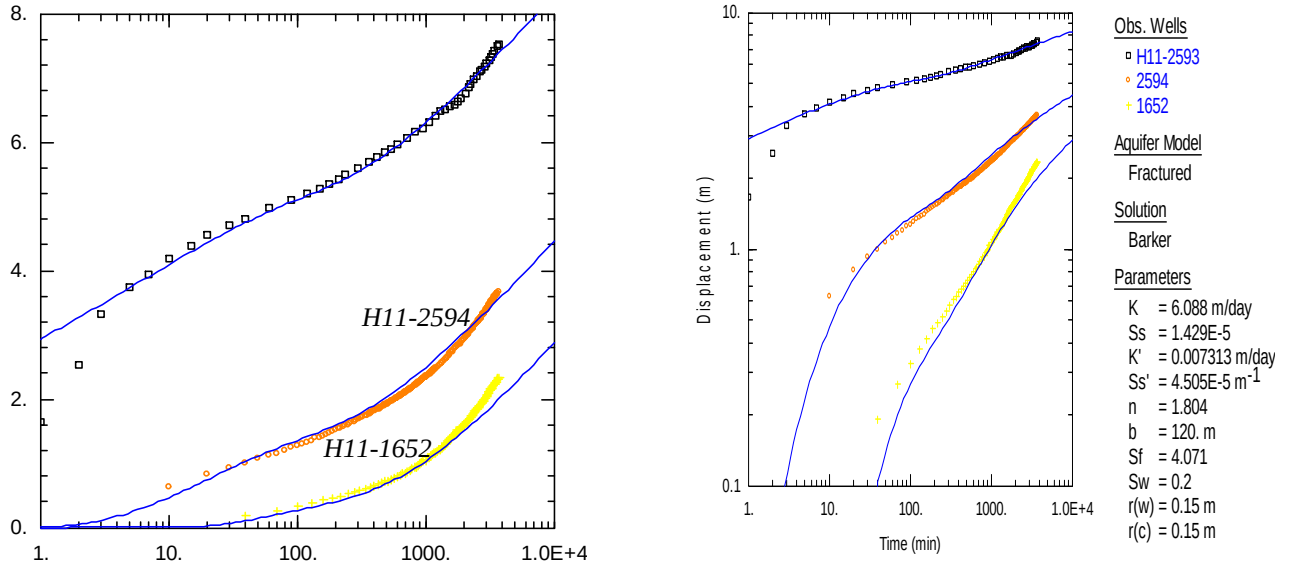

Figure 5.40. Diagnostic plot (semi- log and log-log) fitted with a fracture (Barker, 1988) model of pumping borehole (H11-2593) and observation boreholes (H11-2594 and H11-1652).

The drawdown behaviour of the observation borehole (H11-2595) to the north of the pumping borehole (H11-2593) is illustrated in Figure 5.41. The borehole is characterised by well bore storage followed by a linear flow regime (n=1).

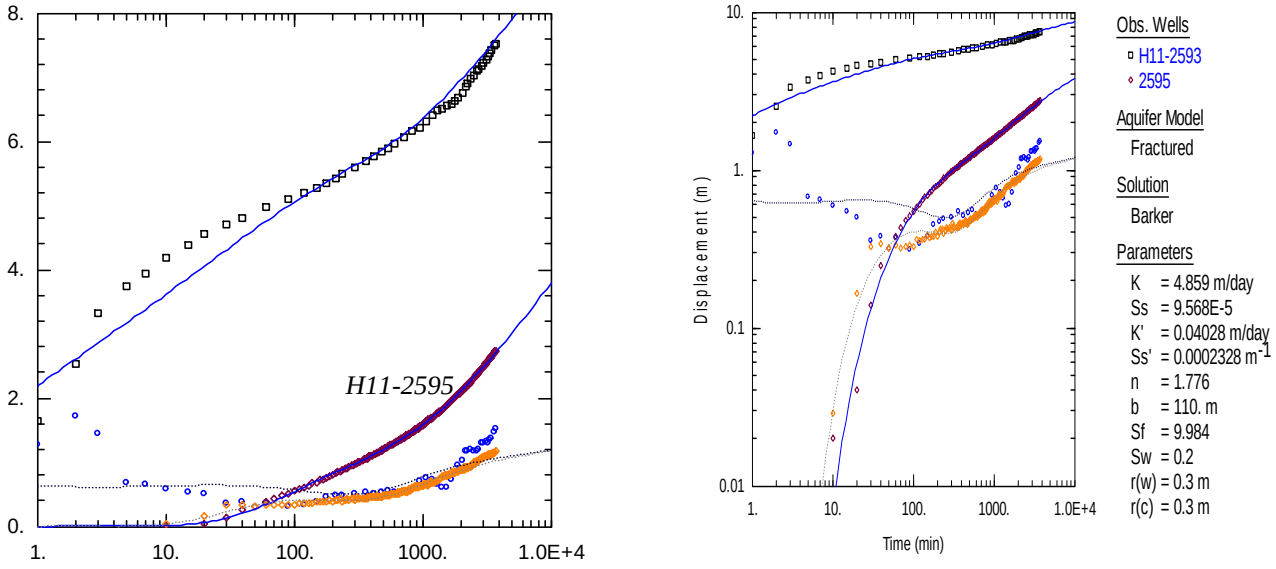

Figure 5.41. Diagnostic plot (semi- log, log-log and derivative) fitted with a fracture (Barker, 1988) model of pumping borehole (H11-2593) and observation borehole (H11-2595).

A summary of the hydraulic parameters obtained from the curve fitting results are illustrated in Table 5.18. Observed responses in all of the boreholes can be matched with type curves based on the Barker (1988) fracture model. Fitting of the model was biased towards the observation boreholes by placing more weight to these observation boreholes. The obvious good fit of the model (both drawdown and derivative) to the data suggests a sound conceptual model and increased confidence in the estimated parameters.

Table 5.18. Summary of hydraulic parameters obtained from well field pumping test analysis.

Observation Boreholes	Distance from abstraction hole (m)	Simultaneous curve fit		
		Hydraulic conductivity (m/day)	Specific storage (S_s)(m^{-1})	Flow dimension
H11-2593	Pump Well	1.9	0.01	n = 1.9
H11-2596 and -1653	38 and 233	5.9	2.1E-06	n = 1.7
H11-2594 and -1652	58 and 215	6.1	1.5E-05	n = 1.8
H11-2595	65	4.9	9.5E-05	n = 1.8

The studied pumping test setting can be regarded as an unconfined aquifer in the weathered zone underlain (and virtually de-connected by a semi-pervious layer) from a deeper (semi-)confined aquifer. The obtained flow dimensions at the scale of the pumping test are around 1.5 to < 2, suggesting an intermediate flow between bilinear (partial flow dimension) and cylindrical flow (like Theis), implying fairly good connectivity of the fracture network. The flow in this anisotropic fractured rock seems to be generated by a sub-horizontal fracture network (suggested by geophysical logging), connected to a second probably sub-vertical to vertical fracture network. The average hydraulic conductivity from the studied pumping test relates to an effective transmissivity of 677 m^2/day and, the average specific storage (4.5E-05 m^{-1}) relates to a storativity

of 0.004 respectively, considering an aquifer thickness of 120 m. The specific storage of 4.5E-05 m^{-1} falls in the upper range of characteristic values (3.3E-06 to 6.9E-05 m^{-1}) for fissured rock (Batu, 1998).

5.5. Geological and geomorphologic influence on borehole productivity

This section outlines the identified relationship between the factors that potentially influence groundwater productivity in the crystalline rocks of the study area. The following factors were considered; 1) the geological and topographic setting, 2) dykes and linear anomalies (including their orientation), 3) regional tectonics (maximum horizontal stress), 4) weathering thickness (erosion surface), and 5) proximity to surface water drainages. In order to identify these factors, the dataset was spatially sub-divided using available GIS layers and related to borehole yield (recommended abstraction rate) and transmissivity. Selection criteria ranged from lithology, weathering thickness, rivers, topography, dykes and lineaments. It must be noted that the assessed boreholes were not drilled randomly, but after preliminary site-investigations. The dataset is in this regard biased towards anomalies and higher yields in comparison to random sampling of basement aquifers. However, the large number of successful as well as unsuccessful boreholes compensates partially for this statistical bias.

The four structural domains identified play a major role in the variability of borehole productivity in the larger study area. The cumulative distribution function in Figure 5.42 indicates that the NW domain is more productive followed by the SW domain, the NE domain and then the SE domain. It should be pointed out that major part of south-eastern comprises the Tzaneen escarpment underlain by the poorly weathered and poorly fractured Duivelskloof leucogranite, which have a low groundwater potential as discussed earlier. This is also confirmed by a visual inspection of the spatial transmissivity distribution map (Figure 5.43). The observed variations in transmissivities are not solely related to the dominant dyke orientation or dyke density that formed the basis of the structural regions, but rather factors such as geology, topography and thickness of weathering.

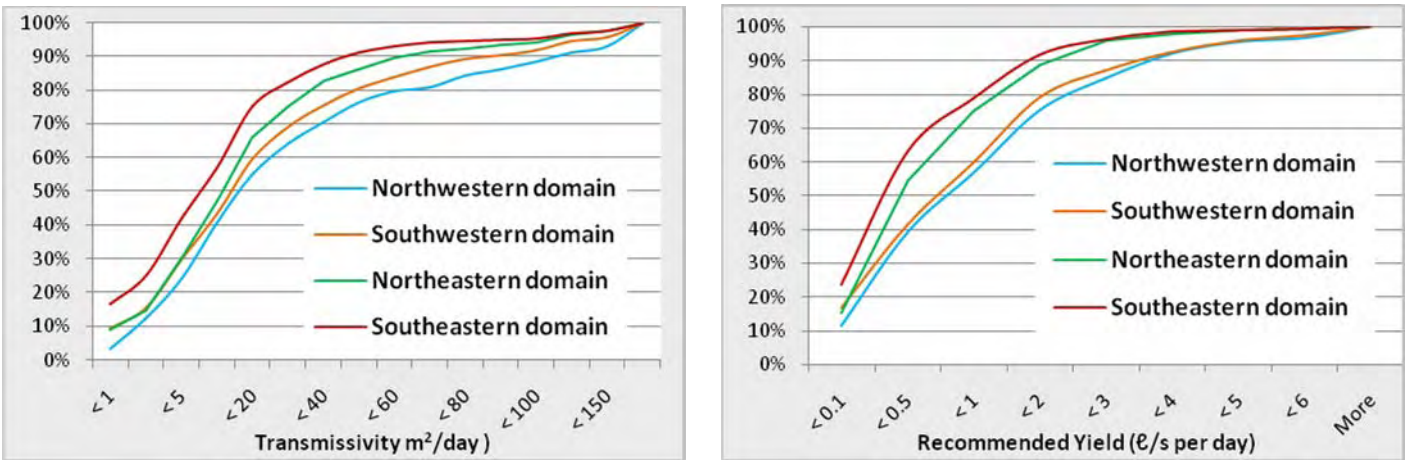

Figure 5.42. Cumulative frequency of transmissivity and recommended yields from boreholes based on the structural domains delineated in section 4.3 Error! Reference source not found.**.**

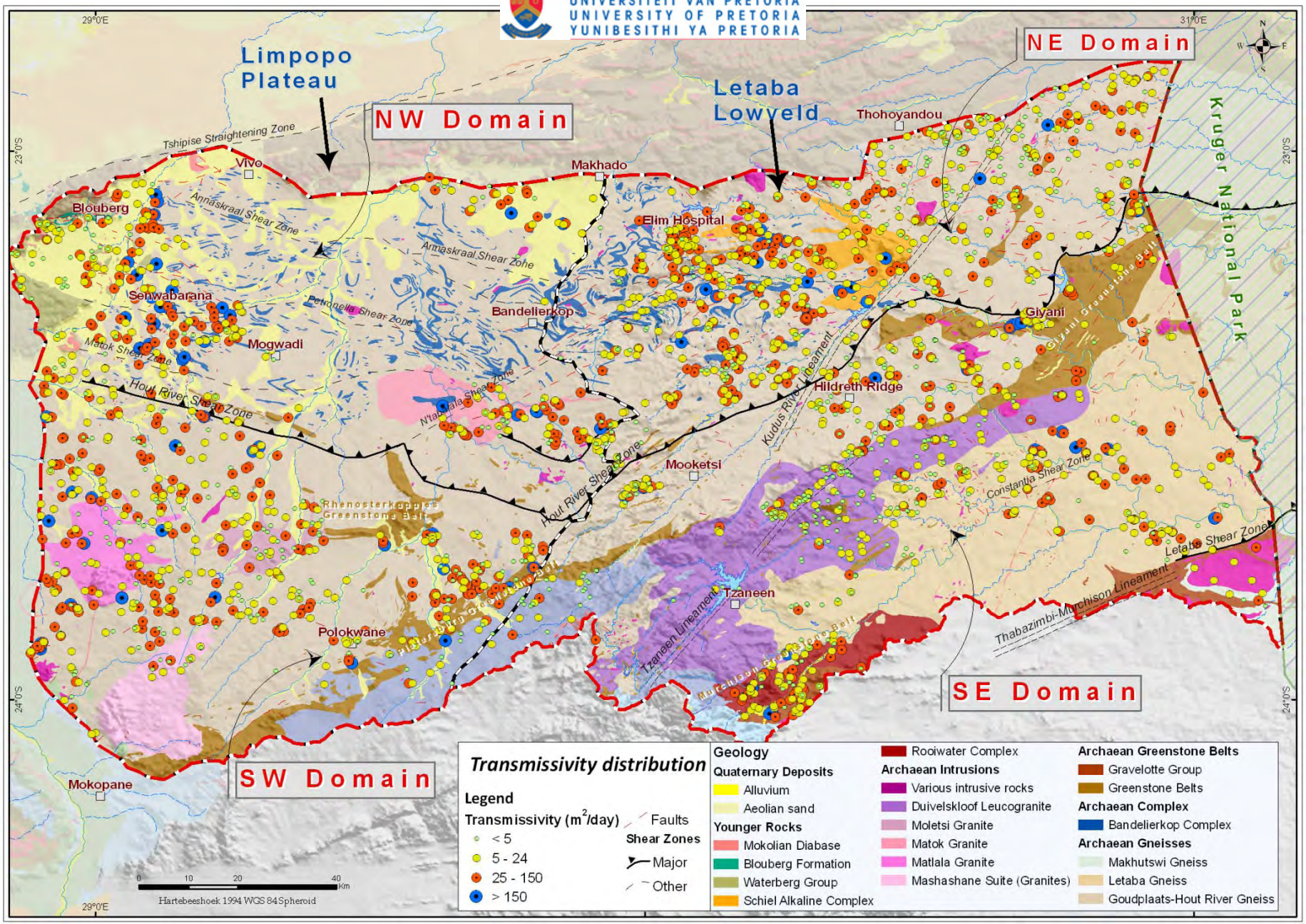

Figure 5.43. Spatial distribution of transmissivity obtained from the GRIP dataset.

5.5.1. Geological setting

The first analysis is based on the lithological information (driller's geological note) captured in the GRIP dataset. Unfortunately 90 percent of the lithology captured pertains to the Letaba Lowveld. Nevertheless the cumulative frequency graph of the major lithologies in the area clearly indicates the relative poor productivity of granites and diabase/dolerite associated with dykes in comparison to pegmatite (Figure 5.44).

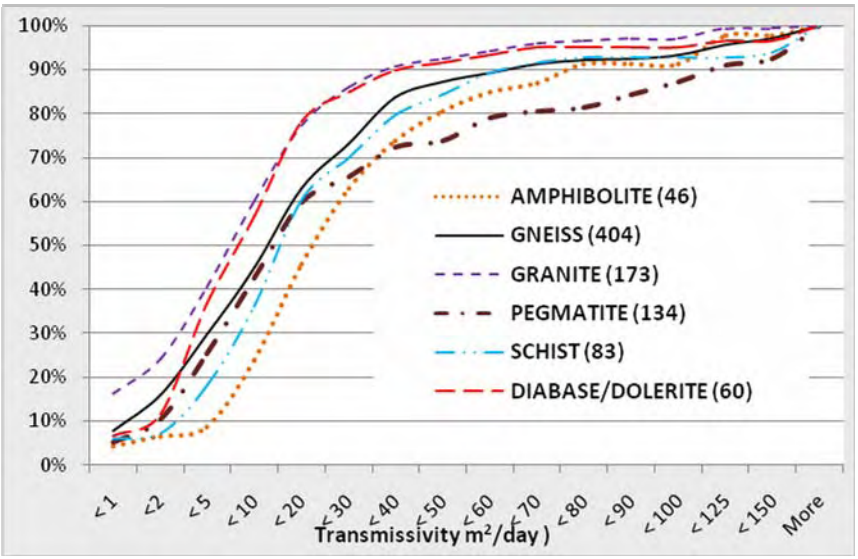

Figure 5.44. Cumulative frequency distributions showing the influence of various rock types on borehole productivity (number of boreholes in brackets).

Pegmatite is clearly more productive especially in the latter ranges of the frequency plot. Eighty percent of boreholes drilled in pegmatite attained transmissivities of 60 m^2/d with a mean value of 44 m^2/d (Table 5.19). Another rock type that supports productive boreholes is amphibolite with a mean transmissivity of 35 m^2/d. These mylonitic rocks are associated with the crushing and intense shearing coupled with the Limpopo Mobile Belt orogeny. As a result the regional amphibolite-grade metamorphism within the Hout River Shear Zone is a favourable groundwater target. Specific rock type clearly plays an important role in the selection of drilling targets in the Limpopo Province, however, rocks such as pegmatite often occurs as veins, forming features of restricted extent rather than a regional groundwater exploratory feature (Cook, 2003).

Table 5.19. Determined hydrogeological parameter based on the geology observed during drilling.

Lithology	Nr. of BH's	Transmissivity m^2/d	Rec. Yield L/s per day
ALL	**827**	**29.6**	**0.85**
Amphibolites	33	35	1.29
Diabase/dolerite	36	20	0.82
Gneiss	426	31	0.97
Granite	140	21	0.74
Pegmatite	117	44	1.13
Schist	75	29	0.94

For the second analysis, the boreholes were grouped according to the geological or lithological setting and the corresponding mean values along were calculated and compared (one-sample Student t-test, see section 3.5.1) to the total population Table 5.20.

Table 5.20. Determined hydrogeological parameter based on the geological setting of boreholes.

Parameter	Transmissivity m^2/d		Rec. Yield ℓ/s per day	
	Nr. of BH's	*Values*	*Nr. of BH's*	*Values*
All data	*2 484*	*30*	3 032	1.04
Alluvium	*200*	***44***	245	**1.63**
Significance		*100 %*		*100 %*
Aureole	*60*	***42***	68	**1.64**
Significance		*95%*		*99 %*
Bandelierkop Complex	*47*	*34*	51	0.89
Significance		*69 %*		*81 %*
Goudplaats-Hout River Gneiss	*1 400*	*33*	1 650	1.14
Significance		*96 %*		*100 %*
Letaba Gneiss	*195*	*24*	281	0.79
Significance		*97 %*		*100 %*
Major Batholith's	*84*	***16***	102	0.72
Significance		*100 %*		*100 %*
Greenstone Belts	*123*	*31*	175	0.90
Significance		*62 %*		*93 %*
Rooiwater Complex	*40*	*29*	48	1
Significance		*53 %*		*83 %*
Alkaline Complex	*50*	*35*	41	1.1
Significance		*93 %*		*86 %*
Leucogranites	*230*	***7***	299	**0.35**
Significance		*100 %*		*100 %*
Waterberg Group	*55*	*12*	72	0.73
Significance		*100 %*		*100 %*

There is a distinct variability in the transmissivities between the lithologies and geological settings of the The highest borehole productivity is - as expected - observed in the primary alluvial aquifers, whilst the least productive boreholes are associated with the elongated granites and leucogranites straddling the escarpment between the Limpopo Plateau and Letaba Lowveld. Similarly low productivities with average transmissivities of 16 m^2/d and average yields of 0.7 ℓ/s are observed in boreholes targeting the granitic batholiths (inselbergs). However, boreholes located along the contact zones of these batholiths provide the highest productivities of the crystalline bedrock. These granitic intrusives can displace the host rocks during intrusion in order to create space for the ascending magma. A number of physical changes occur in the host rock i.e. tension jointing, peripheral cleavage and ductile deformation, enhancing the water bearing characteristics of the host rock (Du Toit, 2001).The younger, large elongated leucogranites together with the main batholiths bodies itself and the sedimentary rocks of the Waterberg group have the lowest transmissivities. The Letaba gneisses which lie to the south of the lecogranites have a slightly lower productivity compared to the Goudplaats-Hout River Gneiss, which may be related to other factors such as fracture density and susceptibility to weathering (Figure 5.43). The Greenstone belts and other igneous complexes have productivities similar to the population mean.

5.5.2. Weathered layer (regolith) and erosion surfaces

To establish the influence of the weathered layer on the productivity of a borehole, the depth of weathering was related to borehole productivity. The scatter diagrams (Figure 5.45) show no correlation between transmissivity and weathering or between yield and weathering.

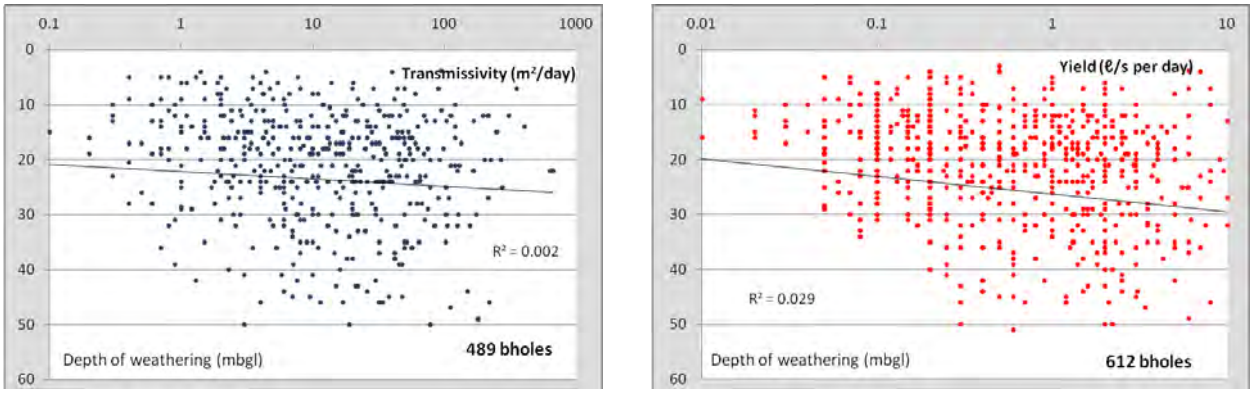

Figure 5.45. Graphs showing the correlation between transmissivity and depth of weathering and between yield and depth of weathering.

Chilton and Foster (1995) highlighted the fact that very few authors if any could obtain significant correlations between regolith thickness and borehole yield from statistical approaches. The authors attributed these poor correlations to the subjectivity of the yield value itself and to the overriding local factors such as well construction and efficiency. The common viewpoint in crystalline hydrogeology is therefore that a deeper weathering profile would be a major controlling factor on the borehole productivity due to the enhanced permeability and storage of this zone. However, in this case the semi-arid environment is characterised by a thin regolith (with less important water strikes) overlying the fractured aquifer where the main water bearing fractures is encountered.

The relationship between borehole productivity and the Post-African, and African erosion surfaces is illustrated in Figure 5.46. The data was compiled through a mutual Water Research Commission and British Geological Survey project known as the Grey Data Project. The results of available case histories from four individual Sub-Saharan countries (Uganda, Zimbabwe, Malawi and South Africa) were used to compare borehole productivities between the African and Post African erosion surface. The distinct high borehole productivity associated with the South African erosion surfaces are related to the high yielding nature of this basement aquifer system, while the post African erosion surface is slightly more comparable with the Malawi results. However, it is difficult to conclude that African (older) do indeed offer a more productive aquifer, due to the complexity and interplay of local factors controlling borehole yields (Figure 5.46).

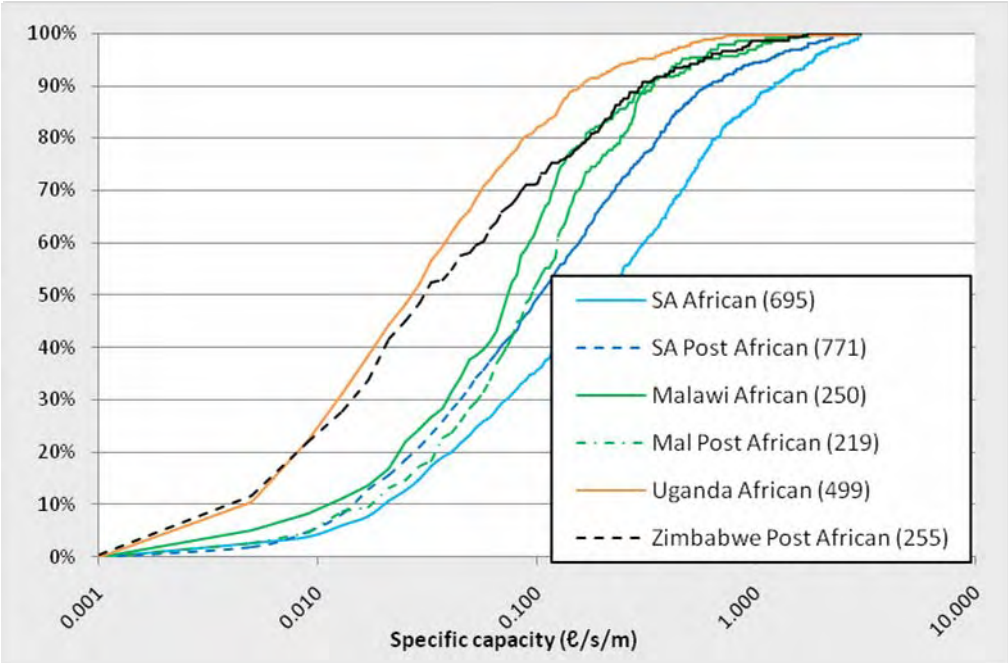

Figure 5.46. Cumulative frequency distributions showing the influence of erosion surfaces on borehole productivity (number of boreholes in brackets).

5.5.3. Topographic setting and drainages

The transmissivity and borehole yield data were filtered according to the topographic setting of the boreholes (as recorded by the driller) (Table 5.21) (Figure 5.47). As expected the boreholes located along rivers (alluvial aquifers) have above average transmissivities and yields, i.e. they represent the most favourable borehole locations from a topographic point of view. Boreholes in mountainous areas are on the other hand the least favourable locations.

Table 5.21. Determined hydrogeological parameter based on the topographic setting of boreholes.

Parameter	Transmissivity m^2/d		Rec. Yield ℓ/s per day	
	Nr. of BH's	*Values*	*Nr. of BH's*	*Values*
All data	*1 449*	*30*	1 837	1.04
Along River	*424*	**33**	245	**1.35**
Significance		*53 %*		*100 %*
Mountain	*23*	**7**	35	**0.32**
Significance		*100 %*		*100 %*
Slope	*300*	26	392	0.84
Significance		*100 %*		*100 %*
Valley	*82*	31	98	0.91
Significance		*66 %*		*98 %*
Flat Surface	*620*	**38**	789	1.15
Significance		*96 %*		*78 %*

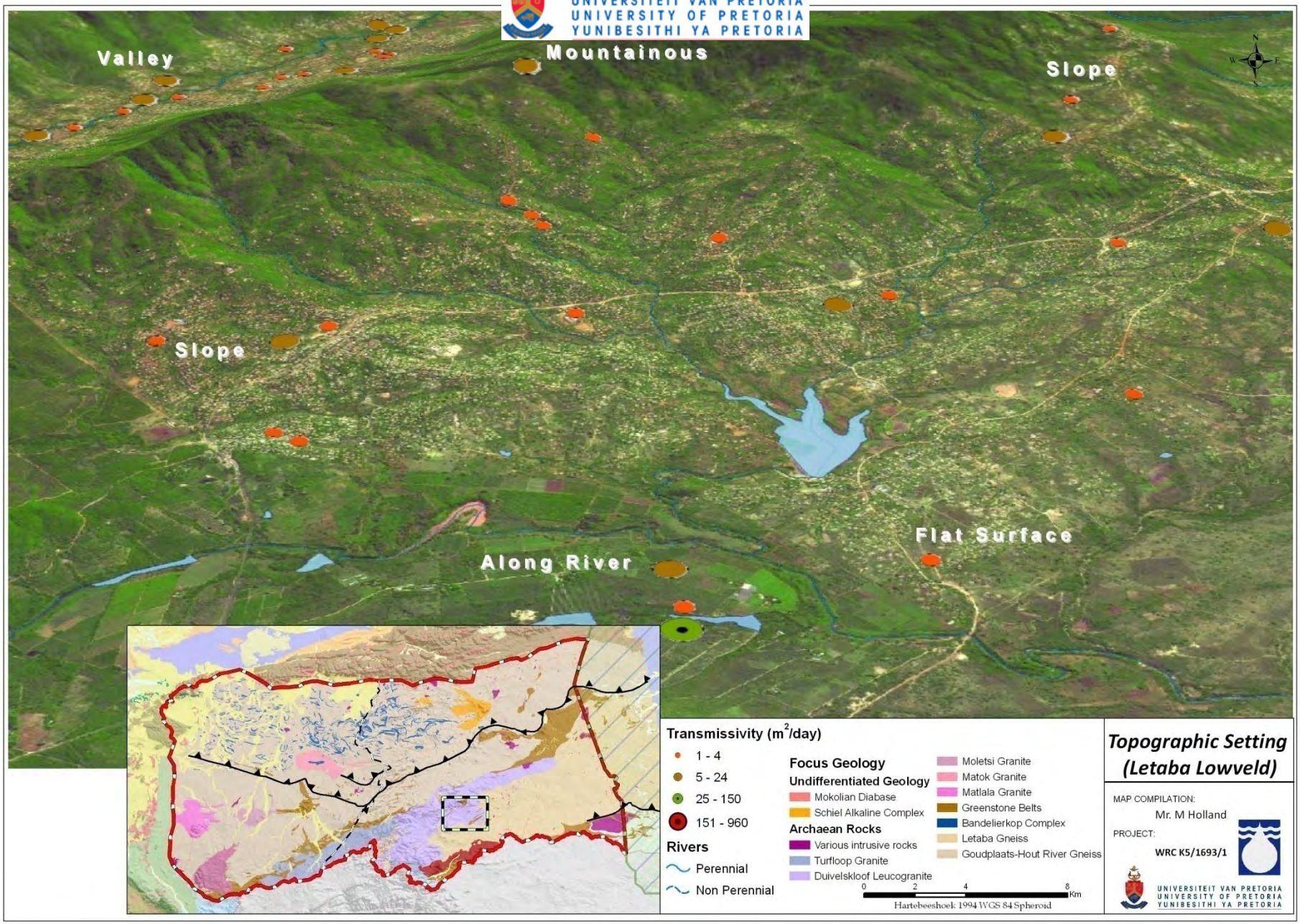

Figure 5.47. Typical setting of boreholes in relation to rivers and topography.

Proximity to rivers

To determine the influence of drainage channels on the borehole productivity, a spatial assessment of proximity was conducted (Table 5.22). 55% of all boreholes in the dataset are drilled within 150 m to streams or rivers as mapped on the 1:50 000 topographic map sheets of South Africa. Furthermore, 19 % of these boreholes are along the major perennial drainage channels. Boreholes close to both minor and major surface drainages have above average transmissivity and yields indicate the strong influence of surface water bodies on borehole productivity.

Table 5.22. Influence of proximity to rivers and streams on borehole productivity.

Area	Parameter	Transmissivity m^2/d			Rec. Yield ℓ/s per day		
		Nr. of BH's	*Mean*	*Median*	*Nr. of BH's*	*Mean*	*Median*
Limpopo	*All data*	**967**	**38**	**15**	**1137**	**1.45**	**0.8**
	Within 150 m (River)	177	**51**	26	206	**2.11**	1.6
	Within 150 m (Stream)	250	36	14	290	1.36	0.8
	Further than 150 m	540	**35**	12	641	1.28	0.7
Letaba	*All data*	**1542**	**24**	**10**	**1925**	**0.80**	**0.4**
	Within 150 m (River)	325	**32**	14	389	**1.03**	0.6
	Within 150 m (Stream)	742	23	9.1	918	0.79	0.3
	Further than 150 m	475	**21**	7.7	618	**0.66**	0.4

It can be concluded that both topography and proximity to rivers has a significant influence on borehole productivity. Drainage channels tend to follow zones of structural weaknesses (i.e. lineaments) in the near surface; therefore rocks in the vicinity of rivers might be more intensely fractured, jointed and/or weathered. From a hydraulic point of view, water levels are generally shallower at topographic lows and present discharge zones, providing more available drawdown and a larger capture zone compared to boreholes in mountainous areas drilled to approximately the same depth below ground surface.

5.5.4. Relationship to dykes

As dykes occur extensively in the study area, it is important to establish their role in the occurrence of groundwater. Based on the geological logs, boreholes which encountered dykes (diabase or dolerite) have generally lower productivity than boreholes devoid of diabase/dolerite (Figure 5.48). Another useful assessment of the role of dykes on borehole productivity is proximity to the mapped (published) dykes and regional aeromagnetic data (inferred dykes). Data from 1000 boreholes shows that drilling in the Limpopo Plateau within 25 m of dykes is more productive compared to wells further away. It is evident that although boreholes intersecting dykes are poor targets, drilling along dykes seems to be promising.

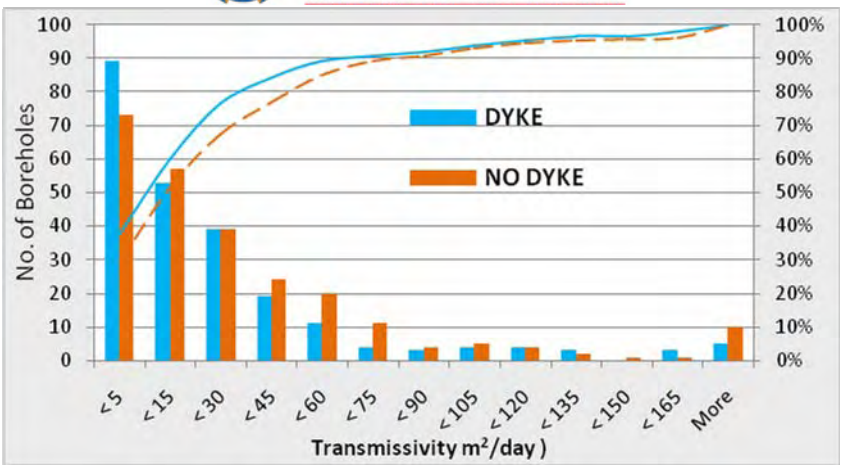

Figure 5.48. Frequency histograms and cumulative distribution showing the influence of dykes encountered on transmissivity estimates.

Due to the generally high transmissivity of the gneisses in the Limpopo Plateau (Figure 5.44), the cross cutting of less permeable dykes may act as flow barriers and, in conjunction with the greater fissuring commonly associated with dykes may enhance the accumulation of water. In contrast, drilling in close proximity to dykes in the Letaba Lowveld neither enhances nor reduces borehole productivity appreciably. Based on 1500 boreholes no significant relationship between transmissivity and distance to dykes exists (Table 5.23). It can be argued the permeability of these closely spaced dykes is not very different from the host rocks, the gneisses or granites, in which they occur. In this regard, their water bearing potential is as variable as the host rock, as they do not act as flow barriers or conduits.

Table 5.23. Transmissivity (m^2/d) of boreholes according to distance to inferred dykes.

	Distance to Dyke	< 25 m	25 – 50 m	50 -150 m	≥ 150 m	Total
Limpopo	N	25	34	96	812	967
	Mean T (m^2/d)	51.4	39.4	27.6	38.7	38.0
	Median T (m^2/d)	26.0	19.5	13.9	15.0	15.0
Letaba	N	65	50	200	1227	1542
	Mean T (m^2/d)	22.6	24.0	21.5	25.1	24.5
	Median T (m^2/d)	10.0	8.8	9.2	10.0	10.0

To evaluate the correlation between borehole productivity and the trend of dykes (azimuth), boreholes occurring within 150 m of dykes were examined more closely within each region (Figure 5.49).Within the Limpopo Plateau NW to NNE (315º to 30º) striking dykes offer evidently poorer water bearing characteristics compared to dykes striking NE (30 to 45º) or ENE (75 to 90º) with median transmissivities above 25 m^2/d. However, the box plots show similar transmissivity ranges (i.e. lower and upper quartiles) for WNW (270-315º) NE to ENE (30 to 90º) trending dykes (Figure 5.49). On the one hand high transmissivity along WNW dyke trends supports the assumption that structures striking parallel to the maximum horizontal stress are open. On the other hand, despite the fact that the effects of the neo-tectonic regime suggest

closure of conduits striking NE, these NE to ENE trending dykes have remained open throughout geological history. These older structures can be regarded as extensional features. The results clearly show the variability in targeting dykes based on their strike, but if any conclusion can be made, it is to reconsider drilling along dykes trending NW to NNE (315-30º). This is also observed in the Letaba Loweld where dykes trending NW to NNE (315-30º) are associated with lowest median transmissivity and also the lowest lower range (Figure 5.49). However, apart from a slightly larger range of transmissivities observed along lineaments with a W to WNW (275-315º) trend, no obvious orientations with significantly increased lower or upper quartiles are evident from the results in the Letaba Lowveld (Figure 5.49). As shown in the previous discussion the significance of drilling within the proximity of a dyke in the Letaba Lowveld is neither positive nor negative and this is supported by the dyke orientation analysis.

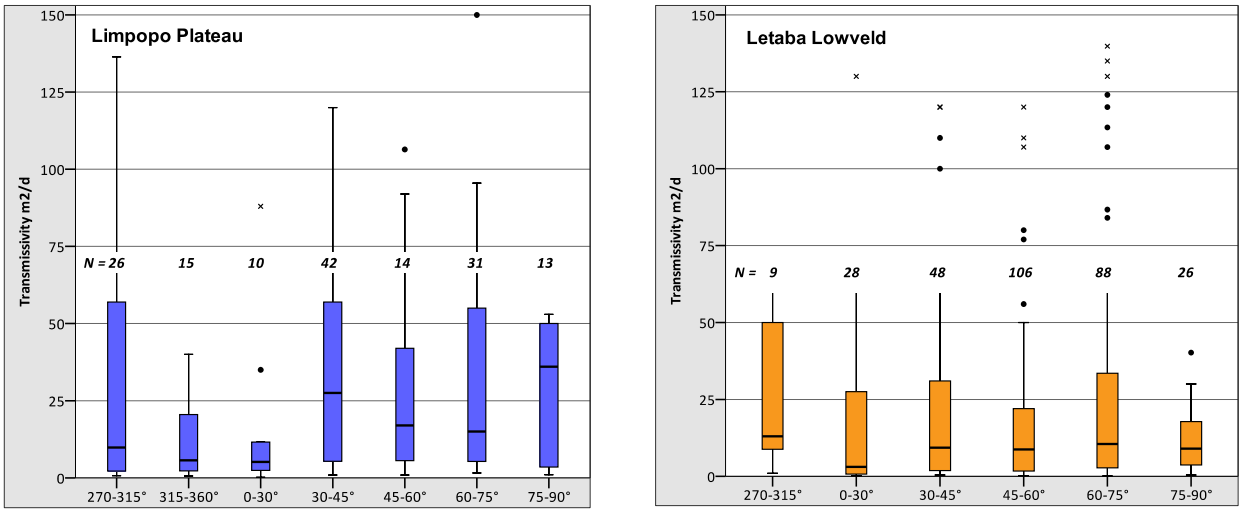

Figure 5.49. Box plot of transmissivity and dyke azimuth for both the Limpopo and Letaba regions. The box represents the 25 and 75 % quartiles, while the median is represented by the *horizontal line within the box*. Outliers are *marked by circles* and *by crosses*. The *vertical lines (whiskers)* connect the smallest and largest non-outliers.

5.5.5. Relationship to lineaments

The most significant correlation between transmissivity and proximity to lineaments is found in the north-western domain where both mean and median transmissivities within 50 m of a lineament exceed the population average (Table 5.24). Results vary slightly for the south-western domain with regards to the arbitrary distance ranges chosen, however, average transmissivities within 150 m of a lineament do show slightly higher borehole productivities compared to further away. Boreholes within 25 m of mapped lineaments in the north-eastern domain have higher median transmissivities compared to boreholes further than 150 m, although mean transmissivities are similar for all distance classes (Table 5.24). In the south-eastern domain notably higher borehole productivities are observed within the 50 – 150 m range compared to boreholes further than 150 m. Based on the results, it can be generally accepted that lineaments have a positive influence on borehole productivity and should be considered for future drilling programs.

Table 5.24. Productivity of boreholes according to distance to inferred lineaments.

Domain	Distance to lineaments	< 25 m	25 – 50 m	50 -150 m	≥ 150 m	Total
NW Domain	*N*	*6*	*13*	*33*	*294*	*346*
	Mean T (m^2/d)	**93.3**	69.8	**32.7**	44.6	45.2
	Median T (m^2/d)	**64**	36	18.4	**15.5**	17
	N	*6*	*13*	*33*	*328*	*380*
	Mean Rec. yield ℓ/s	**2.8**	1.43	1.6	1.64	1.65
SW Domain	N	*16*	*9*	*61*	*459*	*545*
	Mean T (m^2/d)	**38.9**	**27.9**	36.6	37.1	37
	Median T (m^2/d)	**25.5**	22	20	**16**	17
	N	*16*	*9*	*61*	*495*	*581*
	Mean Rec. yield ℓ/s	**2.1**	1.5	1.55	**1.44**	1.47
NE Domain	N	*30*	*28*	*80*	*628*	*766*
	Mean T (m^2/d)	21.8	25.1	**19.6**	**28.4**	27.1
	Median T (m^2/d)	**15.6**	9.4	11	12	12
	N	*30*	*28*	*80*	*682*	*820*
	Mean Rec. yield ℓ/s	**0.69**	0.93	**0.94**	0.94	0.93
SE Domain	N	*23*	*21*	*63*	*668*	*775*
	Mean T (m^2/d)	**21.5**	19.8	**28.3**	22.6	23
	Median T (m^2/d)	**6**	9.5	**12**	8	8
	N	*23*	*21*	*63*	*840*	*947*
	Mean Rec. yield ℓ/s	0.86	**0.41**	**0.94**	0.81	0.81

North-western and South-western domain (Limpopo Plateau)

The NW structural domain has a complex tectonic history and intense shearing and fracturing of the crystalline rocks has created highly productive fractured aquifers (Figure 5.42). The most common lineament strike direction is ENE (70° to 80°), based on the rose diagram developed for each domain (Figure 5.50). This trend is almost parallel with the dominant dyke trend of 66° and oblique to the average azimuth of joints (23°) observed from field measurements (see Figure 4.10). Productive boreholes are not associated with only one lineament trend direction, but the least favourable lineament trend appears to be ENE (60-75°) with below average transmissivities observed (Table 5.25). However, the results are in some cases based on a small borehole population.

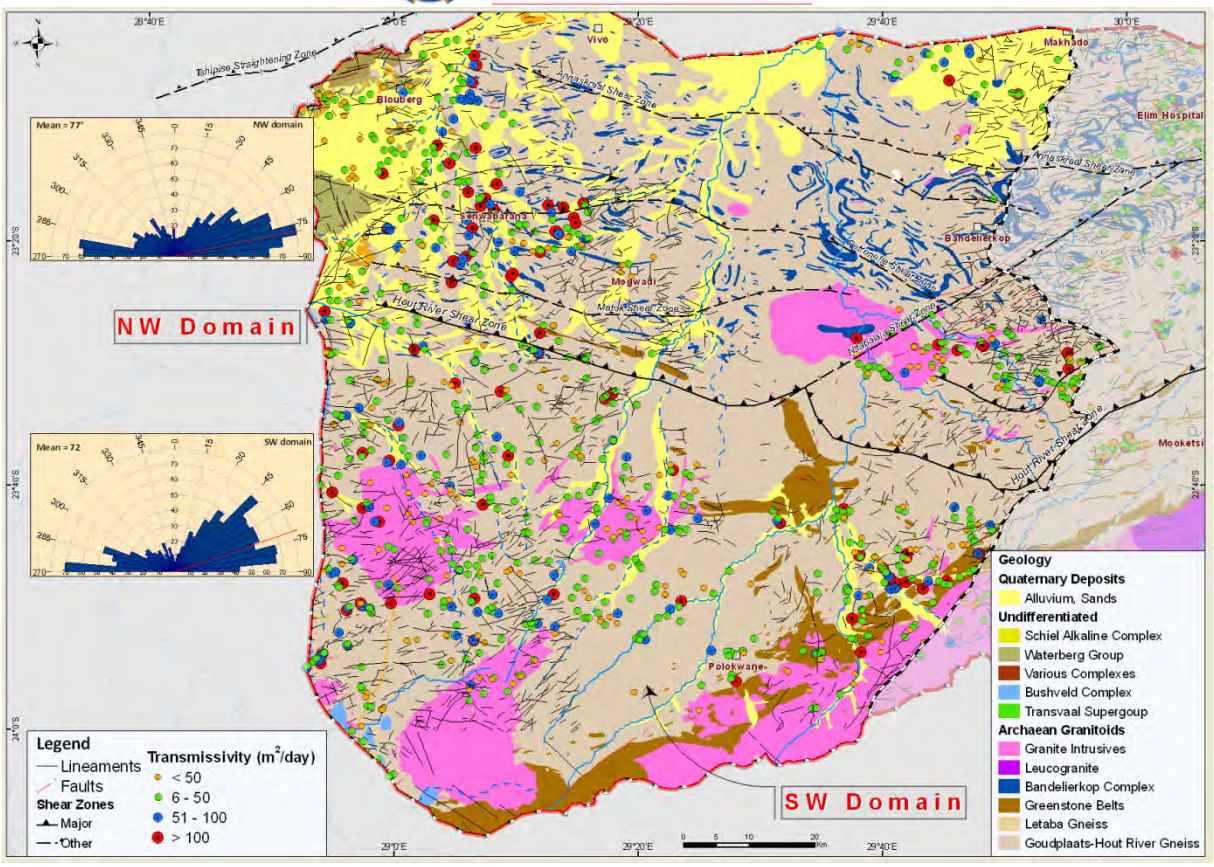

Figure 5.50. Distribution of shear zones, faults and lineaments in the Limpopo Plateau, with the lineament frequency rose diagram showing main structural trends.

Table 5.25. Transmissivity (m^2/d) of boreholes according to distance to inferred lineaments within the Limpopo Plateau.

Domain	Lineament azimuth	270-315°	315-360°	0-30°	30-45°	45-60°	60-75°	75-90°
NW domain	N	*14*	*11*	*2*	*3*	*4*	*6*	*12*
	Mean T (m^2/d)	50.5	49.5	58.0	**57.7**	52.3	11.2	36.3
	Median T (m^2/d)	22.2	11.0	58.0	**42.0**	29.0	4.3	29.0
SW domain	N	*23*	*14*	*11*	*4*	*13*	*13*	*8*
	Mean T (m^2/d)	41.4	21.1	28.4	29.4	**48.6**	39.0	36.6
	Median T (m^2/d)	**37.0**	18.0	11.6	30.5	15.0	23.0	22.0

Considering the borehole populations, median transmissivity and range of transmissivity it is interpreted that the most productive boreholes may be associated with ENE to E trends (75-90°) (Figure 5.51) which is almost perpendicular to the current NW maximum horizontal stress regime. Lineaments striking W to WNW (270-315°) are associated with higher average and median borehole productivities compared to NNW to N (315-360°) (Table 5.25). These trends are slightly oblique to the current horizontal stress regime and it may be interpreted that the W to WNW trends are more favourable targets compared to the latter and may have opened due the this acting stress regime. This is even more apparent in the south-western domain where above average and

median transmissivity are associated with lineament trends striking W to WNW (270-315°) and offer potentially the most productive lineament target. Other high borehole productivities was observed along lineaments striking ENE to E (60-90°) with the least favourable lineaments associated with N to NNE (0-30°) trends (Figure 5.51).

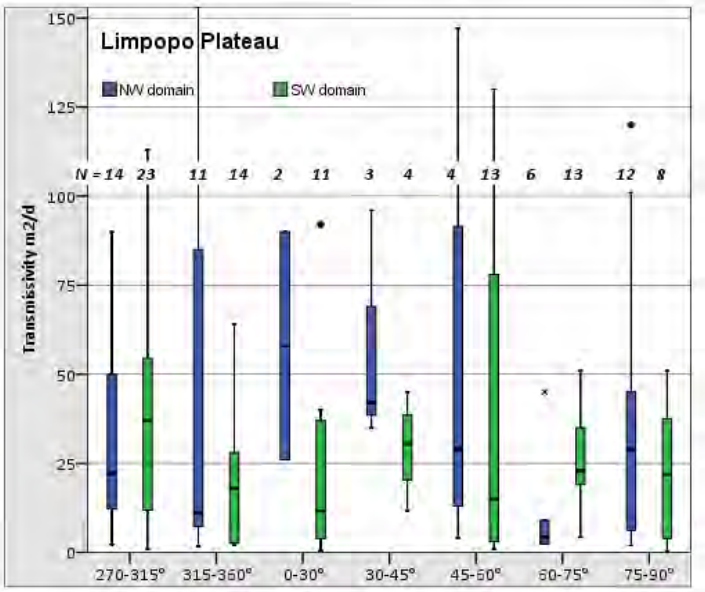

Figure 5.51. Box plot of borehole transmissivity in relation to the lineament azimuth in the Limpopo Plateau.

North-eastern and South-eastern domain (Letaba Lowveld)

The prominent ENE (60-75°) lineament strike direction in the NE structural domain is almost parallel to the observed dyke trend and joint orientations based on field measurements (Figure 5.52). Although no single preferred lineament orientation is distinctly clear, based on the observed average and median transmissivity 45 to 60° provide the least favourable groundwater potential, while it is clear the N to NE (0-45°) and ENE to E (60-90°) is by far superior compared to lineaments striking W to N (270-360°) (Table 5.26) (Figure 5.53). This is in contrast to what is expected under current stress conditions, with lineaments striking perpendicular to the current stress regime providing higher transmissivity.

Table 5.26. Transmissivity (m^2/d) of boreholes according to distance to inferred lineaments within the Letaba Lowveld.

Domain	Lineament azimuth	270-315°	315-360°	0-30°	30-45°	45-60°	60-75°	75-90°
NE domain	*N*	*26*	*14*	*11*	*9*	*13*	*35*	*30*
	Mean T (m^2/d)	17.4	12.9	**36.2**	35.7	6.7	25.2	20.4
	Median T (m^2/d)	11.8	10.6	12.4	12.9	4.0	12.0	**16.7**
SE domain	*N*	*21*	*8*	*15*	*27*	*4*	*15*	*17*
	Mean T (m^2/d)	15.4	15.3	**25.4**	14.5	13.0	21.5	23.0
	Median T (m^2/d)	8.0	13.5	12.0	7.7	10.0	**19.0**	14.0

Similar results is observed in the SE structural domain where preferred lineament orientations are associated with lineament trending ENE to E (60 to 90°), while lineaments striking NE (30 to 60°), which is along the strong main NE lineament trend (Figure 5.53), provide evidently the least favourable groundwater potential.

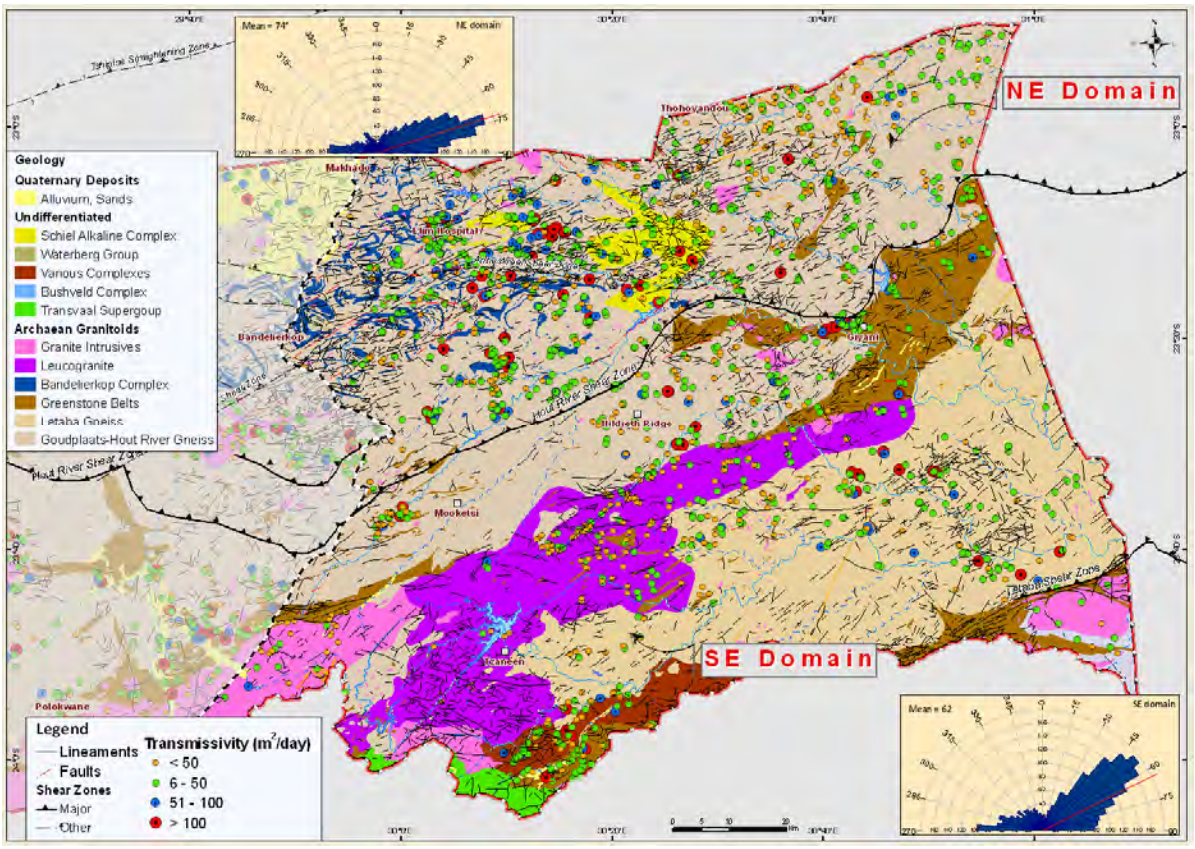

Figure 5.52. Distribution of shear zones dykes, faults and lineaments in the Letaba Lowveld, with the lineament frequency rose diagram showing main structural trends (squares indicate field studies).

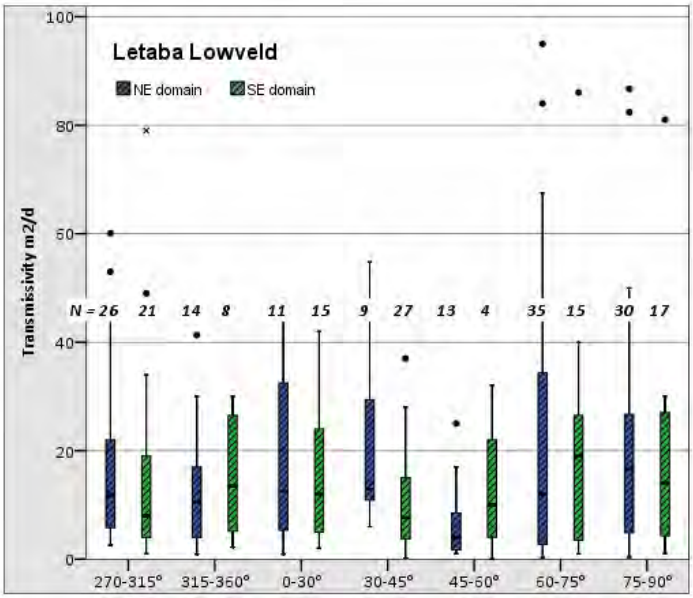

Figure 5.53. Box plot of borehole transmissivity in relation to the lineament azimuth in the Letaba Lowveld.

5.5.6. Field observation (testing the results)

Field verification of the lineament borehole productivity relationship were tested as part of the GRIP programme for the augmentation of a surface water supply scheme in the Great Letaba catchment (SE Domain, see Figure 5.52).

Dzumeri

A 5000 m geophysical profile striking NNE to SSW was conducted to pin-point drilling targets and to verify regional ASTER lineaments and aeromagnetic dykes (Figure 5.54). A number of anomalies from the geophysical profile correspond with the regional lineaments Five out of the 7 boreholes drilled along the profile were successful with an airlift yield of more than 0.1 ℓ/s.

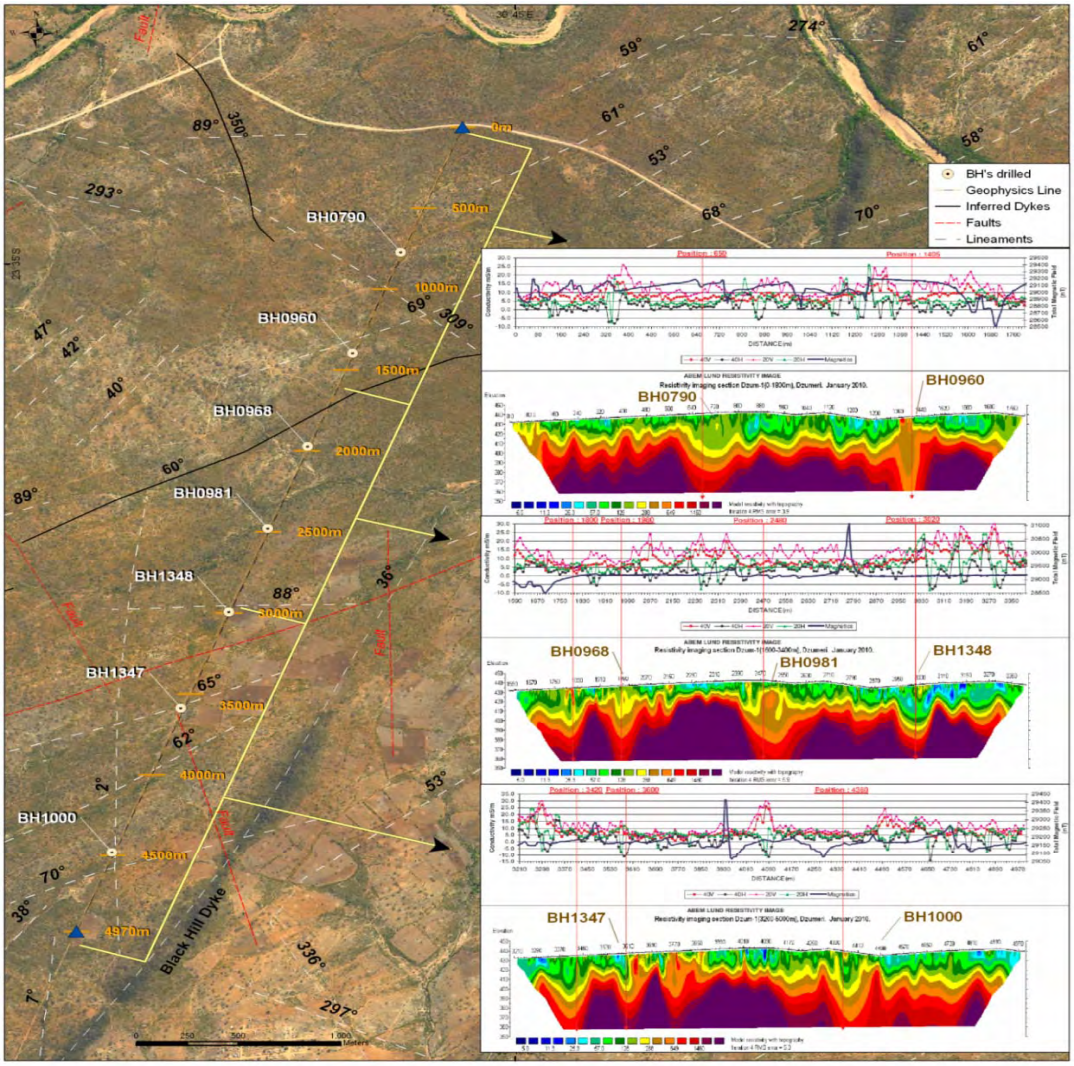

Figure 5.54. Field study location and the 5 km geophysical profile near Dzumeri village.

Throughout the length of the resistivity profile a number of deeper weathering zones (< 100 Ωm) are observed which relates to the lineaments observed in the field. Although boreholes targeting these weathered zones were successful, the yields were relatively low (Table 5.27). In most cases water was encountered below the regolith which highlights the fact that the relatively thin regolith (< 25 m) alone does not produce significant yields for water supply purposes. Fissure zones could be identified from the anomalies detected on the conductivity profile especially from 3 000 m to 3 300 m where borehole BH1348 was drilled. Boreholes targeting these anomalies were not all high yielding (i.e. BH1347 and BH 1000) and this could be related to the fact that some of these fractures are closed to groundwater flow. Two boreholes with an airlift yield of 1 ℓ/s (BH0790) and 7 ℓ/s (BH1348) were drilled on anomalies striking predominantly N305°W and N88°E respectively. The highest yielding borehole (BH1348) is also associated with a deeply weathered and fracture zone evidently to a depth of 30 m.

Bolubedo

An 800 m geophysical profile striking NNE to SSW near Bolobedu highlights three distinct anomalies which correspond spatially reasonably well with the regional ASTER image lineaments (Figure 5.55).

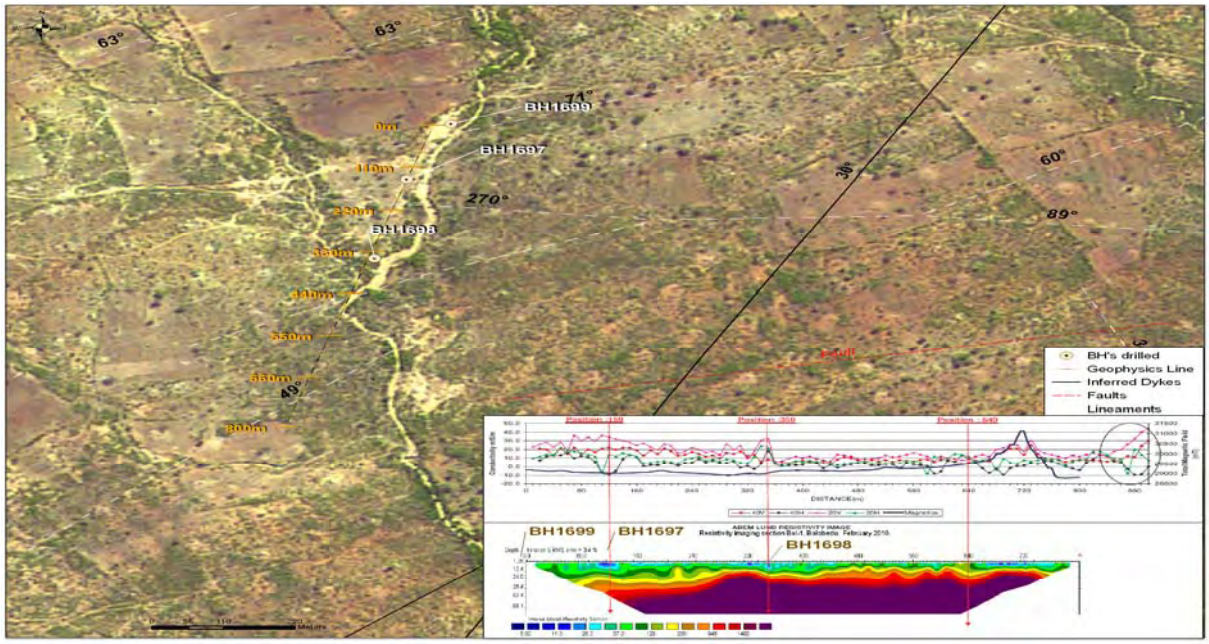

Figure 5.55. Field study location and the 800 m geophysical profile near Bolobedu.

Borehole BH1699 was drilled based on field observations while BH1697 and BH1698 targeted geophysical anomalies at positions 150 and 350 m respectively (Figure 5.55). The highest yielding borehole is associated with a distinct E-W trending lineament while the noisy conductivity profile may suggest a fissured zone. BH1698 lies seemingly on a N60°E trending lineament and produced the lowest yield of the three sites, corresponding to the theory that ENE to E (N60°E to N90°E) striking structures offer potentially higher yields compared to lineaments striking NNE to NE (N30°E to N45°E).

Table 5.27. A summary of drilling results in the Great Letaba Catchment.

Site	*BH Nr.*	Lineament/dyke		Water Strike (m.b.g.l)	BH Depth (m.b.g.l)	Airlift Yield (ℓ/s)	Regolith Depth (m.b.g.l)	Rec. Yield ℓ/s per day	T-value m^2/d
		Dist (m)	Azimuth						
Dzumeri	BH0790	180	305°	66	120	1	22	0.8	9
	BH0960	90	69°	131	156	0.2	32	-	-
	BH0968	204	60°	Dry	144	Dry	16	-	-
	BH0981	475	60°	123	148	0.3	26	-	-
	BH1348	18	88°	35	210	7	43	1.7	3
	BH1347	23	65°	Dry	120	Dry	20	-	-
	BH1000	88	2°	45	114	0.3	30	-	-
Bolobedu	BH1699	30	71°	21	72	2	20	1	5.5
	BH1697	60	270°	23	72	5.2	24	-	-
	BH1698	73	60°	21	72	0.5	18	0.2	2

*- meters below ground level.

5.5.7. Discussion of results

Historical groundwater exploration within the area has successfully targeted structural features and geological contacts at depth within the unweathered bedrock instead of in the rather thin regolith. Regionally, the influence of the weathering layer on borehole productivity is therefore considered poor. However, an ideal borehole or well would still intercept long or interconnected fractures in the solid rock which are in contact with a large volume of overlying, low permeability material that provides a consistent source of water. While the geological analysis of the data set indicates the obvious, that the rock type and lithology influences borehole productivity, the four structural domains identified within the study area show distinct differences in groundwater potential suggesting that the factors involved in controlling borehole productivity vary with each geological setting. Although dykes are poor groundwater targets drilling along these features may prove to be more successful in the Limpopo Plateau, where these dykes may act as barriers to flow. In the Letaba Lowveld dykes can be regarded as part of the host rock with no difference in permeability. These magnetic anomalies may present poor drilling targets with often disappointing results unless their strike direction is considered.

In general, the proximity of lineaments plays a role in borehole productivity and based on the transmissivity results it is assumed that the intensity of fracturing decreases with increasing distance away from the lineament.

Although highly variable, a number of specific lineament orientations provide above average transmissivities. It is generally expected that boreholes influenced by lineaments striking NW-SE (presumed to be under dilation and shear stress caused by the NW-SE maximum horizontal stress direction) should have higher productivities than boreholes associated with lineaments striking perpendicular to that direction. However, based on the results it seems that higher borehole productivities are in fact associated with lineaments and dykes perpendicular to the current stress regime, more specifically ENE to E and WNW to W. A possible explanation for this may be a localised compressive stress regime which is inconsistent with the regional maximum horizontal stress regime of NW-SE as determined by Bird et al. (2006). The ENE-WSW trending Tshipise-Bosbokpoort fault system immediately north of the area under investigation was for example notably reactivated in post-Tertiary times (Brandl 1995). The cause of the rejuvenation of these structures may be related to the southerly propagation of the East African Rift system (Figure 5.56). This would suggest that the Limpopo Plateau and the Letaba Lowveld might be considered to be under N-S extension, which is more pronounced towards the east. The higher transmissivities observed along lineaments trending ENE to E in the Letaba Lowveld support this assumption. In the Limpopo Plateau this model is not as distinct, with higher borehole productivities associated with lineaments trending both NE and WNW.

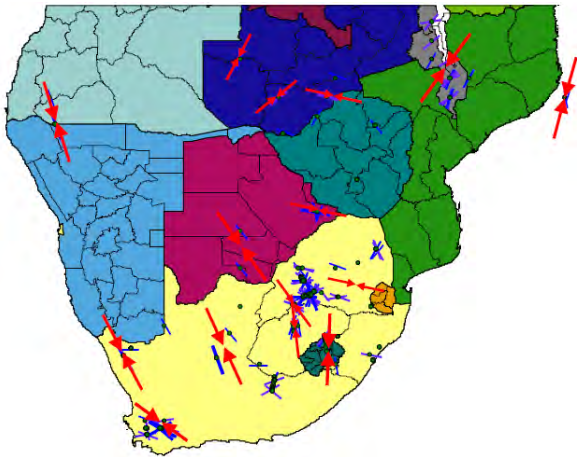

Figure 5.56. Stress orientations of southern Africa (Stacey and Wesseloo, 1998).

Geology has been identified as the main influence on borehole productivity while topography and proximity to surface water drainages have an obvious influence on the groundwater potential. However, since the topographic setting is directly related to the underlying geology, it is not an independent factor. The influence of topography on well yield in fractured rocks has also been shown by Mabee et al. (1994), Henriksen, (1995) and Fernandes and Rudolph, (2001). In all cases the authors found higher well yields in low topographic settings (i.e. valleys). Valleys are often associated with regional fracture features. From a hydraulic point of view, water levels are generally shallower at topographic lows and present discharge zones, providing more available drawdown and a larger capture zone compared to boreholes in mountainous areas drilled to approximately the same depth below ground surface. This may also explain in part the high observed borehole productivities in proximity of surface water drainages. In most cases these high productive boreholes are associated with elongated primary alluvial aquifers. In addition drainage

channels tend to follow zones of structural weaknesses (i.e. lineaments) in the near surface; therefore rocks in the vicinity of rivers might be more intensely fractured, jointed and/or weathered.

A conceptual understanding of the most significant features controlling groundwater occurrence in the Limpopo Basement aquifers is illustrated in Figure 5.57. A summary of the potential groundwater targets based on the knowledge obtained during this investigation is listed in Table 5.28 and presented spatially in Figure 5.58. The occurrence of alluvium aquifers was discussed in previous sections and while this remains a prime target for groundwater exploration it was excluded from the list in Table 5.28.

Table 5.28. Recommended drilling targets per structural domain.

Feature	Limpopo Plateau	Letaba Lowveld
Dykes (proximity)	High borehole productivity within 50 m of dyke	Little influence on the borehole productivity
Dyke (orientation)	NW to NNE (315° to 30°) striking dykes offer evidently poorer water bearing characteristics compared to dykes striking NE (30 to 45º) or ENE (75 to 90º)	No preferred orientation, although W to NNE (315-30°) seem less favourable
Feature	**NW Domain**	**NE Domain**
Lineaments (proximity)	High borehole productivity within 25 m and 50 m of lineament	Slight influence on the borehole productivity (within 25 m of lineament)
Lineaments (orientation)	W to WNW (270-315°) and ENE to E trends (75-90°) are associated with higher borehole productivities compared to NNW to N (315-360°)	N to NE (0-45°) and ENE to E (60-90°) are associated with higher borehole productivities compared to W to N (270-360°)
Neo-tectonics	High borehole productivities observed parallel, perpendicular and oblique to the current NW maximum horizontal stress regime	High borehole productivities observed oblique and perpendicular to the current NW maximum horizontal stress regime
Feature	**SW Domain**	**SE Domain**
Lineaments (proximity)	High borehole productivity within 25 m of lineament	Slight influence on the borehole productivity (within 150 m of lineament)
Lineaments (orientation)	W to WNW (270-315°) and ENE to E (60-90°) with the least favourable lineaments associated with N to NNE trends (0-30°)	ENE to E (60 to 90°) are associated with higher borehole productivities compared to W to NW (270-315°) and NE (30 to 60°)
Neo-tectonics	High borehole productivities observed perpendicular and slightly oblique to the current NW maximum horizontal stress regime	High borehole productivities observed oblique and perpendicular to the current NW maximum horizontal stress regime

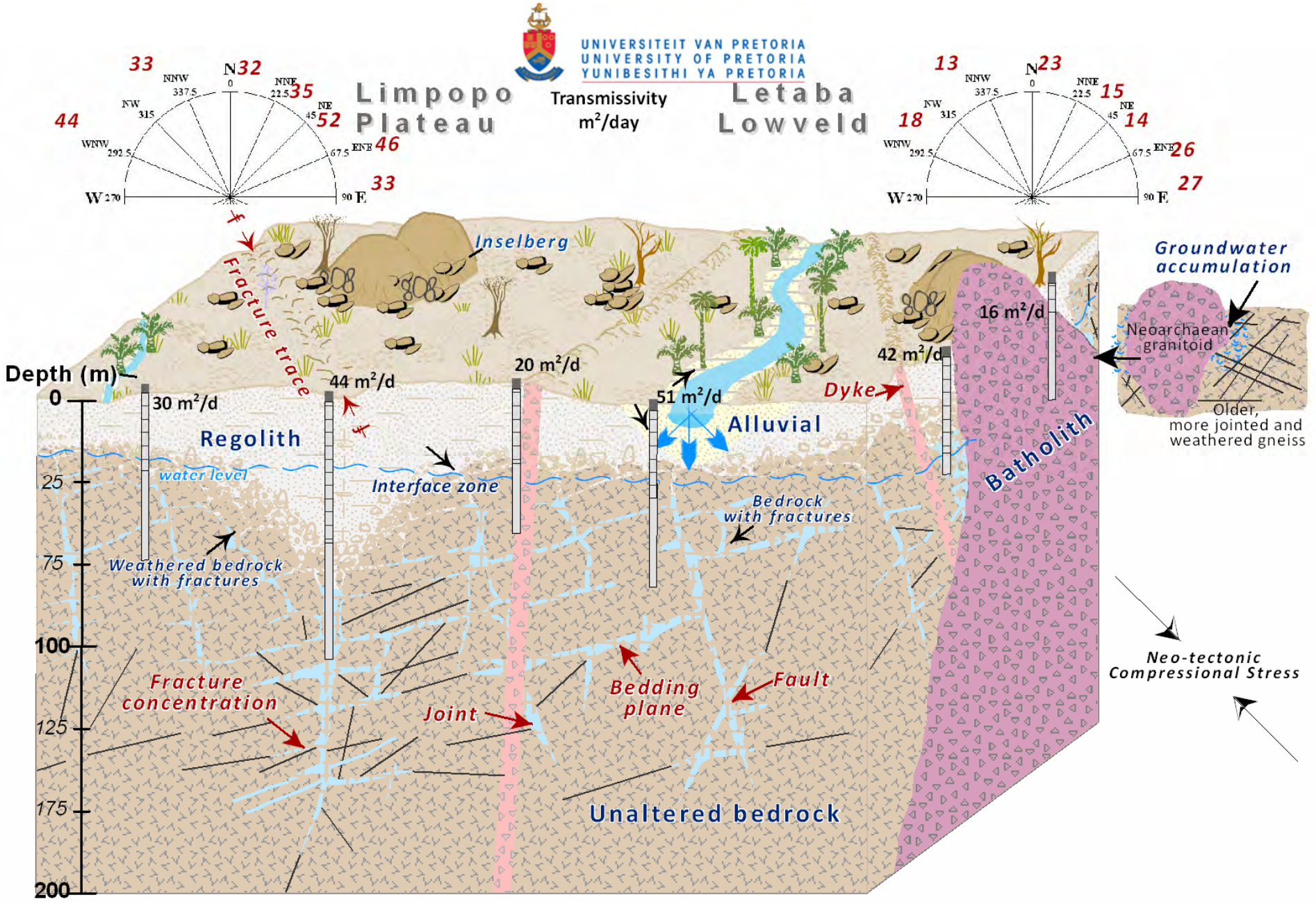

Figure 5.57. Conceptualisation of transmissivity values obtained from various borehole settings in the Limpopo basement aquifers (rose diagram indicating mean transmissivities for selected lineament azimuths based on Table 5.25).

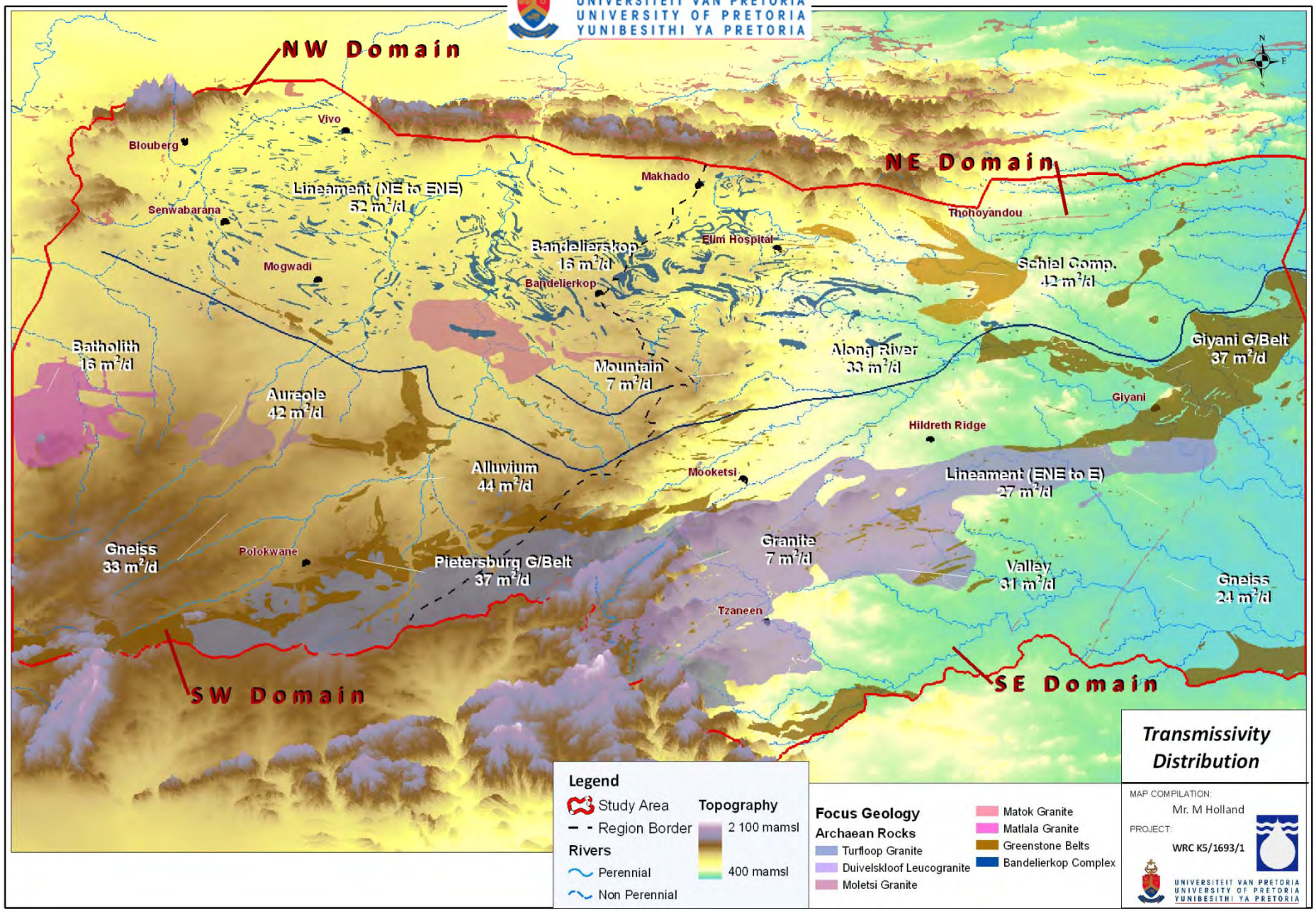

Figure 5.58. Regional distribution of transmissivity to illustrate the potential productive groundwater areas.